UNIVERSITÀ DEGLI STUDI DI PALERMO

PhD School of Biomedicine and Neuroscience
Department of Experimental Biomedicine and Clinical Neuroscience (BioNeC)
SSD BIO/17

CHARACTERIZATION AND ENERGETIC METABOLISM ANALYSIS OF DIFFERENT POPULATIONS OF UMBILICAL CORD MESENCHYMAL STEM CELLS FOR THE TREATMENT OF STROKE

CANDIDATE
DR. ELEONORA RUSSO

PROGRAM DIRECTOR
PROF. FELICIA FARINA

TUTOR
PROF. GIAMPIERO LA ROCCA

CO-TUTOR
PROF. CESAR V. BORLONGAN

CYCLE XXXI
YEAR OF DOCTOR TITLE ATTAINMENT 2018/2019

Dedicated to my grandparents that always encouraged me to study and to be the best person that I could be, hoping that they are proud of me.

<<Education is the most powerful weapon which you can use to change the world>>

Cit. Nelson Mandela

INDEX

LIST OF ABBREVIATIONS

LIST OF FIGURES

LIST OF TABLES

INTRODUCTION

Stroke is the second leading cause of death and disability worldwide behind heart diseases [1]. Ischemic stroke accounts for the 87% of all the cases of stroke [1]. Only one pharmacological treatment approved by the Food and Drug Administration (FDA), alteplase, is available for the treatment of ischemic stroke [1]. Alteplase is a recombinant tissue plasminogen activator (tPA) with thrombolytic action that can restore the blow flow after stroke [2]. However, its limited time window (effective only within 4.5 hours after stroke onset) and high risk of hemorrhages reduce the range of patients able to benefit from it [2]. Therefore, there is a critical need for novel therapeutic strategies for stroke.

A direct consequence of oxygen and glucose deprivation during stroke is the dysfunction of mitochondria that impairs oxidative metabolism and contributes to oxidative stress, neuronal death and inflammation [3]. Indeed, mitochondria are responsible for more than the 90% of the total adenosine triphosphate (ATP) demand of the cell [4]. Accordingly, the decrease of ATP production following glucose and oxygen depletion leads to energy failure, excitotoxicity and calcium overload that, in turn, determine loss of mitochondrial membrane potential [3]. In addition, the mitochondrial dysfunction induces excessive production of reactive oxidative species (ROS), which directly trigger damage of proteins, lipids and deoxyribonucleic acid (DNA) [3]. However, mitochondria exert different hierarchical quality control (QC) mechanisms against oxidative stress including mitochondrial fusion and fission to protect mitochondria against stress and damage, ensuring the selective removal of dysfunctional mitochondria by mitophagy [3]. Finally, excessively damaged mitochondria are characterized by an increase of membrane permeability that allows the release of pro-apoptotic molecules in the cytoplasm triggering apoptotic cell death [3]. Thus, mitochondrial dysfunction plays a central role in stroke injury.

Cell-based therapies aim to replace dead cells and promote the survival of damaged cells, altogether directly aiding exogenous and endogenous repair mechanisms [5]. In addition, the use of stem cells may indirectly promote regeneration by altering the local environment to be more conducive for regeneration by providing trophic support and reducing inflammatory response [5]. Recently, a novel beneficial mechanism of stem cells has been demonstrated to involve the transfer of healthy mitochondria into damaged cells [6]. Mitochondria can be released through

tunneling nanotubes (TNTs), microvesicles, gap junctions, cell fusion and direct uptake of isolated mitochondria [7]. Even though the signals that induce a cell to release its own mitochondria and transfer these organelles to another cell are not still clear, much evidence suggests that this phenomenon can help damaged cells to recover their functions [8]. In the last few years, mitochondrial transfer has been shown to occur between several cell types, including mesenchymal stem cells (MSCs) and pulmonary alveoli, astrocytes and neurons, and bone marrow (BM) derived-MSCs (BM-MSCs) and, rat cortical neuronal cells or, endothelial progenitor cells [9] [10]. Taken together, these observations suggest that the transfer of healthy mitochondria into damaged cells may be a novel therapeutic strategy for stroke.

Treatment strategies for injured/diseased central nervous system (CNS) include transplantation of embryonic stem cells (ESC), stem cells isolated from adult tissues like the MSCs; and induced pluripotent stem cells (iPSC) which are adult somatic cells reprogrammed to pluripotency [11]. MSCs represent highly safe and efficacious transplantable donor cells in regenerative medicine due to their plasticity, and immunomodulatory and anti-inflammatory properties [12]. Moreover, they are non-tumorigenic and are the most widely studied cells in blood-borne diseases [12]. MSCs can be isolated from each adult organ, as well as from fetus-associated perinatal tissues such as placenta, amnion, chorion, amniotic fluid, and umbilical cord [12]. Extraembryonic tissues offer an attractive alternative source to adult MSCs as they are discarded after birth and therefore, the collection procedures are not invasive and without ethical constraints [12].

With their self-renewal and multipotent differentiation potential, immunomodulatory and anti-inflammatory abilities, human umbilical cord (UC)-derived MSCs (UC-MSCs) are an enticing cellular source for regenerative medicine purposes [13] [14]. Harvesting MSCs from UC is practical as it circumvents ethical and logistical issues normally associated with fetal or embryonic tissues. MSCs have been isolated from Wharton's jelly (WJ), perivascular region (PV) and cord lining (CL) of UC. However, it is still unclear whether MSCs from a certain compartment of UC are therapeutically superior to MSCs from other compartments [15]. Interestingly, because UC is composed only of two arteries and a vein, the UC-MSCs are physiologically adapted to survive in a relatively hypoxic and glucose poor environment leading to the overarching hypothesis that these cells may have a beneficial potential for the treatment of ischemic pathologies, such as stroke.

The overall aim of this PhD research project is to characterize the human UC-MSCs based on their neuroprotective, trophic, and immunomodulatory capacities, as well as test their energetic metabolism potential for the treatment of ischemic stroke.

BACKGROUND

1

Stroke

1.1 – Epidemiology

Stroke is a main cause of mortality and morbidity worldwide. In 2015, prevalence of cerebrovascular disease was 42.4 million people and 6.3 million deaths worldwide, making stroke the second leading global cause of death behind ischemic heart disease [1]. On average, every 40 seconds, someone in the United States has a stroke and every 4 minutes, someone dies of a stroke [1]. In the Western world, over 70% of individuals experiencing a stroke are over 65 years of age. Since life expectancy continues to grow, the absolute number of individuals with stroke will further increase in the future as the world population ages [1].

1.2 – Types of stroke

There are two types of stroke: ischemic and hemorrhagic [16]. Hemorrhagic stroke is due to a rupture of a blood vessel and bleeding in brain. The blood accumulates and compresses the surrounding brain tissue that may increase the fluid pressure in the brain, resulting in swelling, hydrocephalus, and vasospasm. On the other hand, ischemic stroke is the most frequent sub-class of stroke, accounting for 87 % of stroke cases in the United States [1] [16]. Ischemic stroke occurs when a cerebral region is deprived of oxygen due to a decrease in local blood flow resulting from an obstruction of a blood vessel, such as embolism or thrombus formation [16].

1.3 – Post stroke outcomes

Following a stroke, 15-30% of stroke survivors are permanently disabled and 20% require institutional care [1]. One of the most severe deficits caused by stroke is motor impairment. Depending on the severity of cerebral infarction, patients may have disabilities in different degrees (mid, acute, severe), in one or both hemispheres and at different body levels: upper (face,

neck), medium (trunk, upper limbs) and lower (lower limbs) [17] [18] [19]. In particular, hemiparesis, defined as muscular weakness or partial paralysis restricted to one side of the body, is an impairment present in 88% of the stroke patients and only 12% shows full recovery after conventional rehabilitation therapy [20] [21]. Cognitive impairments after stroke include difficulties with memory, thinking and language [22]. These deficits are persistent and reduce the quality of life of both patients and family members also in social, professional and economic aspects of the life [23]. In this latest regard, in United States the annual medical direct and indirect cost of stroke is about $40 billion and between 2015 and 2035, the total direct medical stroke-related costs are projected to more than double [1].

1.4 – Stroke timeline

A stroke onset triggers a cascade of events that determines the degree and extent of cerebral ischemic damage, which have been well investigated in pre-clinical and clinical studies [24]. According to a common accepted framework reviewed by Dobkin and Carmichael, the development of stroke can be divided into three key phases: acute, sub-acute and chronic [25]. With the aim to moving forward with the progress on stroke recovery research, the first Stroke Recovery and Rehabilitation Roundtable (SRRR), set in Philadelphia in 2016, updated the stroke timeline subdividing it in hyper-acute, acute, early sub-acute, late sub-acute and chronic [26].

The hyper-acute phase occurs directly in the first 24 hours after the occluding event. In this phase, lack of glucose and oxygen-rich blood flow determines a reduction of ATP production [24] [26]. This causes metabolic deficit, oxidative stress, and excitotoxicity resulting in cell death and edema [24].

The acute phase, which occurs in the hours to days after stroke onset, is characterized by neuroinflammation by the release of cytokines, chemokines, cellular adhesion molecules (CAMs), and matrix metalloproteases (MMPs) from injured neurons and surrounding cells, such as microglia and astrocytes [24] [26]. Expression of MMPs and CAMs are key factors of the increase permeability of the blood brain barrier (BBB) and peripheral leukocytes invasion of the injured site, where they upregulate present inflammatory processes driven by activated microglia and astrocytes [24]. Chronic inflammation can lead to cerebral edema and neuronal death [24].

The sub-acute period, and in particular the early sub-acute phase within 1 month from stroke, is characterized by an increase of endogenous mechanisms of brain repair [25] [26]. Therefore, this critical window of time after stroke is recommended to target functional recovery in clinical trials [26].

1.5 – Current treatments available for stroke

Currently, only one FDA-approved drug, the tPA, is available for the treatment of ischemic stroke [2]. tPA is a thrombolytic agent and its mechanism of action is to break down the clot, allowing the recanalization of the occluded blood vessel [2]. The restoration of blood vessel flow is only effective if the brain tissue of the ischemic area is still viable [2]. Blood flow in the infarct "core" or "focal" area, supplied by the occluded vessel, falls to less than 20% of normal and will be irreversibly damaged during few minutes after stroke. Unfortunately the core becomes necrotic very quickly, whereas the periphery (referred to as the "penumbra" or "peri-infarct area"), which receives some perfusion by adjacent non-ischemic regions, is still salvageable within few hours [2]. Thrombolysis by tPA resulting in successful recanalization potentially saves this ischemic but still viable penumbra, but it has to be administered within 4.5 hours after stroke onset [2] [27]. Moreover, the use of thrombolytic and anti-coagulant agents increases the risk of hemorrhagic transformation [27]. On the other hand, available surgical interventions aim to reduce the acute neurological complications of stroke such as cerebral edema, intracranial pressure and the risk of clot formation [27]. Overall, these treatments are primarily preventive in scope.

Stem cell therapy, on the other hand, can target the sub-acute and chronic phases of ischemic stroke, thereby providing stroke patients a potential solution to the management of chronic symptoms associated with neural ischemia, such as long-term neuroinflammation and localized necrosis [28].

2

Mitochondria as central players in ischemic cell death

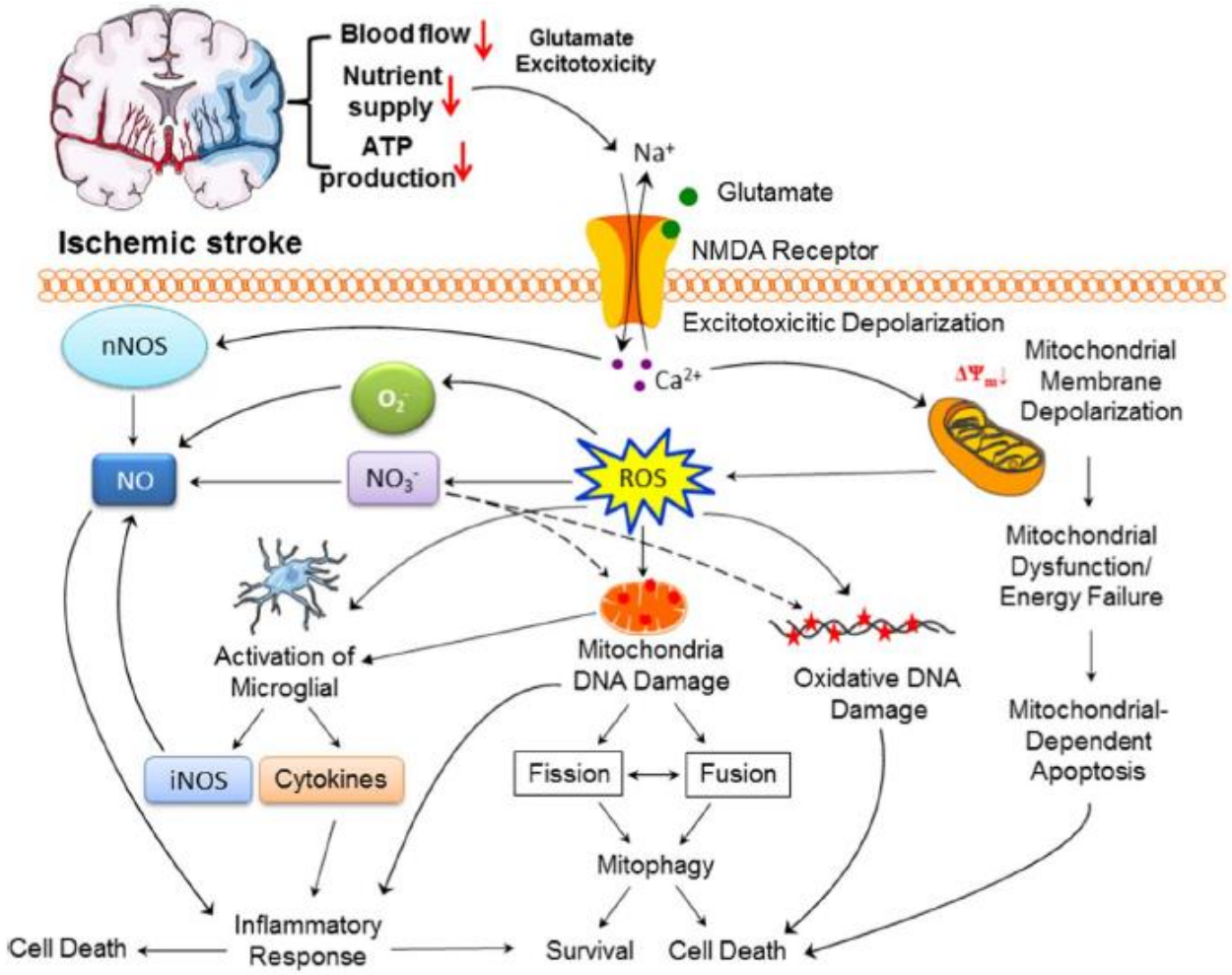

Figure 1. The central role of mitochondrial dysfunction in ischemic cascade (Yang et al. 2018)

Ischemic stroke is caused by a transient or permanent reduction in cerebral blood flow around the occluded artery. The pathophysiology of stroke is complex and involves a cascade of events responsible of the ischemic damage including energy failure, glutamate excitotoxicity, oxidative stress, inflammation, and programmed cell death [16].

A direct consequence of oxygen and glucose deprivation during stroke is the dysfunction of mitochondria that impairs oxidative metabolism and contributes to neuronal death and inflammation (Figure 1) [3]. In particular, mitochondrial impairment after stroke results in reduction of ATP production because mitochondria are responsible for the 92% of the total ATP

production of the cell [3] [4]. Despite the human brain representing only 2% of the body weight, it requires about 20% of the oxygen and 25% of the glucose consumed by the body, and depends almost exclusively on mitochondria for energy production [29].

The energy failure in the core region results in an irreversibly damage within a few minutes after the ischemic event [30]. In the infarct core, neuronal cells undergo necrosis, followed by glutamate release and excitotoxic cell damage to surrounding regions [30] [31]. The peri-infarct area is moderately hypoperfused with impaired mitochondrial functions but preserved structural integrity [30] [31]. As such, the penumbral region is salvageable whether the reperfusion promptly occurs in the early hours following the ischemia or the neuronal demand of oxygen and nutrients is satisfied by the collateral blood circulation [30] [31].

However, the reperfusion can lead to the increase of ROS and, consequently, oxidative stress that exacerbates the mitochondrial damage [3]. This extreme mitochondrial dysfunction triggers apoptotic cell death, as well as other programmed cellular degeneration such as autophagy, necroptosis, and pyroptosis [3]. To this end, mitochondrial dysfunction is a central event in the ischemic injury. A deeper analysis about the role of mitochondrial impairment in ischemic damage following stroke is discussed below.

2.1 – Energetic metabolism failure

The brain is the only organ that requires a continuous supply of glucose for its physiological functions [29] [32]. While all the other tissues, including the heart, can metabolize fatty acids, amino acids, and ketone bodies alternatively to glucose, the BBB prevents rapid influx of these substrates under most conditions. It has been estimated that about 60% to 70% of energy is used to maintain the sodium/potassium (Na^+/K^+) membrane potential required for the transmission of the nerve impulses [29] [32]. In addition, neurons expend much energy for the synthesis of neurotransmitters and their receptors to propagate nerve impulses [29] [32].

Most of ATP is required for ribonucleic acid (RNA) synthesis and amino acids activation for protein synthesis. Following oxygen and glucose deprivation, the cell attempts to store the remaining ATP by decreasing protein synthesis and by selective gene expression earliest in order [33].

The limited production of ATP by mitochondrial oxidative phosphorylation determines the necessity to produce energy via alternative pathways. Phosphocreatine can provide for short-term energy storage, allowing ATP to be regenerated from adenosine diphosphate (ADP) in a reaction catalyzed by creatine kinase [30]. Glycogen is almost exclusively localized in astrocytes in the adult brain [29]. Astrocyte glycogen storage can be converted in lactate that, in turn, can be used from the neighboring neurons during both physiological and pathological conditions [29] [32] [34]. However, due to its limited amount, brain glycogen is completely oxidized in only 5-7 min [33].

Even-though, some alternative substrates can compensate the limited supply of glucose, oxygen cannot be replaced. The absence of oxygen interrupts the mitochondrial oxidative phosphorylation and determines a drastic reduction of ATP production. The reduced availability of oxygen requires an increase of anaerobic glycolysis to compensate the cellular ATP demand [30]. In this context, some of the glucose that reaches the ischemic tissue is metabolized via glycolysis to lactate with an associated decrease in pH [30] [35]. Normal brain pH is about 7.2 [36]. During stroke, anaerobic metabolism of glucose to lactic acid can reduce this to approximately 6.6 in normoglycemic patients and below 6.0 in hyperglycemic ones [36]. While moderate levels of acidosis, pH about 6.7, tend to be neuroprotective in ischemia by inhibiting superoxide production by nicotinamide adenine dinucleotide phosphate hydrogen (NADPH) oxidase, severe reductions in pH exacerbate ischemic brain injury by inducing protein denaturation, activation of acid-sensing ion channels, and release of ferrous iron [36]. The damage of acidosis is associated with cell necrosis and edema [35].

2.2 – Glutamate excitotoxicity and calcium overload

Excitatory glutamatergic synapses represent about the 80% of the total cortical synapses suggesting that at least the 80% of the energy is expended for the glutamate-mediated neurotransmission [3]. Despite the glutamate can be synthesized by multiple metabolic pathways, about the 80% used as a transmitter is synthesized from glutamine by mitochondrial phosphate-activated glutaminase [37].

In glucose-oxygen deprivation condition, the ATP production decreases and consequently the Na^+/K^+-ATPase function fails [38]. The loss of Na^+/K^+-ATPase function generates an intense loss of ionic gradients resulting in the membrane depolarization and thus activation of voltage-gated

calcium channels and release of glutamate in the extracellular space [38] [39] [40]. In physiological conditions, the extracellular glutamate is transported into astrocytes and converted to glutamine by glutamine synthetase [41]. Glutamate transporters need external Na^+, and therefore are strongly linked to the activity of Na^+/K^+ ATPases, which maintain the Na+ concentration gradient [41]. On the other hand, glutamine synthetase requires ATP for its function [41]. The low level of ATP also inhibits the uptake of extracellular glutamate form astrocytes exacerbating the glutamate excitotoxicity [38]. The extracellular pool of glutamate overstimulates the N-Methyl-D-aspartate (NMDA), α-amino-3-hydroxy-5-methyl-4-isoxazolepropionic acid (AMPA) and kainate glutamate receptors resulting in influx of Na^+ and calcium (Ca^{2+}) ions [40]. The elevated level of intracellular Ca^{2+} results in detrimental consequences. The Na^+ and Ca^{2+} cytoplasmic increase is accompanied by influx of Cl^- and water with the consequent cell swelling [40].

In addition to metabolic functions, mitochondria act like sensors of Ca^{2+} intracellular levels [38] [42]. During an excitotoxic insult, mitochondria are implicated in Ca^{2+} sequestration [38]. However, this elevated Ca^{2+} influx causes mitochondrial membrane depolarization [38] [42]. The loss of mitochondrial membrane potential induced by Ca^{2+} induces the opening of the mitochondrial permeability transition pore (PTP) with a consequent release of pro-apoptotic molecules and thus triggering cell death [38]. Moreover, the calcium accumulation is amplified in a positive feedback loop by the activation of Ca^{2+}-dependent calpains that inactivate the Na^+/Ca^{2+} exchanger (NCX3) increasing the intracellular calcium influx [43]. Besides NCX3, the Ca^{2+} can modulate several proteins and enzymes including the neuronal nitric oxide synthase (nNOS) [44]. The accumulation of high concentrations of nitric oxide (NO) leads to irreversible cellular damages and impairment of mitochondrial respiration, that inevitably triggers neuronal death [44].

2.3 – Oxidative stress and apoptotic cell death

Mitochondrial dysfunction induced by the prolonged accumulation of Ca^{2+} is considered a major source of free radicals that are produced after reperfusion [38].

Mitochondria are responsible for about the 90% of the total energy required from a cell by oxidative phosphorylation (OXPHOS) at the electron transport chain (ETC) [45]. ETC consists of a series of complex (CI-CV) in the inner mitochondrial membrane (IM) in which electrons are transferred from flavin adenine dinucleotide ($FADH_2$) and nicotinamide adenine dinucleotide

(NADH) to series of electron acceptors and donors of which molecular oxygen (O_2) is the last acceptor that is reduced to water [45]. The proton motive force generated during the ETC across the IM is used to produce ATP at complex V, otherwise known as ATPase synthase.

Physiologically, about 2% of the total electrons are leaked from the ETC, mainly from complexes I and III [45]. They can be transferred non-enzymatically to O_2 resulting in the formation of the superoxide anion free radical ($O_2^{\bullet -}$) [45]. $O_2^{\bullet -}$ is the precursor of the most of ROS including hydrogen peroxide (H_2O_2) and hydroxyl radical ($^{\bullet}OH$) [45]. All the ROS are able to directly induce damages to the cellular macromolecules such as lipids, proteins and nucleic acids resulting in detrimental consequences for the cell homeostasis [45]. Indeed, ROS are considered key players in the process of aging, as well as in the genesis and progression of cancer, atherosclerosis and several disorders [45].

Mitochondria have evolved towards regulating sophisticated hierarchical quality control (QC) mechanisms for their own and for cellular defense against ROS [45]. These QC mechanisms are gradually activated depending on the severity of the ROS damage, and include antioxidant systems, chaperones, proteases, fusion and fission of mitochondria, mitophagy and, in the worst condition, apoptotic cell death [45].

The antioxidant system is involved in scavenging of free radicals and prevention of cellular damage [38] [46]. The antioxidant system includes enzymatic factors such as superoxide dismutases (MnSOD, SOD2), catalases, glutathione reductase/glutathione peroxidases (GR/GPX), thioredoxin/thioredoxin reductase (Trx/TrxR), peroxiredoxins (Prx), glutaredoxins (Grx) and non-enzymatic molecules such as ascorbic acid, pyruvate, α-tocopherol and glutathione [38] [46]. In stroke pathology, the aberrant ROS production overwhelms the antioxidant defense system of the brain causing oxidative stress [38] [46].

ROS production takes place in three phases [47] [48]. The first generation of ROS is during the oxygen and glucose deprivation involving the mitochondrial depolarization and dysfunction [47] [48]. In particular, the limited oxygen availability interrupts the mitochondrial respiration at complex IV inducing the accumulation of reduced intermediates of ETC that promote electron leakage and subsequently production of ROS [47] [48]. The second phase involves an increase of ROS due to activation of xanthine oxidase (XO) [47] [48]. The reduction of ATP production determines accumulation of ADP and adenosine monophosphate (AMP) [47] [48]. ADP and AMP

can be degraded into hypoxanthine (HX) via purine catabolism [47] [48]. XO reacts with HX forming superoxide as a byproduct, which damages mitochondria, increasing the bioenergetic dysfunction and electron leak with a consequent amplification of ROS formation in a feedback loop [48]. The restoration of the blood flow paradoxically constitutes a crucial part of the stroke injury [38]. The rapid and sudden increase of O_2 level promotes the mitochondrial respiration that sustains the neuronal survival [38]. On the other hand, O_2 becomes a substrate of several enzymes leading to the third phase of ROS generation [38].

The ROS generation phase is also linked to activation of NADPH oxidase (NOX) [38]. NOX family consists of transmembrane proteins involved in the transport of electrons across the membranes [49]. O_2 is used as electron acceptor generating $O_2^{\bullet -}$ [49]. In addition, NOX activation is closely associated with mitochondrial dysfunction [50]. Impaired mitochondria release $O_2^{\bullet -}$ and H_2O_2 to the cytoplasm by redox-sensitive mitochondrial PTP, inner membrane anion channel (IMAC), aquaporins or by diffusion for the increase permeability [50]. These reactive species, along with released Ca^{2+}, determine the activation of redox-sensitive protein kinases (protein kinase C, PKC) and tyrosine kinases (cellular Src kinase, cSrc) that, in turn, activate NOX resulting in the amplification of the cellular oxidative stress [50]. Moreover, NOX4 has been found in intracellular membranes including endoplasmic reticulum, nucleus and also in the inner membrane of mitochondria, which promotes a closer crosstalk between NOX and mitochondria in amplifying oxidative stress and inducing apoptosis [51] [52]. NOX4 has been implicated as the most relevant source of ROS in stroke [47]. In addition, a Ca^{2+} - dependent activation of NOX has been shown to be linked to glutamate excitotoxicity [47].

Other enzymes affected by Ca^{2+} include cyclooxygenase (COX) and phospholipase A2 (PLA2), which produce ROS and cause lipid peroxidation and membrane damage during stroke [38]. PLA2 activity is linked to the products of COX. In addition, mitochondrial PLA2 (mt-PLA2) has been suggested to be activated by ROS [53]. In physiological conditions, mt-PLA2 is involved in balancing mitochondrial biogenesis on the side of biodegradation [53]. mt-PLA2 can modulate the cytochrome c release from mitochondria and influence the permeability transition inducing apoptosis [38] [53].

$O_2^{\bullet -}$ can damage ETC complexes either directly or through interactions with NO, generating reactive nitrogen species (RNS) that lead to deleterious effects on the mitochondrion [28]. Beyond the canonical NOS (nNOS, endothelial NOS, eNOS, and inducible NOS, iNOS), recently a

mitochondrial NOS (mtNOS) has been identified [54]. mtNOS is encoded by nuclear DNA and probably translocates to mitochondria. Contributing to RNS production, mtNOS may correlate with apoptosis after stroke and it is considered a key factor of reperfusion injury [54]. Nitrosative stress induces protein misfolding and aggregation that can contribute to mitochondrial fragmentation [3]. The impairment of the mitochondrial fission-fusion dynamics leads to neurotoxicity [3].

Mitochondria are extremely dynamic organelles able to modify their shape, size and localization through highly regulated mechanisms of fission, fusion and transport along microtubules [45]. The primary function of this dynamism is the distribution of mitochondria into daughter cells during cell division [55] [56]. The role of mitochondrial fusion is the exchange of metabolites, membranes and mitochondrial DNA (mtDNA) between two adjacent mitochondria [55]. The mitochondrial fusion is considered a QC mechanism that allows the salvage of a damaged mitochondrion through the fusion with a healthy mitochondrion [56]. In neurons, mitochondrial fission is crucial for the transport of these organelles along axons and dendrites [57]. Synapses require mitochondria for the supply of ATP and the regulation of Ca^{2+} concentration for neurotransmission [57]. The imbalance of fusion/fission dynamics can compromise the mitochondrial function and transport resulting in impaired neurotransmission and cell death [57]. Indeed, mitochondrial fission has a fundamental role in the segregation of dysfunctional mitochondria ensuring their removal by mitophagy [55]. While physiological or mild levels of mitophagy may favor the neuronal survival by avoiding the release of apoptotic molecules from mitochondria, high levels could be fatal for the cell and may exacerbate the ischemic injury [55]. Mitochondrial oxidative stress may contribute to mitochondrial dysfunction and cell death [55]. In this regard, it has been shown that oxidative stress up-regulates Drp1 expression, a protein involved in mitochondrial fission, resulting in mitochondrial fragmentation and cell death [55]. Mitochondrial fission has been correlated to ischemic cell death. Studies have shown that the prevention of mitochondrial fission may avoid the apoptotic cell death by reducing cytochrome c release [55].

Mitochondrial QC ensures the survival of the cell on three levels. At protein level, chaperones and proteases allow the restoration of the correct protein folding or degradation of mitochondrial damaged proteins [58]. The upper phase of QC is the organelle level involving fusion, fission and mitophagy ensuring the restoration of impaired mitochondria or removal of mitochondria irreversible damaged [58]. The third phase is the cellular level characterized by

extremely damaged mitochondria and the release pro-apoptotic molecules in the cytoplasm, which can induce apoptotic cell death that can affect the neighboring cells [58]. In addition, autophagy contributes to cell death after stroke [59]. These downstream cell death events may be further exacerbated by progressive mitochondrial dysfunction during chronic stroke in the absence of any therapeutic intervention.

2.4 – Mitochondria and inflammation in stroke

Inflammation plays a fundamental role in all the phases of ischemic cascade involving both innate and adaptive immune-cell responses leading to neuronal cell death [3].

Recently it has been reported that mitochondria have a central role in inflammation in stroke [3]. According to endosymbiotic hypothesis of mitochondrial origin, mitochondria retain features of their bacterial ancestry that may trigger inflammatory response from the cell host [3] [60]. Mitochondrial ROS can enhance host defense and inflammation [3]. Oxidative stress can induce mtDNA fragmentation that can be released in cytosol where it can activate the toll-like receptor 9 (TLR9) [3]. Activated TLR9 triggers the NF-kB signaling pathway including the expression of pro-inflammatory proteins, such as tumor necrosis factor-α (TNF- α) and Interleukin (IL)-6 [3]. In addition, the mtDNA can activate the nucleotide-binding domain (NOD)-like receptor protein 3 (NLRP3) inflammasome on the outer mitochondrial membrane causing the cleavage of pro-IL-1β and pro-IL-18 by caspase-1, thereafter resulting in pyroptotic cell death [3] [60]. Mitochondrial dysfunction, induced by increase of ROS, can trigger inflammation and cell death [3].

3

Regenerative medicine and stem cells

According to the National Institutes of Health (NIH), “Regenerative medicine is the process of creating living, functional tissues to repair or replace tissue or organ function lost due to age, disease, damage, or congenital defects. This field holds the promise to regenerate damaged tissues and organs in the body by stimulating previously irreparable organs to heal themselves. Regenerative medicine also empowers scientists to grow tissues and organs in the laboratory and safely implant them when the body cannot heal itself” [61].

The idea of wound repair and organ regeneration has captured the human imagination since the time of the ancient Greeks. Examples are the many-headed Hydra myth, whose two new heads grew up for every one that Heracles cut off, and the myth of liver of Prometheus, devoured by a ravenous eagle each night, but regenerated every morning [62]. Aristotle (384–322 BC) noted that the tails of lizards and snakes, as well as the eyes of swallow-chicks, could regenerate which he reported his observations in the books “Generation of animals” and “The history of animals” [63].

While much interest in regenerative medicine disappeared in the medieval era, the Enlightenment period (late 17th century to the end of 18th century) was the first significant milestone in the history of regenerative medicine. In 1744, Abraham Trembley investigated hydra’s robust regenerative capability in that each half of the hydra regenerated into a complete new hydra, providing the first glimpse into the cellular regenerative potential [64].

The first stem cell research was Harrison’s experiment on nerve fiber development in 1907, more specifically in 1910 [65] [66]. Interested in knowing how the nerve fibers grew, he cultivated a sample of neural progenitor cells into a droplet of frog lymph [65] [66]. Harrison observed that these progenitor cells differentiated in fully formed nerve cells *in vitro*, producing the first in vitro cultures of stem cells, in particular of neural stem cells [65] [66] [67].

In modern-day medicine, research work involving stem cells and organ regeneration started in the 1950s with the first attempts at bone marrow transplantation in animal models.

These pioneering studies paved the way for human bone marrow transplantation, a therapy now widely used for the treatment of various blood disorders [68] [69]. This new therapeutic strategy revealed the existence of stem cells that regenerated adult tissues. Presently, regenerative medicine is a major focus of research not only to find therapies but also to understand basic biology and the pathogenesis of disease. Recent advances in stem cell isolation and cell growth and development have helped scientists to identify and culture specific cell types for regeneration of tissues in various disorders such as Parkinson's (PD), Alzheimer's (AD), or diseases of the heart, muscles, lung, liver, and other organs [70].

Stem cells are clonogenic cells capable of both self-renewal and multilineage differentiation [71]. The first genetic evidence that stem cells exist came from the studies of Till, McCulloch, Wu, Becker and Siminovitch focusing on blood-forming (hematopoietic) stem and progenitor cells [72] [73] [74].

Stem cells are defined simply as cells respecting three basic criteria: self-renewal, clonality, and potency [70]. First, stem cells renew themselves throughout life, in that the cells divide to produce identical daughter cells and thereby maintain the stem cell population [70]. Second, stem cells have the capacity to undergo differentiation to become specialized progeny cells [70]. When stem cells differentiate, they may divide asymmetrically to yield an identical cell, as well as a daughter cell that acquires properties of a particular cell type, for example, specific morphology, phenotype, and physiological properties that categorize the cell as belonging to a particular tissue [70]. The third property of stem cells is that they may renew the tissues that they populate [70]. Specific tissue compartments may contain cells that satisfy the definition of "stem cells", and the rate at which stem cells contribute to replacing cells varies throughout the body [70].

3.1 – Stem cells source and classification

Stem cells can be classified into 5 groups according to their differentiation potenial: totipotent or omnipotent, pluripotent, multipotent, oligopotent, and unipotent [75]. Based on their origin, stem cells can be grouped into five categories: embryonic, fetal, perinatal and adult (resident or tissue-specific). Embryonic and iPSCs are pluripotent, and fetal and perinatal are, in general, multipotent, whereas adult stem cells are usually oligo- or unipotent Figure 2) [11].

Different stem cell types can potentially be used for clinical studies, including ESCs, isolated from the inner cell mass of blastocysts; iPSCs which are adult somatic cells reprogrammed to pluripotency; neural stem cells (NSCs), ESCs- or iPSCs-derived or isolated from fetal or adult brains; MSCs, stem cells isolated from fetal, perinatal or adult tissues.

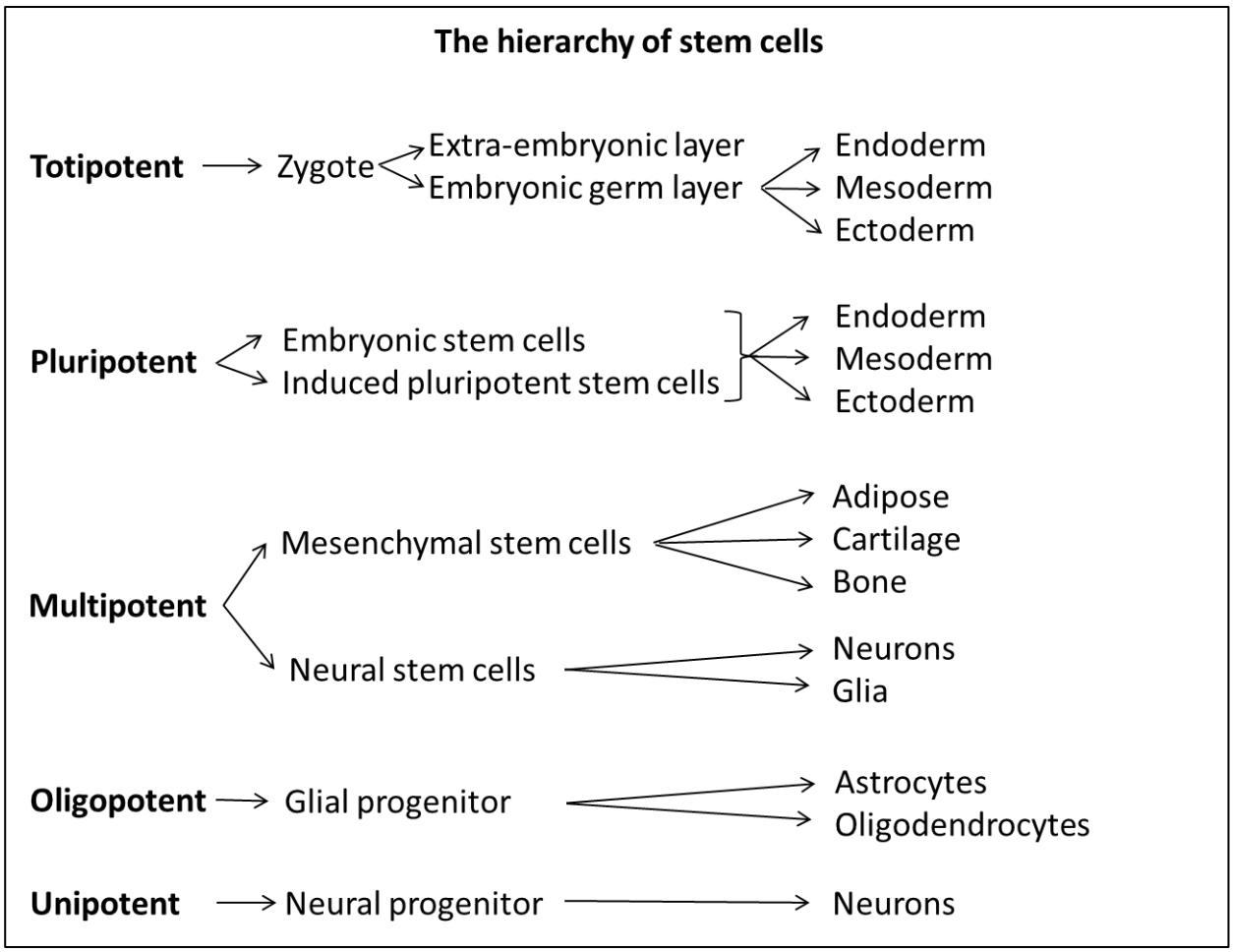

Figure 2. The hierarchy of the stem cells.

3.1.1 – Embryonic stem cells

ESCs are pluripotent stem cells derived from the inner cell mass of blastocyst stage embryos grown in culture within 5 days of fertilization of the oocyte [76] [77]. Human ESCs (hESCs), theoretically, can differentiate into almost all tissues of the human body, but they cannot form the extraembryonic tissues necessary for complete development, such as the placenta and membranes. ESCs are therefore distinct from the totipotent fertilized oocyte and blastomere cells, which are harvested from the first divisions [78].

However, hESCs have limitation for use. The principal limitation is an ethical problem because hESCs are isolated from the embryoblast or inner cell mass destroying the fertilized human embryo [78]. These ethical issues are debated around the world and hESCs-based research is regulated differently from one country to another. HESCs for research purposes are allowed in many European countries [79]. In United Kingdom, new hESC lines can be derived from supernumerary in vitro fertilization (IVF)-derived embryos, as well as after therapeutic cloning (or somatic cell nuclear transfer) [80]. On the contrary, in other countries, including Italy, all the hESC-based research is prohibited [79]. The Italian law on medically assisted fertilization (Law 40/2004) prohibits the use of human embryos for research purposes, as well as the production of embryos through the somatic cell nuclear transfer technique [81]. However, Italian scientists can import hESC lines from abroad but its use is highly limited by lack of oversight regulation and national funding research on hESCs [81]. In United States, several states have complete bans in hESC lines production and limits on usage of lines created prior to August 9, 2001 [82]. On the other hand, other states, including California, Florida and Texas, support ESC research [82].

Beside ethical concerns, hESC-based therapy is highly controversial for safety issues [83]. The pluripotency of hESCs could make them the best choice of stem cells for tissue repair at wide range allowing to generate cell types from all the three germ layers [83]. However, this same plasticity makes hESCs highly tumorigenic. hESCs are immortal because they express high levels of telomerase, which ensure that the telomere ends of the chromosomes are preserved at each cell division and the cells do not become senescent [83]. Studies have shown that teratoma formation is between 33-100% in hESC-transplanted immunodeficient mice [84] [85].

3.1.2 – Induced pluripotent stem cells

iPSCs are somatic cells reprogrammed to the pluripotent state [86]. In 2006, Takahashi and Yamanaka successfully reprogrammed mouse somatic cells (such as fibroblasts) by using a cocktail of four transcription factors (OCT4, SOX2, KLF4 and MYC) that were named “Yamanaka factors” [87]. One year later, two research groups generated iPSCs from human fibroblasts [88] [89]. iPSCs are very similar to hESCs in terms of karyotype, phenotype, telomerase activity and differentiation capacity [86].

IPSC represent an important discovery in regenerative medicine showing the possibility to generate cells similar to hESCs without destruction of embryos and, therefore, avoid ethical

concerns [83] [86]. Moreover, since iPSCs are generated from somatic cells from the same patient who will receive the transplant, there is no risk of immune rejection after their transplantation [83] [86]. However, similar to the transplant concern with hESCs, teratoma formation is the main safety issue on iPSCs clinical use [83] [86].

3.1.3 – Fetal stem cells

Recent interest in human fetal stem cells (hFSCs) derived from aborted fetal tissues [90] because of the potential to harvest different stem cells. Fetal-derived hematopoietic stem cells (HSCs), fetal MSCs and fetal NSCs are the most investigated FSCs [90]. FSCs therapeutic potential is higher compared to the adult stem cells [90]. In addition, the pre-immune status of early FSCs might reduce the risk of reject in transplantation [90].

Fetal neural tissue is one of the main sources of NSCs for replacement therapy in the injured nervous system, with fetal NSCs transplantation has shown effective in several brain-injury models [90]. Clinical studies have also been performed with human fetal neural tissue transplantation in neurodegenerative disorders resulting in symptomatic improvement [90] [91]. However, deleterious side effects were associated with the fetal grafts, and logistical issues accompanied such approach, specifically for the need to harvest up to six fetuses to treat one patient [91].

Notably the hFSCs overcome the ethical issues associated with hESCs, because aborted fetuses are discarded [92]. However, use of fetal tissue is not totally exempted from ethically controversies because it is associated with voluntary interruption of pregnancy which many people object to [92] [93]. Accordingly, the documented side effects, limited supply of fetal tissue, and ethical concerns have led to a search for alternative sources of stem cells for clinical uses.

3.1.4 – Neural stem cells

The discovery that adult neurogenesis occurs throughout life in animals and then in humans led to rapid recognition of the therapeutic potential of NSCs [94] [95].

NSCs are undifferentiated cells with both self-renewal and capacity to differentiate in neurons, astrocytes, and oligodendrocytes [94] [95]. Adult neurogenesis is restricted, under physiological conditions, to two specific ‘neurogenic’ brain regions: the subgranular zone (SGZ) in

the dentate gyrus (DG) of the hippocampus and the subventricular zone (SVZ) of the lateral ventricles [94] [95]. The new neurons generated in the SVZ migrate through the rostral migratory stream (RMS) to the olfactory bulb where they become interneurons [94] [95]. However, it was shown that neurogenesis also occurs in supposed “non-neurogenic” regions such as the striatum, which is adjacent to the lateral ventricle wall and the subcortical white matter [96] [97].

In contrast to fetal NSCs, studies of adult NSCs are limited because the only source for NSCs cultures from adult brain are small pieces of tissue biopsy from patients undergoing epilepsy surgery or traumatic temporal lobe decompression [97]. Despite this logistical limitation, the successful isolation and expansion of viable adult NSCs from the rodent and human brain within a short postmortem interval suggests that postmortem NSCs could potentially become an acceptable alternative stem cell source [98]. However, very few studies have used biopsy sampling from post-mortem patients because of delicate ethical, social, and legal implications, as well as various still-unresolved questions about cell viability of stem cells harvested from aged and diseased tissues due to global ischemia after death [98] [99] [100] [101].

Olfactory bulb also contains NSCs and this finding opens up the possibility to isolate NSCs from non-biopsied source, which is obviously preferable to the highly risky surgical collection of intracerebellar NSCs [102]. For instance, the use of olfactory bulb-derived NSCs could be advantageous for treating diabetes with an autologous transplantation strategy before the disease progresses [103]. This advanced collection of stem cells from the olfactory bulb could become an attractive source of NSCs for autotransplantation for neurodegenerative diseases.

Recently, it was shown that ultrasonic aspirate samples, discarded as biological waste following epileptic surgery, represent another valuable source of neural progenitors cells (NPCs) and they could be similarly used for autologous transplantation [104].

4

Mesenchymal stem cells

The MSCs are considered the most important cell type for regenerative medicine and are the most widely studied in preclinical and clinical trials [105] [106] [12]. Their advantages for clinical application include easy isolation and high *in vitro* yield with elevated genomic stability, high plasticity and differentiation potential as well as few ethical implications [12] [105] [106]. In addition, great interest in these cells is due to their ability to modulate inflammation and to promote cell growth and differentiation [12] [105] [106]. Compared to ESCs and iPSCs, MSCs do not form teratomas after transplantation, ensuring safety to the host [12] [105] [106]. MSC is the designation commonly applied to the plastic-adherent cells isolated from different tissues: fetal [107] [108] [109]; adult (bone marrow [110], adipose tissue [111], dental pulp [112], endometrium [113], menstrual blood [114], peripheral blood [115], salivary gland [116], skin and foreskin [117] [118], synovial fluid [119] muscle [120], corneal stroma [121], heart [122], lung [123]); and perinatal (placenta, chorionic and amniotic membranes [124], amniotic fluid [125], umbilical cord [126] and umbilical cord blood [127]).

The isolation of multi-potent stromal cells from the bone marrow, by Friedenstein in the 1970, led to keen interest in the field of MSCs biology. This was the first report to show that the mesenchyme of a tissue could harbor mesenchymal progenitor/stem cell properties whose potency can be validated in vitro and in vivo [128]. The term “MSC” was popularized in the early 1990s by Caplan, considered the father of MSCs [129] [130]. The Mesenchymal and Tissue Stem Cell Committee of the International Society for Cellular Therapy proposed three criteria to define MSCs: adherence to plastic, specific surface antigen (Ag) expression and multipotent differentiation potential [131]. First, MSCs must be plastic-adherent when maintained in standard culture conditions using tissue culture flasks [131]. Second, ≥95% of the MSCs population must express CD105, CD73 and CD90 [131]. Moreover, these cells must lack expression (5/2% positive) of CD45, CD34, CD14 or CD11b, CD79a or CD19 and HLA (human leukocyte antigen) class II. Third, the cells must be able to differentiate to osteoblasts, adipocytes and chondroblasts under standard in vitro differentiating conditions [131].

MSCs point to a wide range of immunological functions [105]. In particular, it has been demonstrated that MSCs have the capacity to suppress T cell activation and proliferation [105]. Moreover, MSCs modulate the innate function of monocytes, macrophages, natural killer (NK) cells, and dendritic cells (DCs) [105] [132]. Notably, human MSCs are hypoimmunogenic because they express low levels of MHC (major histocompatibility complex) class I and lack expression of MHC class II, indicating that MSCs may potentially avoid immune-rejection in allotransplantation [133]. In addition, MSCs do not express the co-stimulatory molecules CD40, CD40L, CD80 or CD86 required for effector T cell induction, and they secrete immunomodulatory and anti-inflammatory molecules, such as IL-10, indoleamine 2, 3-dioxygenase (IDO), prostaglandin E2 (PGE2) and hepatocyte growth factor (HGF) [133]. Therefore, this immunomodulatory function has promoted use of MSCs in transplantation. However, recent studies have debated the immune-privileged status of MSCs, highlighting the necessity of comparisons between autogeneic and allogeneic MSCs [134].

Bone marrow-derived MSCs (BM-MSCs) are considered the gold standard in MSC biology. However, although BM-MSCs are the most studied and well-documented, they have limitations such as an invasive isolation procedure and a high risk of bacterial and viral contamination [135]. In addition, donor age variations among samples leads to differences in the initial yield of isolation as well as in proliferative and differentiation capabilities [135] [136]. These factors can affect reproducibility between different bone marrow isolates [136]. Moreover, BM-MSCs have limitation in terms of cell numbers, requiring the need for expansion in vitro, which may trigger the risk of loss of stemness properties and induction of artifactual chromosomal changes [136].

The adipose tissue has recently emerged as an alternative source of MSCs. Compared to the bone marrow, the adipose tissue is a rich source of MSCs with up to 10-fold higher yield of MSCs [105] [111]. More recent publications demonstrated that adipose tissue-derived MSCs (AD-MSCs) might also have higher immunomodulatory and immunosuppressive potential in vitro as compared to BM-MSCs [111]. Despite its plentiful nature, an invasive procedure is still required to collect the adipose tissue [105] [111].

Most recently, MSCs have been isolated from extra-embryonic tissues which offer more advantages than embryonic, fetal and adult stem cell sources [137]. Perinatal tissues as a source of stem cells are appealing because they are routinely discarded at delivery and could be stored and used for useful clinical purposes [137]. The extracorporeal nature of these tissues facilitates

isolation, eliminates risks for patients connected with adult stem cell isolation and circumvents ethical concern [137]. Most importantly, the volume of extra-embryonic tissues is comparably greater than all the other stem cell sources that, together with an ease of *in vitro* expansion, increases the number of stem cells that can be isolated [137]. MSCs have been isolated from placenta, chorionic and amniotic membranes [124], amniotic fluid [125], umbilical cord [126] and umbilical cord blood [127]. Perinatal MSCs are used in both pre-clinical and clinical studies [137] [138] [139] [140] [141]. The ability to harvest viable stem cells from adipose tissues, or for that matter any tissue source, should entail a rigorous set of studies to reveal the optimal safety and efficacy of these cells for transplantation therapy in a disease-tailored condition.

5

Umbilical cord: a pivotal source of MSCs

The umbilical cord (UC) is the link between mother and fetus during pregnancy [15]. UC connects the placenta to the uterus and allows the flux of nutrients, oxygen and waste products to and from the fetus [15]. At term, the human UC is about 40–60 cm long, with a girth of 1–2 cm [15]. UC is anatomically a simpler tissue than bone marrow, adipose tissue or placenta and this characteristic, together with other properties which will be described here, makes it a pivotal source of MSCs.

5.1 – Structure of the human umbilical cord

The UC consists of two arteries and one vein surrounded by a connective tissue called "Wharton's jelly" (WJ) and outer single layer of amniotic epithelium [15]. The umbilical arteries carry deoxygenated blood from the fetus to the placenta, while along the umbilical vein there is a flux of oxygenated and nutrient-rich blood from the placenta to the fetus [15]. The umbilical vessels comprise only a tunica intima and media, but lack tunica adventitia unlike other vessels of similar diameter in the human [15]. WJ is considered to play the adventitial roles of vascular support and contractile function [15].

WJ is first described by Thomas Wharton in 1656 [142] and consists of an amorphous substance composed by glycosaminoglycans (GAGs) and collagen. Hyaluronic acid is almost 70% of the GAGs, whereas the sulphated GAGs (such as keratansulphate, heparan sulphate, chondroitin-4-sulphate, chondroitin-6-sulphate and dermatan sulphate) are less abundant [143]. Different types of collagens are observed in umbilical cord stroma, such as collagen type I, III, IV and VI [144]. Two different types of cells are dispersed in WJ: myofibroblasts and fibroblast-like MSCs (also known as WJ-MSCs) [15] [145]. These cells are responsible for the deposition of the extracellular matrix (ECM), which is the main component of WJ. The main role of WJ is to prevent the compression, torsion and bending of the enclosed vessels during movement of the fetus in the womb [15]. Notably, WJ contains no other blood or lymph vessels and is not innervated and it is

thought that it serves as a surrogate lymphatic system [15]. Therefore, the role of the WJ is not simply mechanical, but its functions seem to be more complex. Interestingly, the lack of vascularization within WJ means that the umbilical cord environment is relatively hypoxic and it has given rise to the hypothesis that the stromal cells are adapted to limited nutrient and oxygen supply [146]. This ability of WJ-MSCs could allow them to survive in ischemic environments after transplantation allowing them to confer beneficial effects to the injured tissue or organ, such as the stroke brain. These potential therapeutic properties of WJ-MSCs require further investigations [146].

5.2 – Wharton's jelly MSCs are all the same?

WJ as effective source of MSCs was examined in the '90s with the reports by McElreavey et al. [147] who first isolated fibroblast-like cells from human UC, then by Takechi et al. [148] who phenotypically characterized these cells. Even though the WJ-MSCs have been studied since nearly 30 years, there is little consensus on both the cellular population of WJ and the anatomical structure of this tissue. This conundrum is mainly due to the lack of a standard cellular isolation method.

Notwithstanding cell isolation standardization shortcoming, laboratory evidence supports the hypothesis that WJ consists of three different anatomical regions - perivascular, intermediate and cord lining or subamniotic - with distinctive characteristics and reasonably specific cellular populations (Figure 3) [15]. WJ-MSCs are not distributed uniformly within the UC stroma, but they are more numerous in the perivascular area and more spread out moving towards the amniotic epithelium [15]. The distribution of the MSCs within the UC reflects also the structure of WJ: densest in the perivascular and subamniotic area, and thinnest with clefts in the intermediate stroma [144].

Moreover, a differential distribution pattern of the various ECM proteins has been shown in different zones of umbilical cord. In particular, collagen type IV is expressed abundantly in the basement membrane of the amniotic epithelium and in the perivascular area, but weakly in the intermediate WJ [144]. Collagen type III and type VI are also present in all the UC stroma, but with an increase positivity moving from the vessels towards the amniotic epithelium [144]. In addition, type I collagen, but also type III, is the most abundant form in the intervascular stroma [143].

Instead, collagen type VII is restricted to the epithelial basement membrane [144]. Interestingly, UC stroma composed of collagen X, laminin and fibronectin plays important roles in peripheral nerve regeneration [149]. Moreover, recently we reported that the fibronectin network created by the WJ-MSCs, together with other extracellular proteins identified by mass spectrometry analysis, exerts key function in the ex vivo expansion of hematopoietic stem/ progenitors cells [150]. In addition to a structural and mechanical role, the ECM proteins of UC stroma create a complex network serving as a reservoir of growth factors, proteases and signaling proteins involved in cell proliferation, adhesion, migration, and differentiation activities [150].

The non-perivascular cells within the umbilical cord are thought to be derived from a perivascular lineage and that they simply migrated away from the vessels to the amniotic epithelium [151]. This hypothesis is supported also by the process of fibrotic repair and wound healing in which endothelial cells migrate from the vessels to the injured site in promoting its regeneration [152]. Another hypothesis is that the UC cells correspond to various stages of fibroblast committed towards myofibroblast differentiation [144]. In addition, some studies showed that the MSCs within the umbilical cord display different characteristics depending on the region from which they are extracted [144] [153]. Notably, UC presents two different embryonic origins: arising from the connection between stalk and allantoic mesenchyme, and from the enveloping amniotic membrane [154].

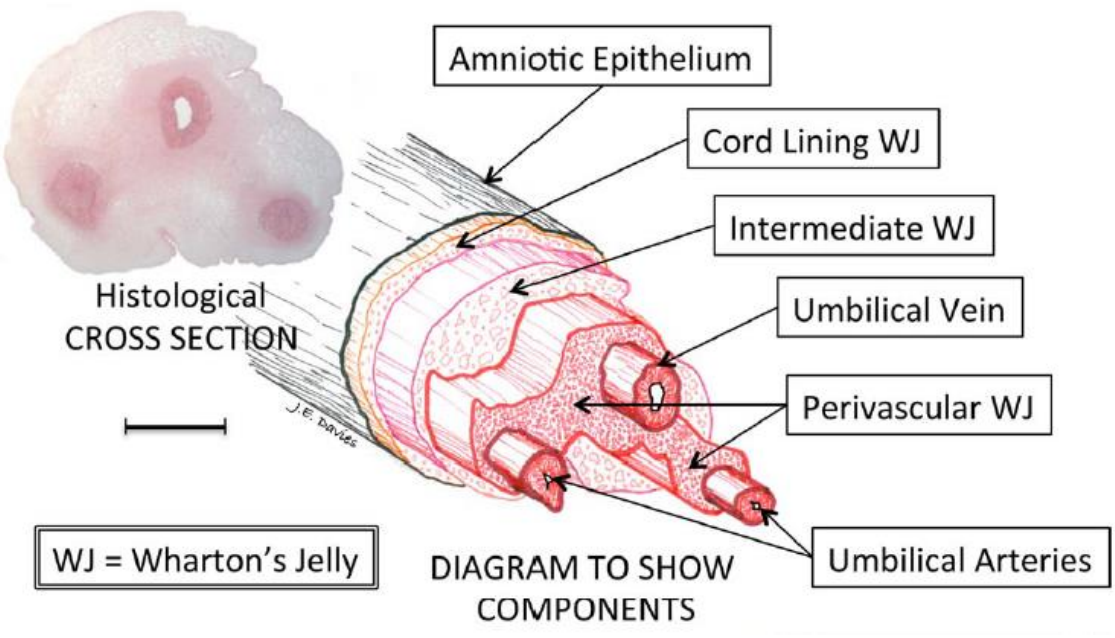

Figure 3. Structure of the umbilical cord (Davies et al. 2017).

However, whether the phenotypes of MSCs within the WJ are equivalent or different is still not clear due to different reasons:

1) Even though all the UC cells show the typical characteristics of the MSCs in surface phenotype, plastic adherence and multipotency, there is still no specific marker or set of markers allowing the distinction between different populations [153].

2) The expression pattern of the MSCs derived from the various compartments of the UC remains not well-defined with contradictory results in literature. The perivascular stem cells are positive for CD14, CD106 and CD117 in some studies, but negative in others [155]. Similarly, it was reported that the subamnion MSCs are positive for CD34, CD45 and SOX2 in one study, but negative in another [155]. Similarly, the MSCs isolated from cultured whole UC pieces (MC) were shown positive for CD106 and CD117 in one report and negative in another [155]. These discrepant results are obtained also for the MSCs derived from the intermediate stroma based on several markers such as CD10, CD45, CD54, CD105, CD106 and CD117 [155]. Discrepancies are also present in the phenotype profile of the MSCs derived from the whole umbilical cord stroma [155]. Even more enigmatic is that proteins such as CD113 and CD235a, exhibited by MSCs harvested from the whole UC stroma, are not detected in MSCs derived from any of the single compartments [155].

3) The MSCs isolation method is not standardized across the studies. Two different methods exist (enzymatic and explant) and various degrees of heterogeneity are employed for harvesting the cells from the UC. Different methods have been employed for the isolation of the MSCs from the various compartments of the UC. Briefly, these methods include: (a) the culture of entire UC pieces containing a mixed population of MSCs [150]; (b) separation of the WJ from the cord lining with a razor blade or scraping off it with a scalpel [156] [157]; (c) squeezing out the enzymatically digested WJ with forceps without removal of vessels and cord lining [158]; (d) separation of the WJ from the cord lining after removal of the blood vessels [156]; (e) after removal of the vessels, enzymatic digestion of the WJ without separating it from the cord lining [159]; (f) the isolation of perivascular MSCs shed out from the blood vessels and culturing them with or without tying the ends into loops [160] [161], (g) culturing separately the perivascular population of MSCs of the umbilical arteries and the vein [161]; (h) collection of a suspension endothelial and subendothelial

MSCs after gentle compression of the intact UC with the vein previously filled on both sides with collagenase [126]; (i) separation of the subamniotic stroma from the amniotic epithelium with enzymatic digestion [162]; (j) culturing the cord lining without separating the subamniotic stroma from the amniotic epithelium, but placing the inner or the outer layer faced down on the culture plate to allow only the cells of one side to detach and then growing in culture [157] [163]. This wide variety of isolation methods means that the comparison of cell populations isolated across studies is hardly feasible.

4) The enzymatic method increases the yield of cell isolation digesting the UC ECMs. However, different types of enzymes and enzyme mixes have been used (see review by Conconi et al.) [155]. Each research group used different types of collagenase (I, II, IV) with or without hyaluronidase type II, trypsin or dispase II [155]. Enzymes concentration and incubation times are also variable between the studies [155]. In particular, the concentration of collagenase type I ranged from 1µg to 500mg per ml, while the hyaluronidase type II from about 0.03 µg to 1mg per ml [155] [164] [165]. Also the digestion time is highly variable from 10 minutes to 24 hours [155] [166] [167] [168]. A reason for this wide variability in the digestion protocols is that the longer incubation periods on equal amount of enzymes could allow a more efficient digestion of the tissues enriching the amount of isolated cells. In the same way, higher concentrations of enzymes, or the use of enzymes mixes, could allow a lesser time of incubation to reach the higher isolation efficiency. Nevertheless, longer times and higher concentrations of enzymes could decrease the cell viability. However, this relationship does not seem very consistent across the protocols since different research groups used the same concentration of enzymes with different incubation times (i.e. collagenase type I at 1mg/ml for 4 hours or for a range of 18-24 hours [160] [169]) or the same incubation time for different enzymatic concentrations (i.e. 0.5mg and 1mg per ml of collagenase type I, both for a range of 18-24 hours [160] [170]). Moreover, different culture media are used such as DMEM-LG, DMEM-HG, DMEM/F12, αMEM, αMEM/F12, M199, RPMI 1640, DF-12, supplemented with fetal bovine serum (FBS, concentrations from 1 to 20%), fetal calf serum (FCS, 10 or 20 %), human serum or umbilical cord blood serum [155]. In addition, some groups supplemented the medium with growth factors [155]. Therefore, this wide heterogeneity and

inconsistency about the isolation methods and MSCs culture conditions contributes to a lack of clarity about the characteristics of the different MSC populations in the UC.

5.3 – Characteristics of MSC populations within the Wharton's Jelly

In view of the reasons mentioned above, to compare MSCs obtained from the different regions of the WJ is very difficult. However, all the UC-derived MSCs (UC-MSCs) meet the characterizing criteria of Mesenchymal and Tissue Stem Cell Committee of the International Society for Cell Therapy [131]. In particular, UC-MSCs express the MSCs-associated markers CD105, CD73 and CD90 and lack the hematopoietic surface antigens such as CD14, CD34, CD38, CD45, and CD133 [155]. Notably, the UC-MSCs show low levels of class I HLA and lacking of class II HLA linked to their immunotolerance in transplantation [155]. In culture conditions, UC-MSCs are plastic adherent and share a fibroblast-like morphology, as well as a high proliferation rate and multipotent differentiation potential [155]. The UC-MSCs can be classified as perivascular (PV), WJ and cord lining (CL)-MSCs according to their anatomical localization in the UC.

5.3.1 – Perivascular MSCs

The perivascular region contains almost the 45% of the cells in the WJ [15]. The arterial perivascular tissue is about 600 microns, while it is thicker around the vein, up to 2,000 microns [15]. The perivascular MSCs (PV-MSCs) express CD29, CD44, and CD54, but lack Oct-4 [155]. Moreover, they express CD10 - a marker of WJ-MSCs, but not of amnion or arterial smooth muscle layers – that supports the hypothesis that PV-MSCs and WJ-MSCs may have the same origin [155]. Interestingly, Schugar et al. showed that the PV-MSCs express CD146, a marker of pericytes which may be an origin for MSCs [171]. In addition, the perivascular origin of the UC-MSCs is also supported by the finding of Xu et al. showing the expression of CD146 is higher in PV-MSCs than WJ-MSCs [172]. Recently, an analysis of PV-MSCs secretome showed the presence of proteins such as HSP27, Galectin 1, Semaphorin 7A, plasminogen activator inhibitor-1 (PAI1) and glia-derived nexin (GDN), which have all been implicated as possessing neuroprotective actions [173]. Moreover, PV-MSCs expressed cardiomyocyte markers such as cTnT, MYH6, SIRPA, and CX43, factors know to influence cardiomyocyte reprogramming and differentiation, which are key factors shown to contribute to an improved cardiac function in a mouse model of acute

myocardial infarction (AMI) [166] [174]. In addition, PV-MSCs may modulate inflammatory response, regulating the switch from infiltration of pro-inflammatory to anti-inflammatory macrophages at the infarct site in an AMI mouse model, probably due to the secretion of IL-10 [175].

5.3.2 – Wharton's jelly MSCs

Wharton's jelly MSCs (WJ-MSCs) are the most studied UC cells. WJ-MSCs fit the minimal criteria for MSCs and their mesenchymal features have been confirmed by the expression of specific lineage cytoskeletal markers, such as αSMA and vimentin [176]. WJ-MSCs are a primitive source of stem cells with stem cell characteristics between ESCs and more mature adult stem cells in the developmental hierarchy. Indeed, ESC markers, such as Oct- 3/4, SSEA4, nucleostemin, SOX-2, and Nanog, have been detected [177] [178] [179]. Interestingly, the La Rocca group demonstrated for the first time that WJ-MSCs express both isoforms of Oct-4 (A and B) and Oct-1 [180]. However, despite these primitive characteristics, no teratoma formation has been reported on transplantation of WJ-MSCs in several animal models [181]. Interestingly remarkable, WJ-MSCs express a high percentage of tumor suppressor genes as compared to other classes of MSCs [181]. Furthermore, WJ-MSCs have the intrinsic ability to secrete factors that can result in cancer cell growth inhibition and/or apoptosis, which are critical therapeutic features when contemplating cell-directed cancer therapy [181].

WJ-MSCs are well-known for their immunomodulatory properties (see reviews by our group and Parolini's group in the book "Placenta: the tree of life") [14]. Notably, it has been demonstrated that WJ-MSCs, like the placental cells, express the HLA-G6 isoform that plays a role in the immune tolerance against the fetus during pregnancy [182]. Moreover, WJ-MSCs lack both CD80 and CD86 costimulatory factors that induce T cell activation and survival [182]. Therefore, the concomitant presence of HLA-G and the lack of CD80 and CD86 suggests that WJ-MSCs are particularly suitable for cell-based therapy with minimal the risk of acute rejection [182]. Moreover, the anti-inflammatory and immunomodulatory role of WJ-MSCs is supported by the cells ability to secrete several cytokines and other factors such as NO, IDO, hemeoxygenase 1 (Hmox1), transforming growth factor-β (TGF-β), TNF α, PGE2, leukemia inhibitory factor (LIF), IL-2, IL-6, IL-8, IL-10, IL-12, IL-15, monocyte chemoattractant protein 1 (MCP-1), macrophage inflammatory protein (MIP-1β), RANTES and others [183] [184].

WJ-MSCs possess great differentiation potential; in fact, they can differentiate into mesodermic but also ecto- and endodermic lineages. It has been shown that WJ-MSCs express the NSC marker neuron-specific enolase (NSE) and neuronal proteins including neuron-specific class III beta-tubulin, neurofilament M and tyrosine hydroxylase, a marker for catecholaminergic neurons after neural induction [185]. Moreover, WJ-MSCs can differentiate to cells that express astrocyte (GFAP) and oligodendrocyte (CNPase, MBP, O4, A2B5, GalC) markers [186]. Interestingly, also naive WJ-MSCs displayed neural progenitor cell markers such as Nestin and Musashi-1 and mature neural markers including MAP-2, GFAP and MBP [187]. Furthermore, they can differentiate into Schwann-cell lineage in vitro indicating that they may contribute to nerve repair in clinical applications [188]. In addition, the transplantation of WJ-MSCs improved the neurological function and the cortical neuronal activity in a rat brain ischemia/reperfusion model [189]. These beneficial effects may be related to the capacity of the transplanted cells to differentiate into glial and neuronal cells, but also into endothelial cells [190]. WJ-MSCs also afford endodermic differentiation potential (see review by our group) [191] [192]. In particular, it has been shown that WJ-MSCs form mature pancreatic islets responsive to glucose challenge and express all the islet hormones [193]. Moreover, it has been shown that WJ-MSCs constitutively express some markers of hepatic lineage, such as albumin, α-fetoprotein, and cytokeratin-19 [194].

The therapeutic potential of WJ-MSCs is not only due to their differentiation ability, but also to their secreted factors. WJ-MSCs express growth factors involved in neuroprotection, neurogenesis and angiogenesis, such as neurotrophin-3 (NTF3), epidermal growth factor (EGF), heparin-binding epidermal growth factor (HBEGF), midkine (MDK), brain-derived neurotrophic factor (BDNF), nerve growth factor (NGF), glial cell-derived neurotrophic factor (GDNF), granulocyte colony stimulating factor (G-CSF), vascular endothelial growth factor (VEGF) and many others [195].

5.3.3 – Cord lining MSCs

The cord lining membrane (subamniotic) MSCs (CL-MSCs) fit the minimal criteria defining MSCs and express mesenchymal cytoskeletal markers αSMA and vimentin [196]. However, it is noteworthy that the expression of CD14 demonstrated by Kita et al. is a receptor for lipopolysaccharide and its binding protein is expressed in monocytes and macrophages [196]. CD14 may function as a sensor for CL-MSCs to detect bacteria, which might explain how CL-MSCs

can home to injured/infected sites [196]. The immunosuppressive characteristics of these cells can be also due to the expression of HLA-E, HLA-G and IDO [197], and even though their expression is relatively low, it can be upregulated by IFNγ – induction [197].

CL-MSCs possess both embryonic stem cells and epithelial cells proprieties. As for the WJ-MSCs, the CL-MSCs also express pluripotent markers, such as Nanog, Oct-4, and SSEA-4 [198]. CL-MSCs may be a progenitor of amniotic epithelium. Indeed, it has been shown that CL-MSCs express cytokeratins (CKs) CK7, CK14 and CK19; MUCIN1, whose function is to protect the epithelium by binding to pathogens; additionally, they express CD151, which is involved in epithelial cell-to-cell adhesion, and p63, an adult epithelial stem cell marker [198].

CL-MSCs display a pluripotent differentiation feature. Indeed, together with adipogenic, chondrogenic and osteogenic differentiation potential, CL-MSCs can differentiate into cardiac cells as evidenced by the expression of cardiac markers desmin, alpha sarcomeric actin, myosin heavy chain (MHC), troponin T and connexin 43 [199]. In addition, they differentiated into neural cell types, expressing typical neural markers of GFAP, NG2, nestin, MAP-2, β-tubulin III, CNPase and O4 [199].

6

Stem cells repair mechanisms

There are two major schools of discipline in stem cell mediated repair mechanisms in brain damage caused by injury or neurodegenerative disorders. The first concept supports the idea that stem cells implanted into the brain directly replace dead or dying cells by neuronal differentiation and reconstruction of the damaged synaptic circuitry ("cell replacement", Figure 4A). The second argues that transplanted stem cells secrete neurotrophic factors, anti-inflammatory substances and anti-oxidative stress molecules that indirectly rescue the injured tissue and stimulate the neurogenesis ("bystander effects of stem cells", Figure 4B).

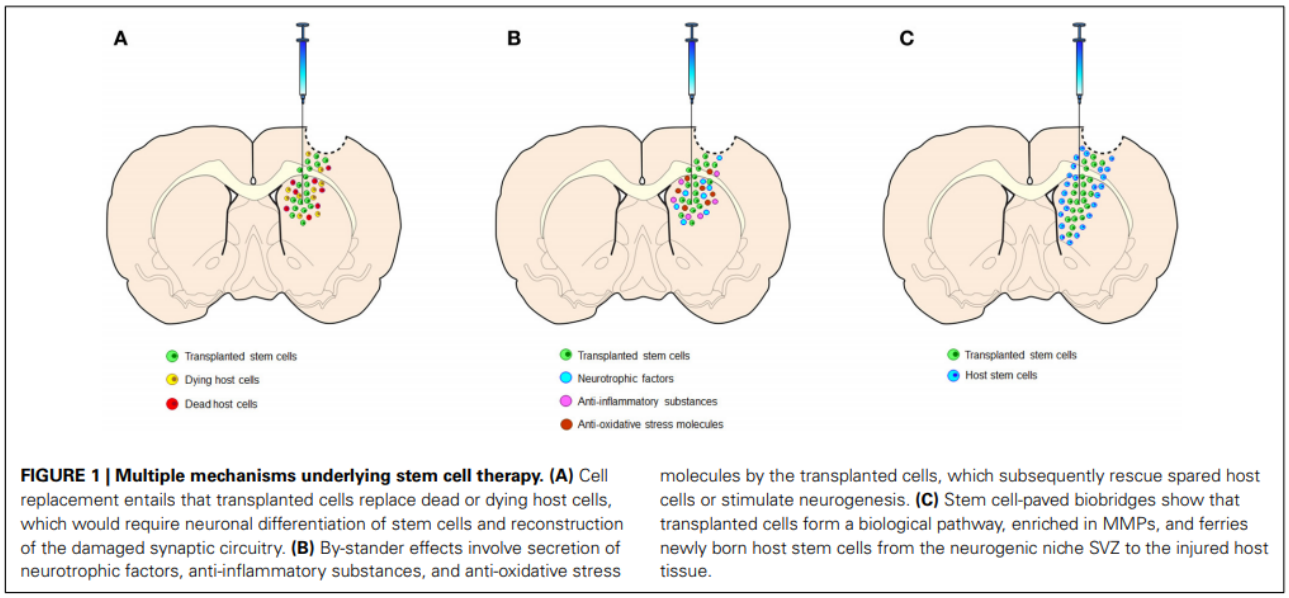

FIGURE 1 | Multiple mechanisms underlying stem cell therapy. (A) Cell replacement entails that transplanted cells replace dead or dying host cells, which would require neuronal differentiation of stem cells and reconstruction of the damaged synaptic circuitry. **(B)** By-stander effects involve secretion of neurotrophic factors, anti-inflammatory substances, and anti-oxidative stress molecules by the transplanted cells, which subsequently rescue spared host cells or stimulate neurogenesis. **(C)** Stem cell-paved biobridges show that transplanted cells form a biological pathway, enriched in MMPs, and ferries newly born host stem cells from the neurogenic niche SVZ to the injured host tissue.

Figure 4. Stem cell repair mechanisms (Tajiri et al. 2014).

Much emphasis is currently placed on the stem cells environment, referred to as it's the cells' "niche". A niche is a subset of tissue cells and extracellular substrates, which in vivo promotes the existence of the stem cells in the undifferentiated state. The niche microenvironment regulates the growth and differentiation of stem cells [200]. Tajiri and colleagues proposed a third stem-cell mediated repair mechanism in brain injury [200]. They observed the capacity of transplanted stem cells to harness a "biobridge" between the neurogenic niche and the site of brain injury, enabling long-distance migration of host neurogenic cells and,

consequently, initiating endogenous repair mechanisms (Figure 4C) [200] [5]. Importantly, it suggests the clinical significance of exploiting this novel stem cell-mediated concept of brain repair for the treatment of brain injury and other neurological disorders [5]. In this regard, neural disorders, presenting a site of cellular degeneration that is physically separated from the area of the brain that could aid in the recovery of dead tissue or lost cells, may benefit from a deeper understanding on the concept of stem cell-paved biobridge [5].

6.1 – Mitochondrial transfer as novel stem cell repair mechanism

Recently, a novel mechanism underlying the therapeutic action of stem cells has been proposed to involve the transfer of healthy mitochondria into damaged cells. It has been reported that mitochondrial transfer can rescue the stressed cells, reprogram the differentiated cells, restore the loss of mitochondrial function in recipient cells, promote cell survival, reduce inflammation, exert neuroprotection and support angiogenesis [8] [9].

As mentioned above, mitochondrial dysfunction is a crucial event in stroke. In addition, mitochondrial impairment is also associated with several degenerative diseases like PD and AD and others disorders such as ischemic heart diseases, cardiomyopathy, lung diseases, and brain injury [8] [9]. Therefore, the therapeutic application of mitochondrial transfer as a regenerative medicine mechanism may pave the way for an innovative stem cell repair strategy. In 2006, Spees et al. first reported the mitochondrial transfer from BM-MSCs to adenocarcinomic human alveolar basal epithelial cells (A549 cell line) restoring the respiratory function of the recipient cells [201]. Since then, several studies have shown the mitochondrial transfer from different type of donor cells (e.g. BM-MSC, iPSC-MSC, AD-MSC, WJ-MSC, endothelial progenitor cells (EPCs) and astrocytes) to various recipient cells (e.g. A549 cell line, pulmonary alveoli, epithelial cells, cardiomyocytes, cardiomyoblasts, macrophages, neurons, endothelial cells, etc) [8] [9].

Mitochondria can be released through TNT formation, gap junctions, microvesicles, cell fusion and transfer of isolated mitochondria (Figure 5) [9]. It has been shown that the mitochondrial Rho-GTPase 1 (Miro1) regulate the movement of mitochondria on microtubules [8] [9]. The down-regulation of Miro 1 results in reduction of TNT formation, while the increase of this motor-adaptor protein leads with an enhanced rescue potential [8] [9]. MSCs are efficient

mitochondrial donors, likely owing in part to MSCs expressing higher levels of Miro1 than the poorer mitochondrial donors, lung epithelial cells and fibroblasts [8].

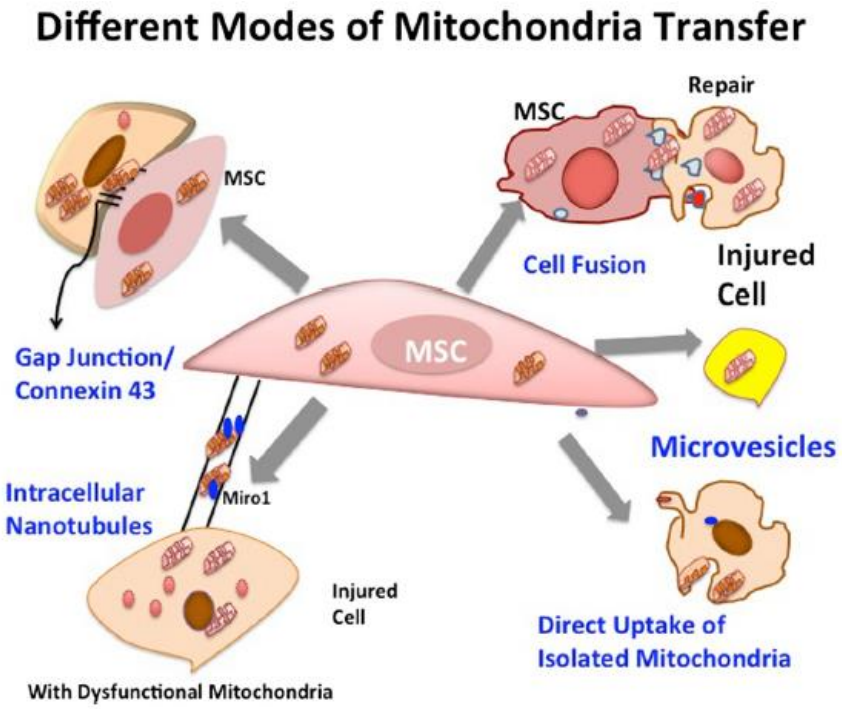

Figure 5. Modalities of mitochondrial transfer (Paliwal 2018).

Despites the growing knowledge about the mechanisms of mitochondrial transfer, the reason why cells donate their own organelles is still unclear. Different hypothesis have been proposed about the signals that trigger the transfer of mitochondria [9]. Oxidative stress of damaged cells might induce neighbor cells to donate mitochondria [9]. Damaged cells can release stress signals including damaged mitochondria, mtDNA and mitochondrial products that are characterized as damage associated molecular patterns (DAMPS) [9]. Notably, mtDNA released by cells with mitochondria dysfunction can be engulfed by MSCs that subsequently enhance mitochondrial biogenesis for mitochondrial donation [9]. Interestingly, ROS released by stressed cells can trigger mitochondrial donation from healthy cells [9]. Indeed, superoxide derived from NOX2 released by acute myeloid leukemia cells stimulates mitochondria transfer from BM-MSCs through TNT [9]. In addition, it has been shown that mitochondrial transfer from astrocytes to neurons is mediated by the Ca^{2+} dependent mechanism of CD38/cyclic ADP ribose signaling pathway that promotes neuroprotective effects and recovery after stroke [202].

Mechanisms underlying the uptake and holding on to the transferred mitochondria are even less clear. Mitochondria are inherited only from the mother, except in rare cases of paternal inheritance leakage [203]. The first phenomenon of mitochondria transfer known is during fertilization. While mitochondria of spermatozoon enter the oocyte, the paternal mitochondria are immediately eliminated by ubiquitin-proteasome pathway [203]. That the mitochondria of spermatozoon are already ubiquitinated suggests that a signal may determine their degradation from the oocyte [203]. It speculated that in the context of mitochondria transfer between a healthy donor cell and a damaged recipient cell their ubiquitination sites could be somehow masked and therefore not recognized like “alien” [203]. The eventual fate of donated healthy mitochondria in the recipient cell is still unresolved and warrants further investigation.

6.2 – Mitochondrial transfer-based stem cell therapies for stroke

Targeting the mitochondria may be a potent approach for the treatment of stroke. Several studies have proposed strategies like activation of the redox state and energy sensor SIRT1 (NAD-dependent deacetylase sirtuin-1), modulation of mitochondrial fission and fusion, purinergic treatment, reduction of electron leakage and increasing ATP production with methylene blue, detoxyfing SOD mimetics, use of antioxidants, as well as calories restriction and exercise [204]. Since the report of successful mitochondrial transfer, mitochondrial-based stem cell therapy has been considered as a feasible treatment of stroke. Hayakawa and coworkers demonstrated the mitochondria transfer between astrocytes and neurons in an in vitro and in vivo model of stroke resulting in neuroprotection and neurorecovery after the ischemic insult [202]. In 2018, the same research group demonstrated mitochondrial transfer from EPCs to brain endothelial cells through extracellular vesicles in an in vitro study [205]. Interestingly, mitochondria transfer stimulated angiogenesis and restored endothelial tightness in an in vitro model of stroke. Recently, our group reported that mitochondria isolated from brains of stroke animals have recovered their OXPHOS capacity after transplantation of EPCs compared to those stroke animals that received vehicle infusion [10]. In addition, the transfer of exogenous mitochondria via in-situ injection or systemic administration reduced cell death and improved the motor performance of stroke rats [206]. These studies taken together support the potential of replacing dysfunctional mitochondria by mitochondrial transfer between stem cells and ischemic cells as a novel strategy for the treatment of stroke.

6.3 – Evidence of UC-MSCs mitochondrial transfer

The ability of UC-MSCs to transfer healthy mitochondria to damaged cells may be an equally effective option to treat diseases characterized by mitochondrial dysfunction. Chen et al. showed that UC-MSCs downregulated autophagy and consequently reduced apoptosis activated T cells of systemic lupus erythematosus (SLE) patients through mitochondria transfer [207]. In a separate study, Lin and coworkers co-cultured WJ-MSCs with mtDNA-depleted human 143B osteosarcoma cells (p° cells) [208]. WJ-MSCs were able to transfer mitochondria to the p° cells and restore the expression of mtDNA-encoded proteins, recover oxygen consumption and respiratory control, as well as the activity of all the ETC mitochondrial complexes including the complex V-inhibitor-sensitive ATP production shifting the energetic metabolism [208]. Subsequently, the same research group tested the use of WJ-MSCs for the treatment of myoclonus epilepsy associated with ragged-red fibers (MERRF), a maternally inherited mitochondrial disease characterized by a mutation in mtDNA [209]. Their findings showed that WJ-MSCs transferred healthy mitochondria to the MERRF cybrid cells resulting in improvement of mt.8344A>G mutation ratio, ROS level, oxidative damage, mitochondrial bioenergetics, mitochondria-dependent viability, balance of mitochondrial dynamics, and resistance against apoptotic stress [209]. Equally a key finding is that WJ-MSCs transferred mitochondria only to the damaged cells but not in the healthy ones suggesting the existence of “help me” signals from the damaged cells recognized from the stem cells [209].

In summary, UC-MSCs may be a promising source of healthy mitochondria for the treatment of mitochondrial dysfunction-related diseases and, potentially, for stroke.

AIMS OF THE PROJECT

The aim of this project is to characterize the MSCs populations of the human UC based on their potential benefits for stem cell treatment in experimental model of stroke. The hypothesis is that UC-MSCs confer therapeutic effects via cell replacement, bystander effect, stimulation of endogenous repair mechanisms and repair of mitochondrial function. To achieve these objectives, this study has been divided in 2 steps characterized by 2 different MSC isolation procedures (Figure 6).

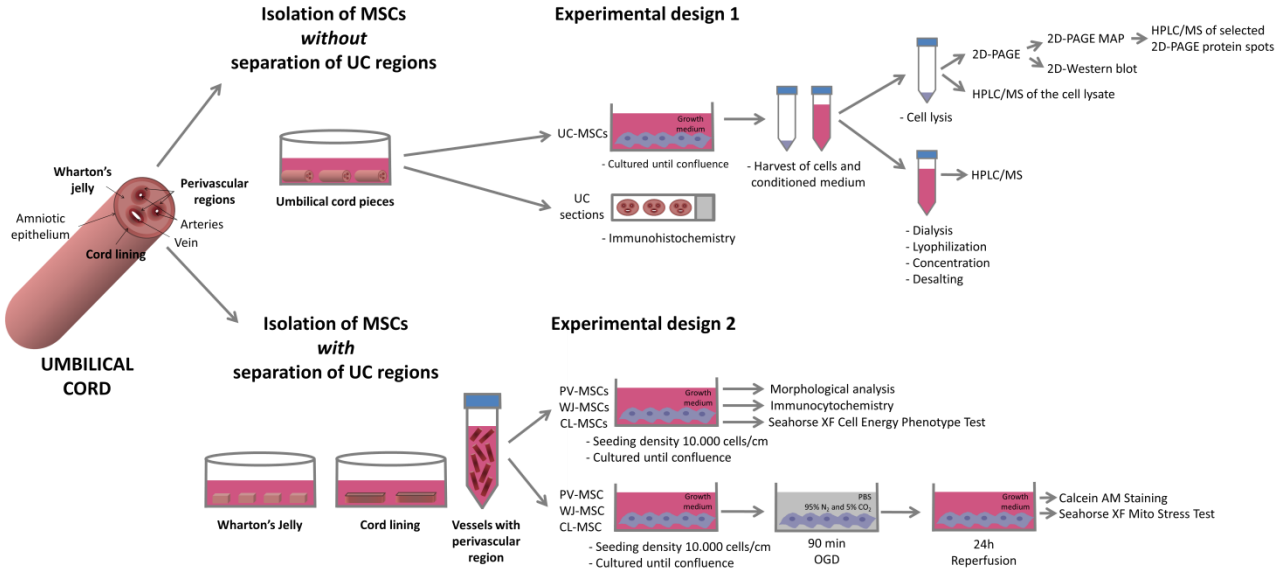

Figure 6. Experimental design.
UC: Umbilical cord, MSC: mesenchymal stem cells, UC-MSC: umbilical cord MSC, PV-MSC: perivascular MSC, WJ-MSC: Wharton's jelly MSC, CL-MSC: cord lining MSC, 2D -PAGE: two-dimensional polyacrylamide gel electrophoresis), HPLC/MS: high performance liquid chromatography coupled with mass spectrometry, OGD: oxygen-glucose deprivation, PBS: phosphate buffered saline.

STEP 1: An explant method without separation of the different anatomic regions of the UC was used for the isolation of a "mixed" population of MSCs called UC-MSCs (Figure 6). Subsequently, a mass spectrometry-based proteomic analysis of cell lysates, by using high performance liquid chromatography coupled with mass spectrometry (HPLC/MS), allowed the characterization of cellular proteins of UC-MSCs. In addition, a two-dimensional polyacrylamide gel electrophoresis map (2D-PAGE MAP) of cell lysates was performed by identification of selected 2D-PAGE protein spots with HPLC/MS. Moreover, the identification of some proteins was validated by 2D Western blot (2D-WB) and immunohistochemistry.

STEP 2: Considering the emerging evidence of three different MSC populations in the human UC, a unique isolation method was used in order to isolate and characterize PV-, WJ- and CL-MSCs (Figure 6). The three UC-MSC populations were characterized by morphological and immunocytochemical analyses. A Cell Energy Phenotype test was performed by using a Seahorse Analyzer to characterize the energetic metabolic profile of the three MSC populations. Furthermore, PV-, WJ- and CL-MSCs were subjected to oxygen and glucose deprivation (OGD) followed by reperfusion (R) to mimics the ischemic condition. Thereafter, a cell viability assay (Calcein AM Staining) and a Seahorse XF Cell Mito Stress Test were performed in both control and after OGD/R to assay the mitochondrial function of PV-, WJ- and CL- in both normal and ischemic conditions.

MATERIALS AND METHODS

Isolation and culture of whole umbilical cord MSCs

Umbilical cords (n= 9) were obtained immediately after full-term births, after normal vaginal delivery or cesarean section. All samples were obtained after mothers' informed consent and treated in accordance with the tenets of the Declaration of Helsinki and local ethical regulations. Umbilical cords were stored aseptically in cold saline and then cellular isolation started within 6 h from partum. The whole umbilical cord MSCs (UC-MSCs) isolation was performed as previously described by La Rocca et al. [180]. Briefly, the cords were washed in 1x PBS in order to remove bloodstains and then rinsed in warm HBSS (Gibco) supplemented by 2x antibiotics/antimycotics (Gibco). Subsequently, the umbilical cord was cut into small pieces of about 1.5 cm length. The cord pieces were sectioned longitudinally to expose the WJ and some incisions were made on the inner matrix with a sterile scalpel to expose a wider area of tissue. Vessels were not removed from the matrix. The cord sections were transferred to 6-well plates (Corning), one cord piece for each well, with the WJ in contact with the plastic surface of the culture plates, and covered completely with culture medium. The isolation and subculture of cells were made using DMEM low-glucose (Sigma), supplemented with 10% FBS (fetal bovine serum gold, PAA), 1x NEAA (non-essential amino acids, Sigma), 1x antibiotics–antimycotics (Gibco), and 2 mM L-glutamine (Sigma). The isolation method did not use proteases to detach cells from the embedding matrix, but employed an explant method, based on cell migratory ability of the MSCs. UC fragments were grown in the culture medium for 15 days in presence of 5% CO_2 at 37°C, with medium changed every second day. Cellular exit from the UC and attachment to the plastic surface of the tissue culture slide was monitored by phase-contrast microscopy. Finally, after 15 days of culture, the remnants of the UC fragments were removed from the wells, and cells attached to wells were cultured until reaching the confluence. After reaching confluence, cells were removed from flasks with TrypLE Select (Invitrogen) and were cultured for up to 6 passages.

Immunohystochemistry

For immunohistochemistry (IHC) analysis, 4.0 µm formalin-fixed paraffin-embedded UC tissue sections were stained. Sections were first deparaffinized and rehydrated in ethanol. The IHC

assay was performed using the ICC/IHC "Histostain Plus 3rd Gen IHC Detection" kit (Invitrogen). The primary antibodies used for this study are diluted with saponin 0.1% in PBS 1x and they are listed in the Table 1. Nuclei were stained with Harris Hematoxylin Solution DC (DC Panreac). The glasses were mounted with Leica CV Mount. The observation of the sections was performed at the automated upright microscope Leica DM5000 B.

Table 1. List of primary antibodies used in IHC analysis.

Antigen	Clone	Host	Clonality	Supplier	Dilution
MMP-2	H76	rabbit	polyclonal	SantaCruz	1:100
MMP-3	1b4	mouse	monoclonal	SantaCruz	1:25
MMP-9	EP1255Y	rabbit	polyclonal	AbCam	1:100
MT-MMP-1	H72	rabbit	polyclonal	SantaCruz	1:100
TIMP-1	G6	mouse	monoclonal	SantaCruz	1:25
TIMP-2	3A4	mouse	monoclonal	SantaCruz	1:25

Separation of proteins by two-dimensional electrophoresis

For the 2D-PAGE of UC-MSCs, 50 µg of total proteins were loaded for the following silver staining and 100 µg for the western blotting of 2D gels.

Proteins extraction and quantization

Protein extraction from UC-MSCs was performed using 8M urea/50mM Tris-HCl (pH 8) in which was added fresh protease inhibitor.

Proteins quantification was performed using the DC Protein assay (BioRad). After determination of the concentration of each sample, they were stored at -20°C until use.

Isoelectric focusing

In the first-dimension run, isoelectric focusing (IEF), proteins were separated according to their isoelectric point (pI) on immobilized pH gradient (IPG) strips. In this study, two 7-cm IPG strips with nonlinear pH gradient and two 7 cm IPG strips with linear pH gradient were used: Immobiline™ DryStrip pH 3-5.6 NL (GE Healthcare), ZOOM® Strip pH 3-10 NL (Invitrogen), Immobiline™ DryStrip pH 6-11 (GE Healthcare), ZOOM® Strip pH 4-7 (Invitrogen). Prior to IEF, each IPG strip for each condition was previously rehydrated with rehydration solution (8 M urea, 2% w/v CHAPS, 0.5% v/v IPG buffer (Amersham), 0.002% bromophenol blue (1% stock solution), double-distilled water), to which was added fresh dithioerythritol (DTE). Samples were diluted in

this solution and allowed to enter IPG strips for 1 h at room temperature, using the ZOOM® IPGRunner™ Cassette (Invitrogen). The first-dimension run included six steps at various voltages ('step and hold' or 'gradient') at different times: (i) hold at 30 V for 720 min, (ii) hold at 100 V for 15 min, (iii) gradient 100 V to 300 V for 30 min, (iv) hold at 300 V for 20 min, (v) gradient 300 V to 3000 V 60 min and (vi) hold at 3000 V for 150 min.

2D-SDS-PAGE

After IEF, protein-separated IPG strips were equilibrated with SDS (sodium dodecyl sulfate) equilibration solution (6 M urea, 75 mM Tris–HCl pH 6.8, 29.3% glycerol, 2% SDS, double-distilled water), then processed to obtain two buffers, one containing DTE as reducing agent (Buffer A) and one containing iodoacetamide (IAA, which alkylates reduced sulfurs) and bromophenol blue (Buffer B). Equilibrated IPG strips were used for the 2D run using 12% SDS-PAGE gels. The 2D run comprised two subsequent steps at different constant currents and different times: 10 mA gel -1 for 10 min; and 20 mA gel -1 for 120 min. The Zoom Dual Power adapter (Life Technologies) was used for both first- and second-dimension runs.

Silver staining and 2D map creation

After 2D electrophoresis, the gels were fixed and stained with the MS compatible Eriochrome black T (EBT) - silver staining method as previously described [210]. The gels were stored in distilled water until use. Stained gels were digitalized to create a 2D map of whole-cell lysate of the UC-MSCs. The Melanie 2D gel analysis software was used to compare images as well as analyze resulting data.

Identification of 2D gels protein spots by mass spectrometry

Excision and de-staining of the protein spots

Protein spots were processed by using mass spectrometry analysis in order to identify the proteins and build a 2D-PAGE map. In particular, selected protein spots were excised from the silver stained 2D gels by scalpel, transferred to sterilized 0.5 ml tubes and stored in -20° C until use. The de-staining of the protein spots was performed using the Destainer A and the Destainer B of the SilverQuest™ Silver Staining kit (Invitrogen).

In-gel digestion

After de-staining, the protein spots were dehydrated with 100% acetonitrile (ACN) to allow the absorption of trypsin solution. For protein digestion, 10 µL of 6.7 ng/µL trypsin (Sequencing Grade Modified Trypsin, porcin, Promega) in 140 µl of ammonium bicarbonate 0.05 M pH 8.2, was added to each sample and incubated overnight at 37°C, according to published procedure [211]. The extract peptide digestion products and extracted gel pieces were stored at -20°C until use.

High performance liquid chromatography and electrospray mass spectrometry

Reverse Phase HPLC (RP-HPLC) separation and MS analysis were performed using UltiMate 3000 RSLCnano System (Dionex) combined with LTQ Orbitrap XL™ Hybrid Ion Trap-Orbitrap Mass Spectrometer (Thermo) via electrospray ionization (ESI) interface (Thermo). The chromatographic separation was on a Discovery BIO Wide Pore C18 column (15 cm x 2.1 mm, 5 µm). Sequential elution of peptides was accomplished using a flow rate of 50 µl min -1 and a linear gradient from solution A (0.1% formic acid, FA) to 98% of solution B (80% ACN; 0.08% FA) in 70 minutes. The gradient elution program was as follows: 0-2 min 98:2 (%A:%B, v/v), 2-4 min 85:13, from 4 to 50 min gradient from 85:13 to 50:50, 50-54 min 2-98, 54-59 min 2:98, 59-60 min 98:2, 60-70 min 98:02 (Figure 7). The column temperature was set at 25°C and the sample tray temperature was maintained at 4°C. For all experiments, a sample volume of 15 µl was loaded by the autosampler using 0.3 ml short thread autosampler vials (Sigma Aldrich). For MS detection, the ESI source was operated in the positive mode and ran with Xcalibur 2.0 software (Thermo Fisher). High purity nitrogen was used as the sheath and the auxiliary gas, while high purity helium was used as the collision gas.

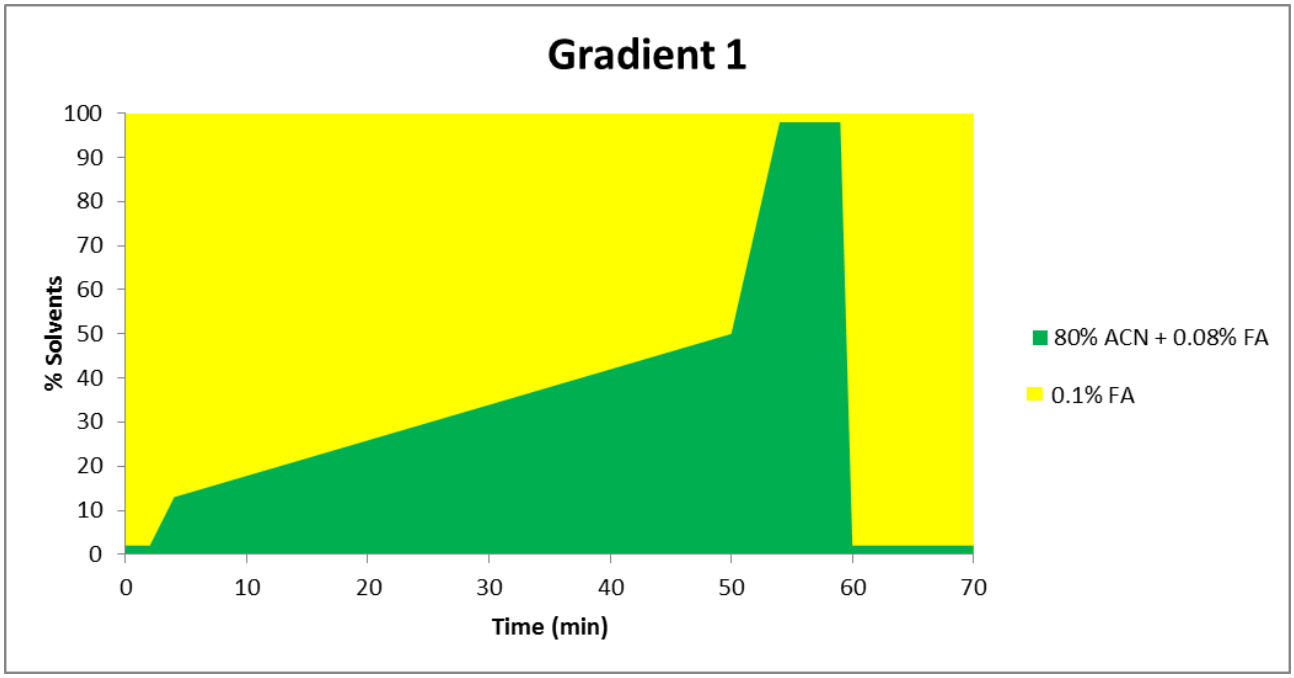

Figure 7. Gradient elution program for RP-HPLC/MS analysis of UC-MSCs 2D gels spots-derived peptides.

Whole-cell lysate analysis by mass spectrometry

After reaching confluence, UC-MSCs were detached from flasks with Tryple Select (Invitrogen) and centrifuged at 4°C for 5 minutes at 1100 rpm. Then, the pellets were stored at -80°C until use. Protein extraction from UC-MSCs was performed using 8M urea/50mM Tris-HCl (pH 8) in which was added fresh proteases inhibitor.

Protein quantification was performed using the DC Protein assay (BioRad). After determination of the concentration of each sample, they were stored at -20°C until use.

In solution digestion

The digestion step was performed adding Trypsin/Lys-C Mix (Promega) to 50µg of proteins at a 25:1 protein/protease ratio (w/w), following the manufacturer's instructions.

Peptides enrichment and desalting

Peptides, obtained after the digestion, were concentrated and desalted with Pierce C18 Spin Columns (Thermo Scientific) following the manufacturer's instructions. Thereafter the samples were lyophilized and suspended in an appropriate buffer (0.1 % FA) for subsequent applications.

RP-HPLC/MS analysis

The peptides mixtures derived from the whole-cell lysates of UC-MSCs were identified by RP-HPLC/MS with the same method used for the 2D gels spots proteins as described above. However, a necessary adjustment of the ACN chromatography gradient was introduced. The gradient was extended to 120 minutes for whole-cell lysates. Since these samples were constituted by peptides derived from a mixture of several proteins, a longer chromatographic run was needed to allow a more efficient separation of the peptides as well as a more successful identification. The gradient elution program was as follows: 2 min 98:2 (%A:%B, v/v), 4 min 87:13; 95 min gradient from 87:13 to 50:50, 104 min 2:98, 109 min 2:98, 110 98:2, 120 min 98:2 (Figure 8).

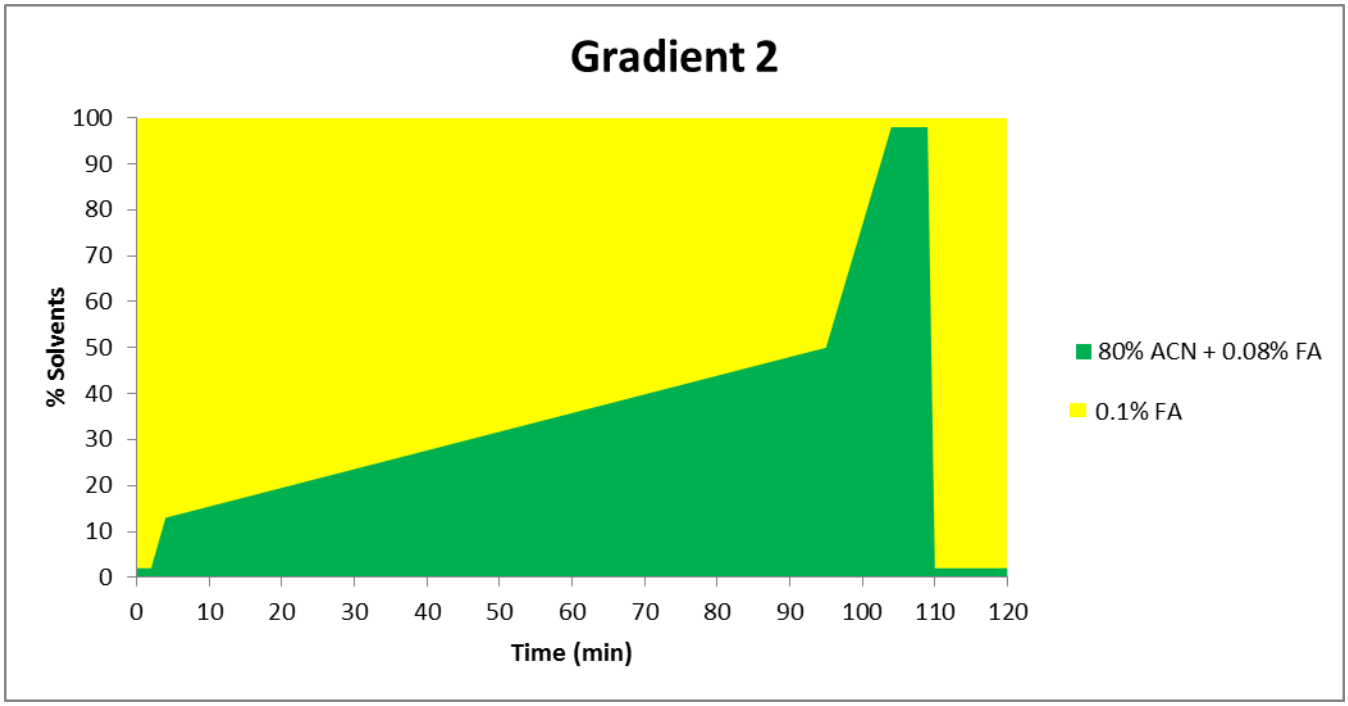

Figure 8. Gradient elution program of RP-HPLC/MS analysis of UC-MSCs whole-cell lysates -derived peptides.

Data analysis

The raw data was processed using Proteome Discoverer version 1.4 (Thermo Scientific). MS/MS spectra were sequentially searched with Sequest HT and MS Amanda, both set against *Homo sapiens* database using the following parameters: full trypsin digest with maximum 2 missed cleavages, fixed modification carbamidomethylation of cysteine (+57.021 Da), variable

modification oxidation of methionine (+15.995 Da) and phosphorilation of tyrosine, serine and threonine (+79.966 Da). Precursor mass tolerance was 10 ppm and product ions fragment ion tolerance was 0.8 Da. Peptide spectral matches were validated using Percolator. In this study, in order to make the identification significant, proteins identified by Proteome Discoverer with ≥ 3 peptides were considered.

Bioinformatics analysis

In order to confirm the identified proteins, *in silico* analysis was carried out using the SWISS-2DPAGE database of the online ExPASy Proteomics Server [212] (http://www.expasy.org) and the UniProt database [213] (http://www.uniprot.org). The Melanie 2D gel analysis software was used for comparing images as well as analyzing resulting data.

For functional analysis of the proteomics data, the Database for Annotation, Visualization and Integrated Discovery (DAVID) (v 6.8, https://david.ncifcrf.gov/) was applied [214].

2D Western blot

Gels obtained from 2D gel electrophoresis were incubated in transfer buffer (Tris 25 mM, Glycin 190 mM, Methanol 20%) for 30 min and then blotted on Hybond ECL nitrocellulose membranes (Amersham) at 0,35 A for 1 hour in wet conditions. To check for success of transfer, the membranes were stained with the Ponceau Red (2% Ponceau S in 30% trichloracetic acid and 30% sulfosalicylic acid) and the gels with Coomassie Blue (a mixture of water/acetic acid/methanol with the addition of Coomassie Brilliant Blue R-259 0,2 % in weight). After antigen blocking for 1 h with 3% BSA in 0.05% Tween-20 Tris-buffered saline (T-TBS) pH 7.6, membranes were exposed overnight at 4°C to specific primary antibodies listed in Table 2. All antibodies were diluted in antibody buffer (1% BSA, 0.05% T-TBS). Membranes were then incubated with specific horseradish peroxidase (HRP)-labeled secondary Abs, Goat Anti-Mouse IgG Antibody (Millipore), for 1 hour. They were exposed to chemo-luminescent substrate (Immobilon Western, Millipore) for 5 min and then developed in a dark room on Hyperfilm ECL (GE Healthcare).

Table 2. List of the antibodies used in 2D Western blot analysis.

Antigen	Clone	Host	Clonality	Supplier	Dilution
B7-H3	G12	mouse	monoclonal	SantaCruz	1:800
Galectin 1	-	mouse	monoclonal	AbCam	1:1000

Isolation and culture of MSCs from different regions of umbilical cord

Umbilical cords (n= 2) were purchased from Zen-Bio and they were obtained after mothers' informed consent, immediately after full-term births with normal vaginal delivery. The isolation of MSCs from perivascular, WJ and cord lining regions of the umbilical cord was performed as previously described [161] [164] [196]. In particular, an enzymatic method was chosen for the isolation of PV-MSCs in order to increase the cellular harvested yield around the vessels, according to Sarugaser et al. [164]. On the other hand, an explant method was performed for the isolation of both WJ- and CL-MSCs, according to Kita et al. and Mennan et al. [161] [196]. For all the three cellular types, the culture was made using DMEM low-glucose (Sigma), supplemented with 10% FBS (Gibco), 1x NEAA (Sigma) and 1x antibiotics–antimycotics (Gibco) and replaced every 2–3 days until the cells were ready for sub-culture (complete medium).

In summary, the UCs were washed in 1x PBS in order to remove bloodstains and then rinsed in warm HBSS (Gibco) supplemented by 2x antibiotics/antimycotics (Gibco). Subsequently, the UC was cut into pieces of about 5-6 cm length and then carefully sectioned longitudinally to expose the WJ and the blood vessels.

For the isolation of PV-MSCs, the three vessels were isolated using forceps and scalpel and placed in 40 ml of HBSS supplemented with 100 U/mL Type I Collagenase and 0.01 U/mL Hyaluronidase in a 50 mL Falcon tube and left to digest in for 4 hours at 37°C. After the digestion was completed, all the vessels were removed from the suspension using forceps. The suspension, containing the cells, was centrifuged at 285 g for 10 minutes. Subsequently, the supernatant was discarded and the cellular pellet was treated with 50 ml of 0.8% ammonium chloride and incubated at room temperature for 5 min to lyse the erythrocytes. After that, the tube was centrifuged for 10 min at 285 g and the supernatant was discarded. The cells, obtained from the perivascular region of each umbilical cord, were counted and plated in one T-75 tissue culture flask with complete medium and put it in 5% CO_2 incubator at 37°C.

After removing the vessels, the remaining cord was cut in smaller pieces with a length of about 1.5 cm and each piece was placed in a wall of a 6walls culture plate with complete medium and incubated overnight in 5% CO_2 at 37°C. The following day, the WJ absorbed the complete medium containing phenol red and, thus, it can be distinguished from the CL that is about 1mm width. The WJ was separated from the CL from each piece of umbilical cord by using a scalpel. The collected WJ was plated in a wall of a 6walls culture plate and each piece of the remaining CL was plated in a wall of other 6walls plate with the sub-amnion side touching the bottom of the wall to

allow the sub-amnion cellular exit and attachment to the culture plate. The WJ and CL were cultured with complete medium changed every 2-3 days over for 15 days in culture, and the cellular exit from both tissues, as well as the attachment to the plastic surface of the tissue culture plate, was monitored by phase-contrast microscopy. After 15 days, the WJ and CL tissues were removed and the attached cells were cultured until reaching the confluence.

The isolated cells were subcultured until passage 4 for all the three cellular types. Morphological analysis was performed by observing the cells at the phase contrast microscope Olympus.

Immunocytochemistry

Cells were seeded at the density of $1X10^4$ cells /cm^2 in 8 wells chamber slides and cultured for 2 days. Subsequently the cells were fixed with 4% paraformaldehyde in PBS (phosphate buffered saline) for 20 min at room temperature. After a wash with PBS, 0.1% Triton X-100 (w/v) in PBS was added and kept incubated for 5 min to allow the permeabilization. After rinsing with PBS, nonspecific binding was blocked by incubating 3% normal goat serum (Invitrogen 50-062Z) in 0.1% Triton-X100 in PBS for 1h at room temperature. Each primary Ab was diluted in blocking buffer and incubated with samples overnight at 4°C. Dilution of each primary Ab is specified in **Error! Not a valid bookmark self-reference.**. After 3 washes (5 min for each wash) with PBS, secondary Abs were added for 1h at room temperature (**Error! Not a valid bookmark self-reference.**). Then, additional 3 washes were performed, each 5 minutes with PBS, then the slides were mounted with Antifade Mounting Medium with DAPI (Vectashield HardSet H-1500) and fluorescent images were collected using a Zeiss microscope.

Table 3. Antibodies used for the immunofluorescent staining.

Antigen	Host	Clonality	Supplier	Code	Dilution
CD90	Rabbit	Monoclonal	Abcam	AB133350	1:100
CD73	Mouse	Monoclonal	Abcam	AB54217	1:500
Oct4	Rabbit	Polyclonal	Abcam	AB19857	1: 400
CD146	Rabbit	Monoclonal	Abcam	AB75769	1: 100
CD14	Mouse	Monoclonal	Abcam	AB181470	1: 100
Goat anti-mouse IgG H&L alexa fluor 488	Goat	Polyclonal	Abcam	AB150117	1: 500
Goat anti-rabbit IgG H&L alexa fluor 594	Goat	Polyclonal	Abcam	AB150080	1: 500

Oxygen-glucose deprivation/reperfusion

PV-, WJ- and CL-MSCs were seeded at the density of 10,000 cells/ cm^2 and cultured until reaching confluence. The cells were exposed to OGD/R to mimic the ischemic condition following stroke as previously described [215]. Briefly, after the removal of the growth medium, the cells were exposed to PBS and placed in an anaerobic chamber (Plas Labs) containing nitrogen (95% N_2) and carbon dioxide (5% CO_2) for 15 min at 37°C. Finally, the chamber was sealed and incubated for 90 min at 37°C (hypoxic–ischemic condition). OGD was terminated by removal of PBS, and addition of the growth medium, the cell cultures were then reintroduced to the regular 95% O_2 and 5% CO_2 incubator (normoxic condition) at 37°C for 24 h, which represented a model of "reperfusion."

Measurement of cell viability

Measurement of cell viability was performed using fluorescent live cells assay. Both control and OGD/R treated cells were incubated with 1 µM Calcein-AM (Trevigen) for 30 minutes in the regular 95% O_2 and 5% CO_2 incubator at 37°C. The green fluorescence of the live cells was measured by the EnSpire Multimode Plate Reader (Ex/Em = 490/520; Perkin Elmer). In addition, a morphologiacal analysis was performed using a phase contrast microscope (Olympus).

Seahorse assay

The Seahorse XF96 Analyzer allows a sensitive kinetic measure of the oxygen consumption rate (OCR), and the extracellular acidification rate (ECAR). OCR is the rate of the decrease of oxygen concentration in the assay medium and, therefore, it is an indicator of mitochondrial respiration. ECAR corresponds to the rate of increase in proton concentration (or decrease in pH) in the assay medium and, therefore, it is a measure of the rate of glycolysis. In this study, the Cell Energy Phenotype test and Cell Mito Stress test assays were performed.

Cell Energy Phenotype test

The Agilent Seahorse XF Cell Energy Phenotype Test measures mitochondrial respiration and glycolysis under baseline and stressed conditions, showing the three key parameters of cell energy metabolism: Baseline Phenotype, Stressed Phenotype, and Metabolic Potential (Figure 9).

The Baseline phenotype corresponds to the OCR and ECAR of cells at starting assay conditions, while the Stressed phenotype represents the OCR and ECAR of cells under an induced energy demand (specifically, in the presence of stressor compounds). The Metabolic potential is the percentage increase of stressed OCR and ECAR over the corresponding baseline OCR and ECAR, and measures the cells' ability to meet an energy demand via mitochondrial respiration and glycolysis.

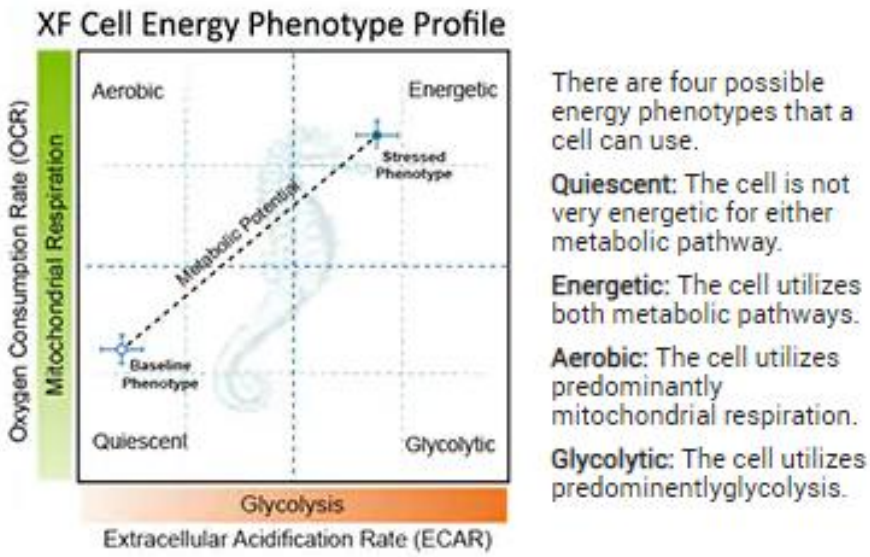

Figure 9. Seahorse XF Cell Energy Phenotype Profile showing the 4 possible cellular energy phenotypes (www.agilent.com).

PV-, WJ- and CL-MSCs were seeded into the Seahorse XF96 Cell Culture Microplates (Agilent) at the cell density of 10,000 cells/cm^2 and cultured until confluence. Prior to the start of the Seahorse XF Cell Energy Phenotype test, a sensor cartridge was hydrated in Seahorse XF Calibrant (Agilent) following the manufacturer's instruction (Agilent). On the day of the assay, the cells were washed once and incubated in XF Seahorse Base Medium DMEM (Agilent) supplemented with 10 mM glucose, 1 mM sodium pyruvate, and 2mM L-glutamine. The XF Seahorse Base Medium DMEM was prepared following the manufacturer's instruction (Agilent). Even though the Agilent protocol suggests two washes, the cells were rinsed only one time to avoid the risk of detaching the cells from the plate. After calibration of the Seahorse XF96 Analyzer, the sensor cartridge was removed from the instrument and Seahorse XF96 Cell Culture Microplate was inserted. For all the three types of cells, the OCR and ECAR readings were taken over time under basal conditions and after the addition of mitochondrial inhibitors Oligomycin (1µM) and carbonilcyanide p-triflouromethoxyphenylhydrazone (FCCP, 1µM). With the

simultaneous injection of these stressor compounds two events occurred: Oligomycin inhibited ATP production by the mitochondria and, consequently, there was a compensatory increase in the rate of glycolysis. FCCP depolarized the mitochondrial membrane that increased the OCR because the mitochondria attempted to restore the mitochondrial membrane potential.

In addition, Hoechst 33342 (Fluka, Biochemika) at the concentration of 1:3000/well was added and the absorbance was measured with EnSpire Multimode Plate Reader (Ex/Em = 358/461 nm; Perkin Elmer) for the normalization of the Seahorse data. The total run was 1 hour and 12 minutes and the run protocol is described in Table 4. Results were exported by using the Seahorse Wave 2.4 XF-96 software and the data obtained were normalized to the absorbance (abs) per well and expressed in pmol/min/abs.

Table 4. Seahorse XF Cell Phenotype Test Run Protocol.

Command	**Time (min)**	**Port**	**Drug**
Calibrate			
Equilibrate	12		
Mix (x 5)*	3		
Measure (x5)*	3		
Inject		A	Oligomycin + FCCP
Mix (x5)**	3		
Measure (x5)**	3		
Inject		B	Hoechst 33342
End protocol			

**After the equilibration, the baseline step consisted of 5 "mix and measure" cycles.*

***After the injection of Oligomycin + FCCP, 5 "mix and measure" cycles were performed.*

Cell Mito Stress Test

The Agilent Seahorse XF Cell Mito Stress Test measures key parameters of mitochondrial function by directly measuring the OCR of cells. Through the serial injections of inhibitors of mitochondrial ETC, the Seahorse XF Cell Mito Stress Test measures basal respiration, ATP production, proton leak, maximal respiration, spare respiratory capacity, and non-mitochondrial respiration (Figure 10).

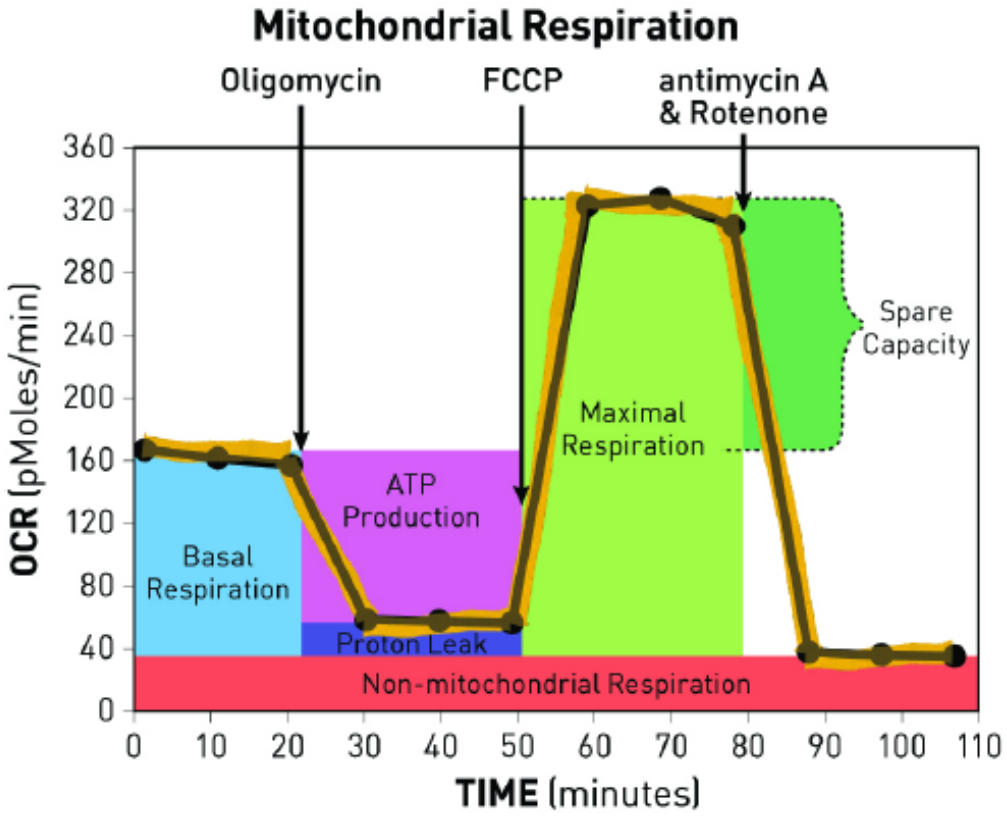

Figure 10. Seahorse XF Cell Mito Stress Test profile of the key parameters of mitochondrial respiration (www.agilent.com).

The drugs (oligomycin, FCCP, and a mix of rotenone and antimycin A) were sequentially added to measure ATP production, maximal respiration, and non-mitochondrial respiration, respectively. By using these parameters and basal respiration, proton leak and spare respiratory capacity were then calculated. Oligomycin inhibited ATP synthase (complex V), FCCP uncoupled oxygen consumption from ATP production, and rotenone and antimycin A inhibited complexes I and III, respectively.

The basal respiration measured the energetic demand of the cell under baseline conditions and modulated proton leak pathways.

ATP production approximated the mitochondrial respiration sensitive to oligomycin.

The proton leak measured the rate of mitochondrial respiration uncoupled with ATP production and it can be a sign of mitochondrial injury or a normal physiological mechanism regulating the mitochondrial ATP production.

The maximal respiration corresponded to the maximum OCR that the cell can achieve after adding FCCP. The mitochondrial ETC was stimulated by FCCP to work at its maximum capacity

determining a rapid oxidation of sugars, fats, and amino acids, altogether simulating a physiological energy demand.

The spare respiratory capacity represented the difference between the basal and maximal respiration showing the capacity of a cell to meet an increased energy demand.

PV-, WJ- and CL-MSCs were seeded into the Seahorse XF96 Cell Culture Microplates (Agilent) at the cell density of 10,000 cells/cm^2 and cultured until confluence. The cells were exposed to OGD/R as described above. Prior to the start of the Seahorse XF Cell Energy Phenotype test, a sensor cartridge was hydrated in Seahorse XF Calibrant (Agilent) following the manufacturer's instruction (Agilent). The day of the assay, the cells were washed one time and incubated in XF Seahorse Base Medium DMEM (Agilent) supplemented with 10 mM glucose, 1 mM sodium pyruvate, and 2mM L-glutamine. The XF Seahorse Base Medium DMEM was prepared following the manufacturer's instruction (Agilent). For both control and OGD/R conditions, OCR and ECAR readings were taken over time under basal conditions and after the addition of mitochondrial inhibitors (1 µM oligomycin, 1 µM FCCP and 0.5 µM rotenone/antimycin).

In addition, Hoechst 33342 (Fluka, Biochemika) was added at the concentration of 1:3000/well. The absorbance was measured with EnSpire Multimode Plate Reader (Ex/Em = 358/461 nm; Perkin Elmer) and the nuclei count was performed with a fluorescent phase contrast microscope (Olympus) for the normalization of the Seahorse data.

The total run was 1 hour and 24 minutes and the run protocol is described in Table 5. Results were exported by using the Seahorse Wave 2.4 XF-96 software and the data obtained for each condition were normalized to the cell number per well and expressed in pmol/min/cells.

Table 5. Seahorse XF Cell Mito Stress Test Run protocol.

Command	**Time (min)**	**Port**	**Drug**
Calibrate			
Equilibrate	12		
Mix (x 3)*	3		
Measure (x3)*	3		
Inject		A	Oligomycin
Mix (x3)**	3		

Measure (x3)**	3		
Inject		B	FCCP
Mix (x3)**	3		
Measure (x3)**	3		
Inject		C	Rotenone/Antimycin
Mix (x3)**	3		
Measure (x3)**	3		
Inject		D	Hoechst 33342
End protocol			

**After the equilibration, the baseline step consisted of 3 "mix and measure" cycles.*

***After the injection of Oligomycin, FCCP and Rotenone/Antimycin follow 3 "mix and measure" cycles.*

RESULTS

UC-MSCs 2D-PAGE map

In order to create a 2D-SDS-PAGE protein fingerprint map of UC-MSCs, 50 µg of total proteins extract were resolved into 7 cm IPG strip having a pH range of 3–5.6 and subsequently separated on the basis of mass using 12% SDS-PAGE in second dimension (Figure 11). A total of 70 protein spots were excised from the gel and enzymatically digested. Subsequently, they were processed for HPLC/MS analysis and 17 spots were identified. The results of the 40 proteins identified were reported in Table 6. The proteins identified with mass spectrometry are indicated in the figure by using the Melanie 2D gel analysis software (Figure 12).

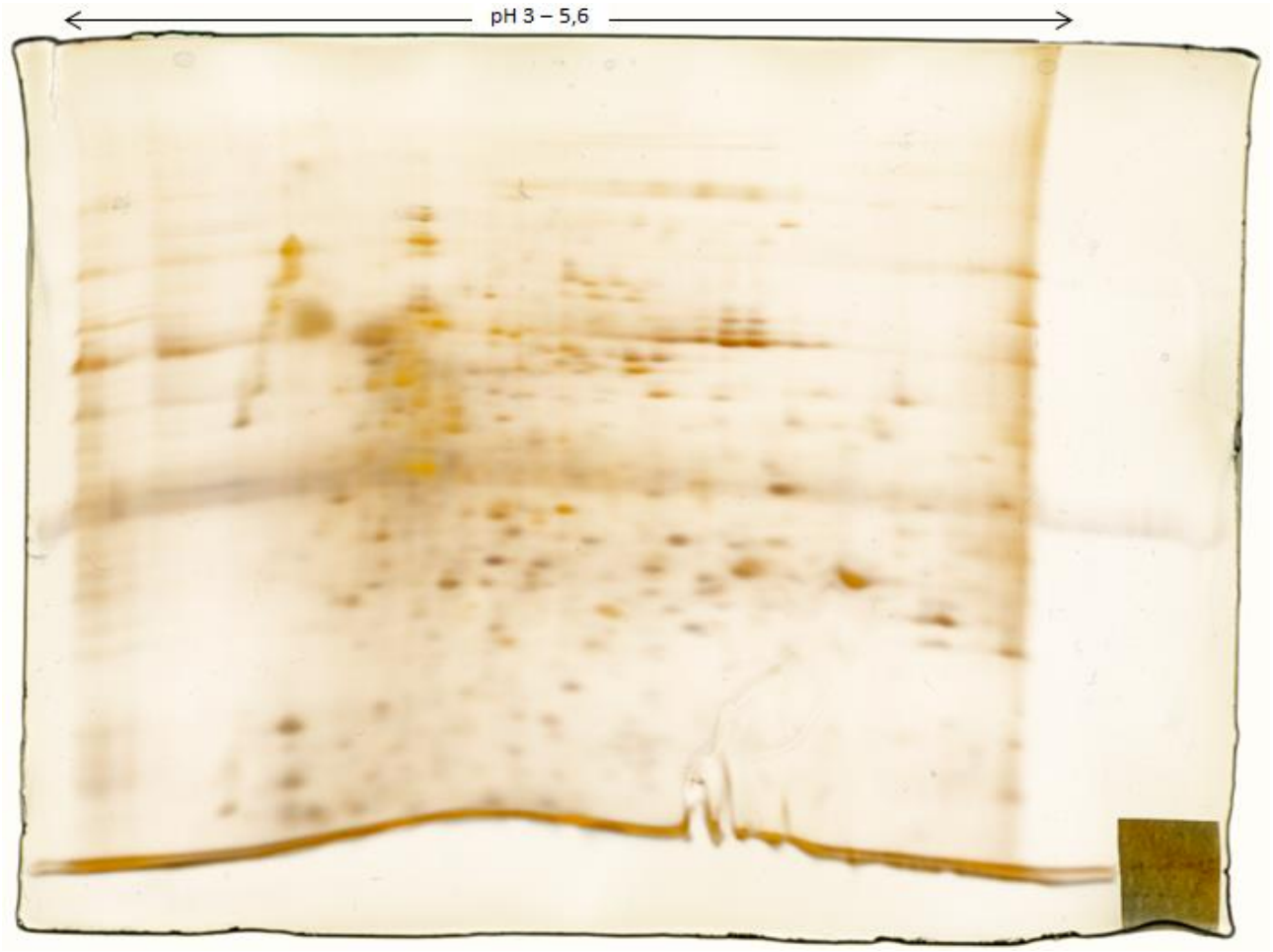

Figure 11. Silver-stained 2D gel of UC-MSCs proteome. 50 µg of total proteins extract of UC-MSCs were separated by IEF in a 7-cm-long IPG strip containing a nonlinear pH gradient 3-5.6, followed by SDS-PAGE in a 12% gel.

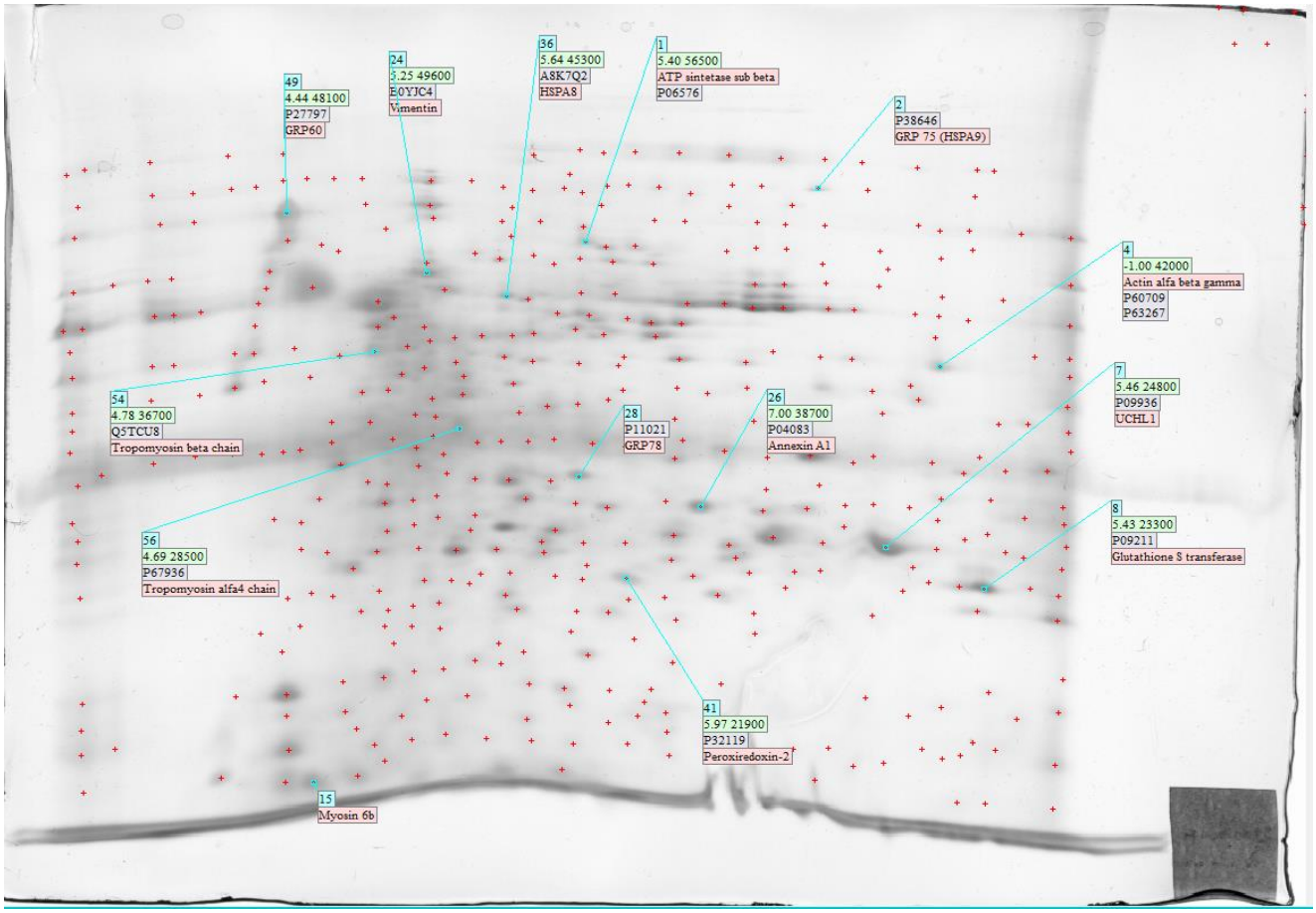

Figure 12. 2D map of UC-MSCs proteome. 17 spots were identified by using RP-HPLC/MS analysis and they are indicated in the figure by using the Melanie 2D gel analysis software. For each identified spot, the name of the identified protein (red), the number of the spot (blue), the pI and the molecular weight in Dalton (green) and the Uniprot accession number (white) are indicated.

Table 6. Identified proteins in UC-MSCs proteome with RP-HPLC/MS analysis of 2D gel protein spots.

# Spot	Protein	Uniprot entry	Coverage	Peptides	MW	pI
1	ATP sintetase sub β	P06576	27.79%	8	56.5 kDa	5.4
2	GRP 75 (HSPA9)	P38646	10.46%	5	73.6 kDa	5.2
4	Actin α	P68133	32%		42 kDa	
	Actin β	P60709	41%	12	41.7 kDa	5.18
	Actin y	P63267	41%		4.8 kDa	
5	Actin β	P60709	29%	12	41.7 kDa	5.22
	Actin y	P63267	19%		41.8 kDa	
7	UCHL1	P09936	56.05%	6	24.8 kDa	5.46
8	Glutathione S transferase	P09211	69.48 %	9	23.3 kDa	5.43
	UMP-CMP Kinase	P30085	18.37%	3	22.2 kDa	5.57
9	Cofilin 1	P23528	36.68%	5	18 kDa	8.2
15	Myosin 6b	P60660	55%	10	17 kDa	4.56
24	Vimentin	B0YJC4	22.04%	9	49.6 kDa	5.25
26	Annexin A1	P04083	12.43 %	3	38.7 kDa	7
28	GRP 78	P11021	12.39%	5	76 kDa	4.98
36	Heat shock cognate 71 (HSPA8)	A8K7Q2	11.71%	4	45.3 kDa	5.64
	Heat shock cognate 71 (HSPA8)	E9PNE6	9.60%	4	54.9 kDa	5.68
	Heat shock cognate 71 (HSPA8)	E9PKE3	7.66%	4	68.8 kDa	5.52
	Heat shock cognate 71 (HSPA8)	P11142	7.43%	4	70.9 kDa	5.52
41	Peroxiredoxin-2	P32119	37.88%	8	21.9 kDa	5.97
49	GRP 60	P27797	73.38 %	21	48.1 kDa	4.44
54	Tropomyosin β chain	Q5TCU3	57.04%	18	32.8 kDa	4.68
	Tropomyosin β chain	P07951	45.42%	16	32.8 kDa	4.70
	Tropomyosin β chain	Q5TCU8	40.06%	16	36.7 kDa	4.78
	Tropomyosin α1 chain	P09493	24.65%	8	32.7 kDa	4.74
	Tropomyosin α3 chain	P06753	22.81%	8	32.9 kDa	4.72
	Tropomyosin α3 chain	J3KN67	22.81%	8	33.2 KDa	4.77
	Tropomyosin 1 (alpha) isoform CRA_f	Q6ZN40	21.47%	8	37.4 kDa	4.72
	Tropomyosin α1 chain	B7Z596	14.18%	5	31.7 kDa	4.89
56	Tropomyosin α4 chain	P67936	68.95%	22	28.5 kDa	4.69
	Tropomyosin β chain	P07951	23.24%	10	32.8 kDa	4.70
	Tropomyosin β chain	Q5TCU3	23.24%	10	32.8 kDa	4.68
	Tropomyosin β chain	Q5TCU8	20.50%	10	36.7 kDa	4.78
	Tropomyosin 1 (alpha) isoform CRA_m	FSH7S3	20.41%	7	28.7 kDa	4.82
	Tropomyosin α1 chain	H0YK48	20.16%	7	28.6 kDa	4.77
	Tropomyosin α1 chain	B7Z596	18.18%	7	31.7 kDa	4.89
	Tropomyosin α1 chain	P09493	17.61%	7	32.7 kDa	4.74
	Tropomyosin 1 (alpha) isoform CRA_f	Q6ZN40	15.34%	7	37.4 kDa	4.72
62	Heat shock cognate 71 (HSPA8)	A8K7Q2	19.27%	5	45.3 kDa	5.64
	Heat shock cognate 71 (HSPA8)	E9PNE6	15.8%	5	54.9 kDa	5.68
	Heat shock cognate 71 (HSPA8)	E9PKE3	12.6%	5	68.8 kDa	5.52
	Heat shock cognate 71 (HSPA8)	P11142	12.23%	5	70.9 kDa	5.52

Name of the identified protein, number of 2D gel spot, number of peptides identified and percentage of sequence protein coverage by HPLC/MS analysis, Uniprot entry, molecular weight (MW) in kiloDalton (kDa) and isoelectric point (pI) are shown for each identified protein.

Immunomodulatory and anti-inflammatory properties of the UC-MSCs.

UC-MSCs can modulate the inflammation. In particular, these cells can reduce the pro-inflammation cytokines and chemokines, and increase anti-inflammation molecules [14]. These anti-inflammatory properties of UC-MSCs indicate that these cells are a pivotal source of transplantable stem cells with reduced risk of immune-rejection.

A major finding here is that immunomodulatory proteins Galectin-1 (Gal-1) and B7-H3 were detected in western blot experiments conducted on 2D-SDS-PAGE gels (2D-WB, Figure 13).

Gal-1 is a key regulator of such immune responses as T-cell homeostasis and survival [216]. Gal-1 is a lectin with a sequence of 135 amino acids, with a molecular weight of 14.7 kDa, and a carbohydrate recognition domain responsible for β-galactoside binding [216]. The glycosylated form of Gal-1 is about 29 kDa [216]. Interestingly, three spots at 14.7 kDa and one at 29 kDa were detected in 2D-WB analysis of UC-MSCs cell lysate (Figure 13A). The three spots at 14.7 kDa correspond to different post-translational modifications. In order to investigate the structure of Gal-1, a mass spectrometry of analysis of UC-MSCs whole cell lysate was conducted. Gal-1 was identified in mass spectrometry analysis with the 73.33% of protein sequence coverage. Additionally, two post-translational modifications were detected: cysteine (C) carbamidomethylation (cysteine residues: C6, C12 and C15) and methionine oxidation (methionine residue M9) (Table 7). The carbamidomethylation on cysteine is a fixed modification of 2D-SDS-PAGE. Mass spectrometry was initiated after treatment with IAA and revealed that cysteine and methionine residues in proteins were both sensitive to reversible oxidation and reduction reactions. Based on the literature, the reduced form of Gal-1 has been shown to be critical for its inflammatory and pro-apoptotic activity, while oxidized Gal-1 has been reported to promote neurite outgrowth and enhance axonal regeneration in peripheral and central nerves [216]. In addition, during axonal regeneration, cytosolic oxidized Gal-1 is secreted in extracellular space, which induces macrophages to secrete an axonal regeneration promoting factor that influences Schwann cells, fibroblasts and perineuronal cells [216]. Taken together, these results show that the immunomodulatory and neuroregenerative functions of UC-MSCs could be linked to the cytosolic Gal-1. However, further analysis will be needed to better identify the corresponding gel spots of 2D-WB to determine its post-translational modifications.

The second immunodulatory protein identified by using 2D-WB is B7-H3 (Figure 13), which belongs to the B7 superfamily, a group of molecules that co-stimulate or down-modulate T cell responses [217]. The functional role of B7-H3 is controversial. This receptor was originally described as a potent costimulatory molecule and inducer of interferon γ (IFN-γ) in human T cells [218]. On the other hand, B7-H3 has been shown to potently and consistently down-modulate human T cell responses by decreasing the expression of IL-2 [217] [219]. These opposite effects could be explained by the existence of four different isoforms of B7-H3 produced by alternative splicing. Indeed, isoform 2 has been shown to enhance the induction of cytotoxic T-cells and selectively stimulate IFN-γ production in the presence of T-cell receptor signaling [218]. For the first time in UC-MSC, La Rocca's research group demonstrated in both undifferentiated and chondrogenic-like cells the presence of B7-H3 in both immunohistochemistry and RNA level [13]. Here, 2D-WB confirmed the expression of B7-H3 in UC-MSCs at protein level revealing two spots at 57.2 kDa and one bigger spot at about 100 kDa that corresponded with the glycosylated form of the protein (Figure 13B). The four isoforms of the human B7-H3 have a molecular weight of 57.23, 33.79, 52.76 and 57.16 kDa respectively [213]. In order to avoid concerns about the identification of B7-H3 isoforms, the antibody used in this study was specific for an epitope common to all the four isoforms, mapping between amino acids 82-107 near the N-terminus of B7-H3 of human origin (see Materials and Methods section). The 2D-WB result showed that UC-MSCs expressed only the isoform 1 of B7-H3. However, the expression of isoform 4 cannot be excluded because it varies from isoform 1 for only 70 Da and this extremely minimal difference could not be clearly delineated in the 2D-WB. Notwithstanding, the presence of two spots at about 57.2 kDa could be post-translational modifications of isoform 1 or both the isoform 1 and 4 of B7-H3. Further investigations with mass spectrometry are in progress to identify the protein structure of B7-H3 in UC-MSCs.

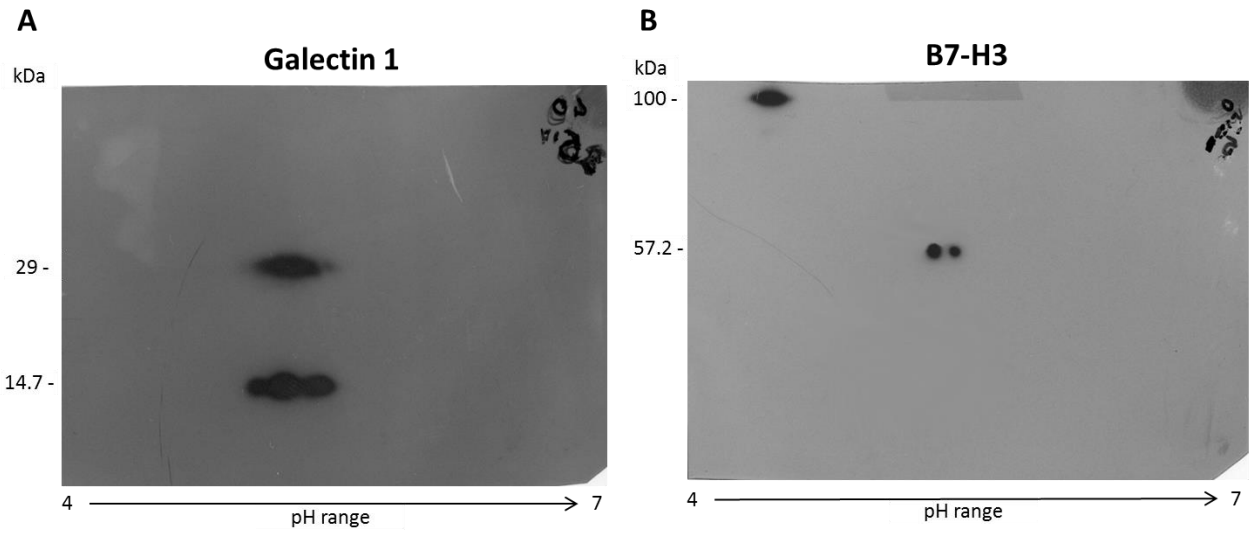

Figure 13. 2D-WB detection of immunomodulatory selected proteins B7-H3 and Galectin 1. 100 µg of total proteins extract of UC-MSCs were separated by IEF in a 7-cm-long IPG strip containing a linear pH gradient 4-7 followed by SDS-PAGE in a 12% gel. A) Galectin-1, B) B7-H3.

Table 7. Identification of Galectin-1 in UC-MSCs whole-cell lysate by mass spectrometry.

Identification of cytosolic Galectin-1			
Uniprot entry	**Description**	**% Coverage**	**# Identified Peptides**
P09382	Galectin-1	73,33	8
#	**Peptidic Sequence**	**Modifications**	**MH+ [Da]**
1	LNLEAINYMAADGDFK		1784,86
2	EAVFPFQPGSVAEVCITFDQANLTVK	C15(Carbamidomethyl)	2867,44
3	LNLEAINYMAADGDFK	M9(Oxidation)	1800,85
4	FNAHGDANTIVCNSK	C12(Carbamidomethyl)	1647,76
5	DSNNLCLHFNPR	C6(Carbamidomethyl)	1486,69
6	LNLEAINYMAADGDFKIK		2026,04
7	DGGAWGTEQR		1076,48
8	SFVLNLGK		877,51
9	VRGEVAPDAK		1041,57

Proteomic analysis of UC-MSCs cellular proteins

Cell lysates were collected and analyzed by using mass spectrometry. In this study, in order to make the identification significant, only the proteins identified with ≥ 3 peptides were considered.

Furthermore, a GO analysis of UC-MSCs control cell lysates was performed to know the regenerative potential of these cells. Several proteins identified were related to neurogenesis; gliogenesis; neuron and glia differentiation; axonogenesis; synaptic signaling; neurotransmitter transport; myelination; learning or memory; adult behavior; angiogenesis; blood vessel development and morphogenesis; endothelial cell migration; regulation of cell death; response hypoxia, oxidative stress and pH; immunomodulation; ECM organization and remodeling; these proteins are listed in

Table 8. UC-MSCs express neural markers and neurotrophic markers, as well as factors that promote angiogenesis and remodeling of ECM that could be advantageous for neurovascular unit repair. In addition, several proteins identified with HPLC/MS indicating these proteins' relevance to immunomodulatory and anti-inflammatory properties of UC-MSCs. Moreover, the UC-MSCs ability to survive in ischemic conditions could be ascribed to identify proteins involved in response to oxidative stress, hypoxia and pH variations as well as the different proteins involved in the regulation of programmed cell death. Altogether, these protein readouts support the potential role of UC-MSCs for the treatment of stroke.

These findings support the beneficial potential of UC-MSCs in regenerative medicine, in particular stem cell therapies for CNS diseases including stroke.

Table 8. GO analysis of UC-MSCs cell lysates

N	Uniprot entry	Protein
		Neurogenesis, gliogenesis, neuron and glia differentiation, axonogenesis
1	Q6IQ32	ADNP homeobox 2(ADNP2)
2	P36405	ADP ribosylation factor like GTPase 3(ARL3)
3	Q8NFD5	AT-rich interaction domain 1B(ARID1B)
4	Q8N157	Abelson helper integration site 1(AHI1)
5	P10415	BCL2, apoptosis regulator(BCL2)
6	Q8TD84	DS cell adhesion molecule like 1(DSCAML1)
7	P32004	L1 cell adhesion molecule(L1CAM)
8	Q07954	LDL receptor related protein 1(LRP1)
9	P54802	N-acetyl-alpha-glucosaminidase(NAGLU)
10	Q92597	N-myc downstream regulated 1(NDRG1)
11	A0A1B0GUJ1	NMDA receptor synaptonuclear signaling and neuronal migration factor(NSMF)
12	Q01851	POU class 4 homeobox 1(POU4F1)
13	Q9Y566	SH3 and multiple ankyrin repeat domains 1(SHANK1)
14	S4R3Q7	adhesion G protein-coupled receptor B3(ADGRB3)
15	E9PQE6	adrenomedullin(ADM)
16	P15514	amphiregulin(AREG)
17	E9PG40	amyloid beta precursor protein(APP)
18	Q9UBB4	ataxin 10(ATXN10)
19	P19022	cadherin 2(CDH2)
20	Q9NYQ7	cadherin EGF LAG seven-pass G-type receptor 3(CELSR3)
21	A0A087X097	cadherin related 23(CDH23)
22	P32297	cholinergic receptor nicotinic alpha 3 subunit(CHRNA3)
23	Q02246	contactin 2(CNTN2)
24	A0A0J9YWG3	contactin associated protein-like 2(CNTNAP2)
25	H7C1N2	cordon-bleu WH2 repeat protein(COBL)
26	P21728	dopamine receptor D1(DRD1)
27	Q9UHG0	doublecortin domain containing 2(DCDC2)
28	P50570	dynamin 2(DNM2)
29	F8W717	echinoderm microtubule associated protein like 1(EML1)
30	O14682	ectodermal-neural cortex 1(ENC1)
31	A0A0A0MRA8	erythrocyte membrane protein band 4.1 like 3(EPB41L3)
32	D6RBH3	glycoprotein M6A(GPM6A)
33	P07686	hexosaminidase subunit beta(HEXB)
34	Q6UXK2	immunoglobulin superfamily containing leucine rich repeat 2(ISLR2)
35	Q9NZI8	insulin like growth factor 2 mRNA binding protein 1(IGF2BP1)
36	O60229	kalirin, RhoGEF kinase(KALRN)
37	Q96Q89	kinesin family member 20B(KIF20B)
38	O60282	kinesin family member 5C(KIF5C)
39	P55145	mesencephalic astrocyte derived neurotrophic factor(MANF)
40	A0A075B6F8	Microcephalin (MCPH1)
41	Q09666	Neuroblast differentiation-associated protein AHNAK (AHNAK)
42	P21359	neurofibromin 1(NF1)
43	Q9Y422	neurogenin 3(NEUROG3)
44	C9JYY6	neuronal cell adhesion molecule(NRCAM)
45	C9J5P6	nitric oxide synthase 1(NOS1)
46	Q92597	N-myc downstream regulated 1(NDRG1)
47	Q9UM47	notch 3(NOTCH3)
48	Q9HCM2	plexin A4(PLXNA4)
49	O15031	plexin B2(PLXNB2)
50	Q9ULL4	plexin B3(PLXNB3)
51	H0Y8A4	receptor-like tyrosine kinase(RYK)
52	Q9NQC3	reticulon 4(RTN4)
53	Q14563	semaphorin 3A(SEMA3A)
54	Q9NS98	semaphorin 3G(SEMA3G)
55	Q9C0C4	semaphorin 4C(SEMA4C)
56	F8WAT5	semaphorin 5B(SEMA5B)
57	Q8NFY4	semaphorin 6D(SEMA6D)
58	P07093	serpin family E member 2(SERPINE2)
59	E7EW28	solute carrier family 4 member 10(SLC4A10)
60	O15020	spectrin beta, non-erythrocytic 2(SPTBN2)
61	Q9BUD6	spondin 2(SPON2)
62	O43426	synaptojanin 1(SYNJ1)
63	Q9NT68	teneurin transmembrane protein 2(TENM2)
64	Q6NT89	TMF1-regulated nuclear protein 1(TRNP1)
65	Q13509	tubulin beta 3 class III(TUBB3)
66	Q6ZN44	unc-5 netrin receptor A(UNC5A)
67	A0A087X152	unc-5 netrin receptor C(UNC5C)
		Synaptic signalling, neurotransmitter transport
68	P28335	5-hydroxytryptamine receptor 2C(HTR2C)
69	Q8NFD5	AT-rich interaction domain 1B(ARID1B)
70	A0A1B0GUJ1	NMDA receptor synaptonuclear signaling and neuronal migration factor(NSMF)
71	A0A087WZQ7	NSF attachment protein beta(NAPB)
72	O75145	PTPRF interacting protein alpha 3(PPFIA3)
73	Q99497	Parkinsonism associated deglycase(PARK7)
74	Q9Y566	SH3 and multiple ankyrin repeat domains 1(SHANK1)
75	H0YHD6	acid sensing ion channel subunit 1(ASIC1)
76	Q9UPA5	bassoon presynaptic cytomatrix protein(BSN)
77	P32297	cholinergic receptor nicotinic alpha 3 subunit(CHRNA3)
78	Q8WVH0	complexin 3(CPLX3)
79	Q02246	contactin 2(CNTN2)
80	E9PDN6	contactin associated protein like 4(CNTNAP4)
81	A0A087WV24	dopa decarboxylase(DDC)
82	P21728	dopamine receptor D1(DRD1)
83	A0A0G2JM26	dopamine receptor D4(DRD4)
84	C9JEN8	fibroblast growth factor 12(FGF12)
85	G3V0J0	fragile X mental retardation 1(FMR1)
86	O00591	gamma-aminobutyric acid receptor subunit pi (GABRP)
87	P39905	glial cell derived neurotrophic factor(GDNF)
88	P14136	glial fibrillary acidic protein(GFAP)
89	Q13003	glutamate ionotropic receptor kainate type subunit 3(GRIK3)
90	O00222	glutamate metabotropic receptor 8(GRM8)
91	O75311	glycine receptor alpha 3(GLRA3)
92	O60229	kalirin, RhoGEF kinase(KALRN)
93	P21359	neurofibromin 1(NF1)
94	Q8TDF5	neuropilin and tolloid like 1(NETO1)
95	Q9Y2I1	nischarin(NISCH)
96	C9J5P6	nitric oxide synthase 1(NOS1)
97	Q9Y6V0	piccolo presynaptic cytomatrix protein(PCLO)
98	P05129	protein kinase C gamma(PRKCG)
99	Q13332	protein tyrosine phosphatase, receptor type S(PTPRS)
100	O95197	reticulon 3(RTN3)
101	P07093	serpin family E member 2(SERPINE2)
102	O43426	synaptojanin 1(SYNJ1)
103	Q16563	synaptophysin like 1(SYPL1)
104	Q8NB66	unc-13 homolog C(UNC13C)
		Myelination
105	Q92597	N-myc downstream regulated 1(NDRG1)
106	Q01484	ankyrin 2(ANK2)
107	Q02246	contactin 2(CNTN2)
108	A0A0A0MRA8	erythrocyte membrane protein band 4.1 like 3(EPB41L3)
109	P07686	hexosaminidase subunit beta(HEXB)
110	P21359	neurofibromin 1(NF1)

N	Uniprot entry	Protein
		Learning or memory
111	Q9Y566	SH3 and multiple ankyrin repeat domains 1(SHANK1)
112	H0YHD6	acid sensing ion channel subunit 1(ASIC1)
113	S4R307	adhesion G protein-coupled receptor B3(ADGRB3)
114	E9PG40	amyloid beta precursor protein(APP)
115	Q02246	contactin 2(CNTN2)
116	A0A0J9YWG3	contactin associated protein-like 2(CNTNAP2)
117	P21728	dopamine receptor D1(DRD1)
118	P06744	glucose-6-phosphate isomerase(GPI)
119	P42858	huntingtin(HTT)
120	O60229	kalirin, RhoGEF kinase(KALRN)
121	P21359	neurofibromin 1(NF1)
122	Q8TDF5, J3QRI	neuropilin and tolloid like 1(NETO1)
123	P05129	protein kinase C gamma(PRKCG)
124	O43426	synaptojanin 1(SYNJ1)
125	Q9C0D5	tetratricopeptide repeat, ankyrin repeat and coiled-coil containing 1(TANC1)
		Adult behaviour
126	O15118	NPC intracellular cholesterol transporter 1(NPC1)
127	Q99497	Parkinsonism associated deglycase(PARK7)
128	Q9Y566	SH3 and multiple ankyrin repeat domains 1(SHANK1)
129	E9PG40	amyloid beta precursor protein(APP)
130	P32297	cholinergic receptor nicotinic alpha 3 subunit(CHRNA3)
131	Q02246	contactin 2(CNTN2)
132	A0A0J9YWG3	contactin associated protein-like 2(CNTNAP2)
133	P21728	dopamine receptor D1(DRD1)
134	A0A0G2JM26	dopamine receptor D4(DRD4)
135	C9JEN8	fibroblast growth factor 12(FGF12)
136	O60229	kalirin, RhoGEF kinase(KALRN)
137	O15020	spectrin beta, non-erythrocytic 2(SPTBN2)
		Response to oxidative stress
138	Q6IQ32	ADNP homeobox 2(ADNP2)
139	P10415	BCL2, apoptosis regulator(BCL2)
140	Q99497	Parkinsonism associated deglycase(PARK7)
141	P15514	amphiregulin(AREG)
142	E9PG40	amyloid beta precursor protein(APP)
143	P27540	aryl hydrocarbon receptor nuclear translocator(ARNT)
144	E9PJL7	crystallin alpha B(CRYAB)
145	P50570	dynamin 2(DNM2)
146	P04062	glucosylceramidase beta(GBA)
147	P09211	glutathione S-transferase pi 1(GSTP1)
148	A0A1B0GTF3	Heat shock 70 kDa protein 12A (HSPA12A)
149	Q53FA3	Heat shock 70 kDa protein 1-like (Fragment) (HSPA1L)
150	A0A087WYC1	Heat shock 70 kDa protein 4 (HSPA4)
151	P34932	Heat shock 70 kDa protein 4 (HSPA4)
152	P11142	Heat shock cognate 71 kDa protein (HSPA8)
153	H0YBT7	Heat shock factor protein 4 (Fragment) (HSF4)
154	P04792	Heat shock protein beta-1 (HSPB1)
155	K7EP04	Heat shock protein beta-6 (HSPB6)
156	P07900	Heat shock protein HSP 90-alpha (HSP90AA1)
157	P08238	Heat shock protein HSP 90-beta (HSP90AB1)
158	U3KPY4	Membralin (TMEM259)
159	Q06830	Peroxiredoxin-1 (PRDX1)
160	P32119	Peroxiredoxin-2 (PRDX2)
161	Q13162	Peroxiredoxin-4 (PRDX4)
162	P30044	Peroxiredoxin-5, mitochondrial (PRDX5)
163	P30041	Peroxiredoxin-6 (PRDX6)
164	Q8TED1	Probable glutathione peroxidase 8 (GPX8)
165	P07602	prosaposin(PSAP)
166	P05129	Protein kinase C gamma type (PRKCG)
167	Q9NZJ4	Sacsin OS=Homo sapiens (SACS)
168	P38646	Stress-70 protein, mitochondrial (HSPA9, GRP75)
169	P00441	Superoxide dismutase [Cu-Zn] (SOD1)
170	P04179	Superoxide dismutase [Mn], mitochondrial (SOD2)
171	O95881	Thioredoxin domain-containing protein 12 (TXD12)
172	P10599	Thioredoxin (TXN)
173	P30048	Thioredoxin-dependent peroxide reductase, mitochondrial (PRDX3)
		Response to hypoxia
174	E9PQE6	adrenomedullin(ADM)
175	P55786	aminopeptidase puromycin sensitive(NPEPPS)
176	Q9Y264	angiopoietin 4(ANGPT4)
177	Q15327	ankyrin repeat domain 1(ANKRD1)
178	P27540	aryl hydrocarbon receptor nuclear translocator(ARNT)
179	P10415	BCL2, apoptosis regulator(BCL2)
180	E9PJL7	crystallin alpha B(CRYAB)
181	H0YDZ5	hypoxia inducible factor 3 alpha subunit(HIF3A)
182	Q9Y4L1	hypoxia up-regulated 1(HYOU1)
183	P05362	intercellular adhesion molecule 1(ICAM1)
184	P50281	matrix metallopeptidase 14(MMP14)
185	Q92597	N-myc downstream regulated 1(NDRG1)
186	P21359	neurofibromin 1(NF1)
187	C9J5P6	nitric oxide synthase 1(NOS1)
188	Q15185	prostaglandin E synthase 3 (PTGES3)
189	P04179	superoxide dismutase 2, mitochondrial(SOD2)
190	Q9NQ88	TP53 induced glycolysis regulatory phosphatase(TIGAR)
191	P61812	transforming growth factor beta 2(TGFB2)
192	Q6EMK4	vasorin(VASN)
		Response to pH
193	H0YHD6	acid sensing ion channel subunit 1(ASIC1)
194	P15289	arylsulfatase A(ARSA)
195	P04062	glucosylceramidase beta(GBA)

N	Uniprot entry	Protein
		Blood vessel development and morphogenesis, angiogenesis, endothelial cell migration
196	O00522	KRIT1, ankyrin repeat containing(KRIT1)
197	A2A3C6	adhesion G protein-coupled receptor B2(ADGRB2)
198	S4R307	adhesion G protein-coupled receptor B3(ADGRB3)
199	P15144	alanyl aminopeptidase, membrane(ANPEP)
200	Q12904	aminoacyl tRNA synthetase complex interacting multifunctional protein 1(AIMP1)
201	P15144	aminopeptidase N (AMPN)
202	C9JTS3	angio associated migratory cell protein(AAMP)
203	Q4VCS5	angiomotin(AMOT)
204	Q9Y264	angiopoietin 4(ANGPT4)
205	Q9Y5C1	angiopoietin like 3(ANGPTL3)
206	Q9Y574	ankyrin repeat and SOCS box containing 4(ASB4)
207	Q15327	ankyrin repeat domain-containing protein 1 (ANKR1)
208	H0YM23	ankyrin repeat domain 17(ANKRD17)
209	P07355	annexin A2(ANXA2)
210	Q9H6X2	anthrax toxin receptor 1(ANTXR1)
211	P27540	aryl hydrocarbon receptor nuclear translocator (ARNT)
212	P02452	collagen type I alpha 1 chain(COL1A1)
213	A0A087WTA8	collagen type I alpha 2 chain(COL1A2)
214	P02461	collagen type III alpha 1 chain(COL3A1)
215	P02462	collagen type IV alpha 1 chain(COL4A1)
216	P20908	collagen type V alpha 1 chain(COL5A1)
217	P27658	collagen type VIII alpha 1 chain(COL8A1)
218	P02751	Fibronectin, fibroblast activation protein alpha(FAP)
219	Q8N387	fibronectin 1(FN1)
220	P35916	fms related tyrosine kinase 4(FLT4)
221	Q08431	lactadherin (MFGE8)
222	P50281	matrix metallopeptidase 14(MMP14)
223	Q969H8	myeloid derived growth factor(MYDGF)
224	J3KNQ4	parvin alpha(PARVA)
225	P11464	Pregnancy-specific beta-1-glycoprotein 1 (PSG1)
226	P35916	Vascular endothelial growth factor receptor 3 (VEGFR3)
		Immunomodulation
227	F5GZS6	4F2 cell-surface antigen heavy chain
228	O43865	Adenosylhomocysteinase 2
229	Q9BY15	Adhesion G protein-coupled receptor E3
230	H0YM23	Ankyrin repeat domain-containing protein 17 (Fragment)
231	P04083	Annexin A1
232	A0A140T9T7	Antigen peptide transporter 1
233	P10415	Apoptosis regulator Bcl-2
234	H0YH65	Armadillo repeat-containing protein 6 (Fragment)
235	Q8IUR7	Armadillo repeat-containing protein 8
236	Q8N143	B-cell CLL/lymphoma 6 member B protein (BCL6B)
237	O00512	B-cell CLL/lymphoma 9 protein (BCL9)
238	P51572	B-cell receptor-associated protein 31 (BAP31)
239	A0A075B6Q3	BCL-6 corepressor-like protein 1 (Fragment) (BCL-6)
240	P61769	Beta-2-microglobulin (B2MG)]
241	P15391	B-lymphocyte antigen CD19 (CD19)
242	P14902	Indoleamine 2,3-dioxygenase 1 (IDO-1)
243	A0A0N4SWI6	Indoleamine 2,3-dioxygenase 2 (IDO-2)
244	P09382	Galectin-1 (Gal-1)
245	Q96DT0	Galectin-12 (Gal-12)
246	P17931	Galectin-3 (Gal-3)
247	Q08380	Galectin-3-binding protein(Gal-3BP)
248	P28799	Granulins(Grn)
249	P30685	HLA class I histocompatibility antigen, B-35 alpha chain (HLA-B)
250	P10319	HLA class I histocompatibility antigen, B-58 alpha chain (HLA-B)
251	P30508	HLA class I histocompatibility antigen, Cw-12 alpha chain (HLA-C)
252	Q95604	HLA class I histocompatibility antigen, Cw-17 alpha chain (HLA-C)
253	H0YBZ2	HLA class II histocompatibility antigen gamma chain (Fragment) (CD74)
254	A2AAZ0	HLA class II histocompatibility antigen, DQ beta 1 chain (HLA-DQB1)
255	K4DIA0	ICOS ligand (B7-H2, CD275)
256	A0A0G2JP11	Immunoglobulin alpha Fc receptor (CD89)
257	Q8TDY8	Immunoglobulin superfamily DCC subclass member 4 (IGDCC4)
258	O75054	Immunoglobulin superfamily member 3 (IGSF3)
259	P05362	Intercellular adhesion molecule 1 (ICAM1)
260	B5MCZ0	Interferon gamma receptor 2 (IFNGR2)
261	K4DIA5	Interferon regulatory factor 2 (Fragment) (IRF2)
262	Q13325	Interferon-induced protein with tetratricopeptide repeats 5 (IFIT5)
263	Q7Z2Y8	Interferon-induced very large GTPase 1 (GVINP1)
264	B4DY09	Interleukin enhancer-binding factor 2 (ILF2)
265	K7EMZ8	Interleukin enhancer-binding factor 3 (Fragment) (ILF3)
266	K7EQR9	Interleukin enhancer-binding factor 3 (Fragment) (ILF3)
267	Q9NZN1	Interleukin-1 receptor accessory protein-like 1(IL1RAPL1)
268	H0YD11	Interleukin-15 receptor subunit alpha (Fragment) (IL15RA)
269	Q9NRM6	Interleukin-17 receptor B (IL17RB)
270	Q9NS15	Latent-transforming growth factor beta-binding protein 3(LTBP3)
271	F8W6G6	Leukocyte immunoglobulin-like receptor subfamily B member 3 (LILRB3)
272	Q08722	Leukocyte surface antigen CD47 (CD47)
273	P22897	Macrophage mannose receptor 1 (MRC1)
274	P14174	Macrophage migration inhibitory factor (MIF)
275	P41279	Mitogen-activated protein kinase kinase kinase 8 (MAP3K8)
276	Q9BZM6	NKG2D ligand 1 (N2DL1)
277	Q8TD07	NKG2D ligand 4 (N2DL4)
278	P19838	Nuclear factor NF-kappa-B p105 subunit (NFKB1)
279	O95644	Nuclear factor of activated T-cells, cytoplasmic 1 (NFATC1)
280	Q13469	Nuclear factor of activated T-cells, cytoplasmic 2(NFATC2)
281	Q6P4R8	Nuclear factor related to kappa-B-binding protein (NFRKB)
282	P11464	Pregnancy-specific beta-1-glycoprotein 1 (PSG1)
283	Q00888	Pregnancy-specific beta-1-glycoprotein 4 (PSG4)
284	Q14005	Pro-interleukin-16 (IL16)
285	Q8N3R3	T-cell activation inhibitor, mitochondrial (TCAIM)
286	P06729	T-cell surface antigen CD2 (CD2)
287	B7ZAN3	Tetraspanin CD37 (CD37)
288	E9PJK1	Tetraspanin CD81 (CD81)
289	Q7L0X0	TLR4 interactor with leucine rich repeats (TRIL)
290	P61812	Transforming growth factor beta-2 (TGFB2)
291	Q15582	Transforming growth factor-beta-induced protein ig-h3 (BIGH3)
292	O43557	Tumor necrosis factor ligand superfamily member 14 (CD58)
293	A0A087X228	Tumor necrosis factor ligand superfamily member 8 (CD30L, CD153)
294	A0A0D9SF52	Tumor necrosis factor receptor superfamily member 14 (Fragment) (CD270)
295	P23458	Tyrosine-protein kinase JAK1 (JAK1)
296	P06239	Tyrosine-protein kinase Lck (LCK)
297	Q6EMK4	Vasorin (VASN)

N	Uniprot entry	Protein
		Extracellular matrix organization
298	P01023	alpha-2-macroglobulin(A2M)
299	E9PG40	amyloid beta precursor protein(APP)
300	P07355	annexin A2(ANXA2)
301	P23352	anosmin-1 (ANOS1)
302	Q9H6X2	anthrax toxin receptor 1(ANTXR1)
303	A0A087X2B5	basigin (Ok blood group)(BSG)
304	P21810	biglycan(BGN)
305	P02452	collagen type I alpha 1 chain(COL1A1)
306	A0A087WTA8	collagen type I alpha 2 chain(COL1A2)
307	P02461	collagen type III alpha 1 chain(COL3A1)
308	P02462	collagen type IV alpha 1 chain(COL4A1)
309	P20908	collagen type V alpha 1 chain(COL5A1)
310	P25940	collagen type V alpha 3 chain(COL5A3)
311	A0A087X0S5	collagen type VI alpha 1 chain(COL6A1)
312	P12110	collagen type VI alpha 2 chain(COL6A2)
313	P12111	collagen type VI alpha 3 chain(COL6A3)
314	P27658	collagen type VIII alpha 1 chain(COL8A1)
315	D6RGG3	collagen type XII alpha 1 chain(COL12A1)
316	Q05707	collagen type XIV alpha 1 chain(COL14A1)
317	A0A0C4DFX3	elastin microfibril interfacer 1(EMILIN1)
318	G5E950	elastin(ELN)
319	A0A0C4DFX3	EMILIN-1 (EMILIN1)
320	Q9BXX0	EMILIN-2 (EMILIN2)
321	P35555	fibrillin 1(FBN1)
322	Q12884	fibronectin, fibroblast activation protein alpha(FAP)
323	P02751	fibronectin 1(FN1)
324	Q8N387	mucin-15 (MUC15)
325	Q8WXI7	mucin-16 (MUC16)
326	Q7Z5P9	mucin-19 (MUC19)
327	Q02817	mucin-2 (MUC2)
328	A0A0G2JR84	mucin-20 (MUC20)
329	P10915	hyaluronan and proteoglycan link protein 1(HAPLN1)
330	Q6ZMP0	thrombospondin type 1 domain containing 4(THSD4)
331	P04004	vitronectin(VTN)
		Blood vessel development and morphogenesis, angiogenesis, endothelial cell migration
332	O00522	KRIT1, ankyrin repeat containing(KRIT1)
333	A2A3C6	adhesion G protein-coupled receptor B2(ADGRB2)
334	S4R307	adhesion G protein-coupled receptor B3(ADGRB3)
335	P15144	alanyl aminopeptidase, membrane(ANPEP)
336	Q12904	aminoacyl tRNA synthetase complex interacting multifunctional protein 1(AIMP1)
337	P15144	aminopeptidase N (AMPN)
338	C9JTS3	angio associated migratory cell protein(AAMP)
339	Q4VCS5	angiomotin(AMOT)
340	Q9Y264	angiopoietin 4(ANGPT4)
341	Q9Y5C1	angiopoietin like 3(ANGPTL3)
342	Q9Y574	ankyrin repeat and SOCS box containing 4(ASB4)
343	Q15327	ankyrin repeat domain-containing protein 1 (ANKR1)
344	H0YM23	ankyrin repeat domain 17(ANKRD17)
345	P07355	annexin A2(ANXA2)
346	Q9H6X2	anthrax toxin receptor 1(ANTXR1)
347	P27540	aryl hydrocarbon receptor nuclear translocator (ARNT)
348	P02452	collagen type I alpha 1 chain(COL1A1)
349	A0A087WTA8	collagen type I alpha 2 chain(COL1A2)
350	P02461	collagen type III alpha 1 chain(COL3A1)
351	P02462	collagen type IV alpha 1 chain(COL4A1)
352	P20908	collagen type V alpha 1 chain(COL5A1)
353	P27658	collagen type VIII alpha 1 chain(COL8A1)
354	P02751	Fibronectin, fibroblast activation protein alpha(FAP)
355	Q8N387	fibronectin 1(FN1)
356	P35916	fms related tyrosine kinase 4(FLT4)
357	Q08431	lactadherin (MFGE8)
358	P50281	matrix metallopeptidase 14(MMP14)
359	Q969H8	myeloid derived growth factor(MYDGF)
360	J3KNQ4	parvin alpha(PARVA)
361	P11464	Pregnancy-specific beta-1-glycoprotein 1 (PSG1)
362	P35916	Vascular endothelial growth factor receptor 3 (VEGFR3)
		Extracellular matrix remodeling
363	Q8N6G6	ADAMTS-like protein 1 (ADAMTSL1)
364	Q6UY14	ADAMTS-like protein 4 (ADAMTSL4)
365	P01023	alpha-2-macroglobulin(A2M)
366	P54802	alpha-N-acetylglucosaminidase (ANAG)
367	P52849	bifunctional heparan sulfate N-deacetylase/N-sulfotransferase 2 (NDST2)
368	Q9UKJ8	disintegrin and metalloproteinase domain-containing protein 21 (ADAM21)
369	F8WAD8	disintegrin and metalloproteinase domain-containing protein 22 (Fragment) (ADAM22)
370	P50281	matrix metalloproteinase-14 (MMP14, MT-MMP1)
371	Q9NR99	matrix-remodeling-associated protein 5 (MXRA5)
372	P35625	metalloproteinase inhibitor 3 (TIMP3)
373	P56730	neurotrypsin (NETR)
374	Q6IE37	ovostatin homolog 1 (OVOS1)
375	Q12884	prolyl endopeptidase FAP (SEPR)
376	P55786	puromycin-sensitive aminopeptidase (PSA)
377	Q6ZMP0	thrombospondin type-1 domain-containing protein 4 (ADAMTSL6)
378	C9J6G4	WAP, Kazal, immunoglobulin, Kunitz and NTR domain-containing protein 2 (GASP1)
379	Q5T6H7	xaa-Pro aminopeptidase 1 (XPNPEP1)
380	P12955	xaa-Pro dipeptidase (PEPD)

Extracellular matrix remodeling potential of the UC-MSCs.

Proteomic analysis of lysates identified several proteins involved in ECM organization and remodeling (

Table 8). Recently, the focus of many studies on MSCs is the connection between cells and matrix signals. Matrix metalloproteases (MMPs) and tissue-specific inhibitors of metalloproteases (TIMPs) are crucial for matrix remodeling processes, a key step towards regeneration. MMPs are a family of zinc-dependent proteolytic enzymes involved in the degradation of ECM components [220]. They are regulated by several MMP-specific inhibitors called TIMPs from TIMP-1 to TIMP-4. MMPs aid in the differentiation of MSCs into different lineages (adipogenic, chondrogenic, osteogenic and endothelial differentiation). Moreover, MSCs express MMPs and TIMPs to regulate different processes such as angiogenesis, proliferation, migration [221]. Moreover, MMPs and TIMPs are involved in BBB opening and neuroinflammation in stroke as well as in promoting stem cells endogenous repair mechanisms [5] [222].

Proteomic analysis identified MT-MMP1 and TIMP-3 in UC-MSCs lysates (

Table 8). In order to further validate the expression of MMPs and TIMPs in the UC-MSCs, IHC experiments were performed. UC-MSCs have shown high expression of MMPs and low expression of TIMPs (Figure 14).

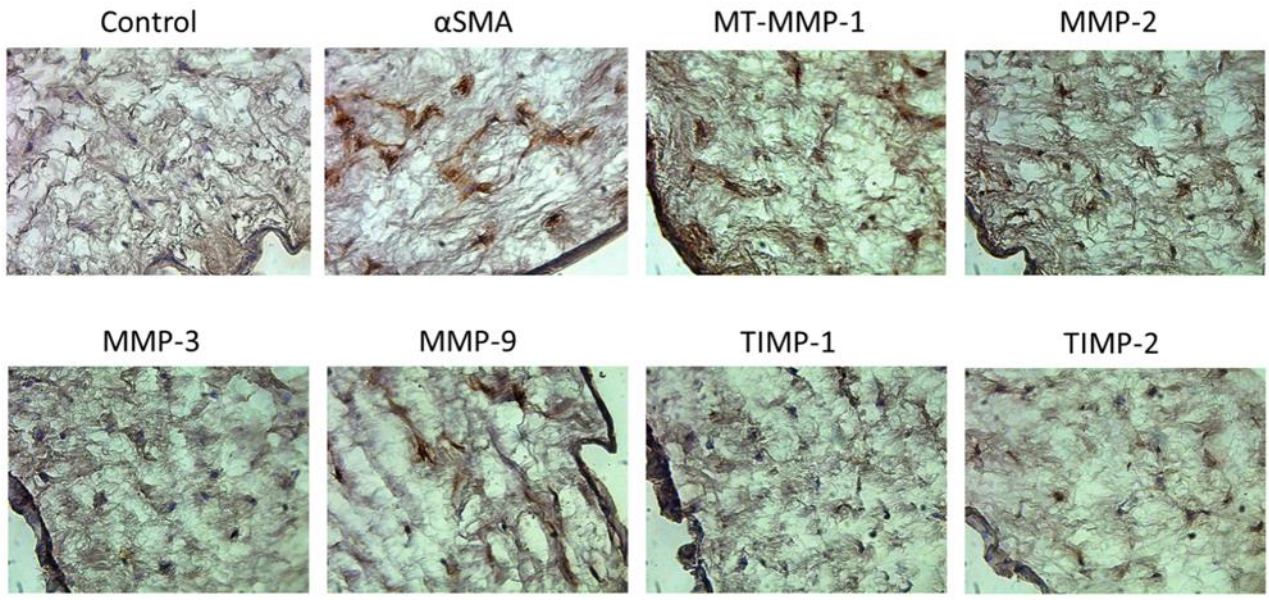

Figure 14. Expression of different MMPs and TIMPs in UC sections. αSMA is used as positive control. Magnification 40x.

Characterization of the three MSCs populations of UC

In view of accumulating evidence of the existence of three different populations of MSCs in UC as well as the necessity of a phenotypic characterization with a greater clarity of their properties, we next embarked in isolating PV-, WJ- and CL-MSCs from UC as described in the Methods section. The number of cells obtained from 2 human UCs is shown in Table 9. The morphological analysis is shown in Figure 15. Immunofluorescence staining showed that they all expressed mesenchymal markers CD90 and CD73 (Figure 16). In addition, PV-MSCs expressed CD146, WJ-MSCs expressed Oct4 and CL-MSCs expressed CD14, according with confirmed previous findings by Sarugaser et al. 2009, Kita et al. 2010 and Shaikh et al. 2012 [164] [196] [223].

Table 9. Number of cells at P0 at confluence.

	Cord 1 ♂	Cord 2 ♀	Total (Cord 1 + Cord 2)
PV-MSCs	4.12×10^6	2.18×10^6	6.3×10^6
CL-MSCs	9.8×10^6	7.95×10^6	17.75×10^6
WJ-MSCs	10.7×10^6	14.55×10^6	25.25×10^6

PV= perivascular; CL = cord lining; WJ = Wharton's jelly.

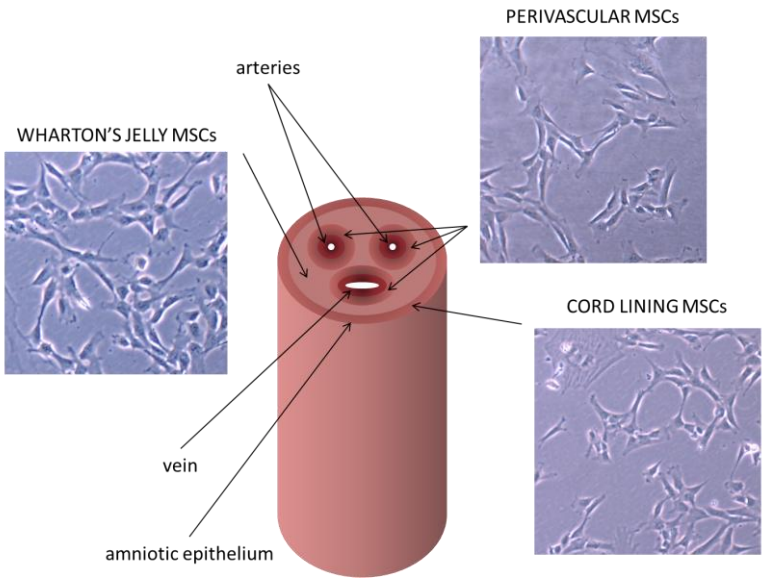

Figure 15. Morphological analysis of the three MSC populations of the UC. Magnification 20x.

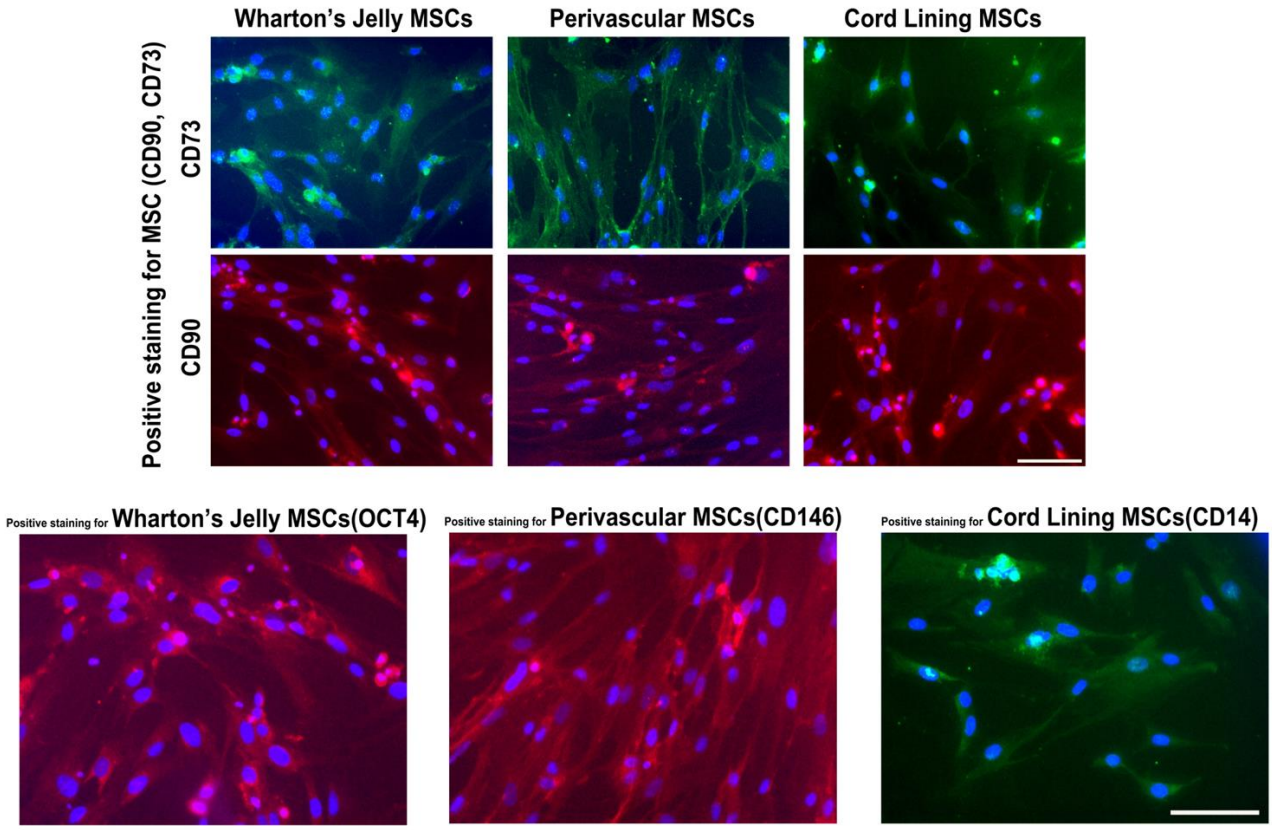

Figure 16. Immunolocalization of CD90, CD73, Oct4, CD146 and CD14. Magnification 20x. Bar 50µm.

Mitochondrial function of PV-, WJ- and CL-MSCs

Because UC is composed only of three blood vessels, the UC-MSCs are likely adapted to survive in a relatively hypoxic and glucose-poor environment advancing the concept of beneficial potential of these cells for the treatment of ischemic pathologies such as stroke. A direct consequence of oxygen and glucose deprivation during stroke is impaired function of mitochondria that contributes to cellular death. Emerging findings of mitochondria transfer provide the basis for the replenishment of healthy mitochondria as a strategy for the treatment of stroke.

In order to understand the metabolic energy profile and mitochondrial function of PV-, WJ- and CL-MSCs, Cell Energy Phenotype and Cell Mito Stress tests were performed by using the Seahorse XF96 Analyzer. The first step was to analyze the metabolic energy profile of the three UC-MSCs populations (upper part of Figure 17).

XF Cell Energy Phenotype Test revealed that all 3 UC-MSCs populations displayed a comparable metabolic phenotype (Figure 18). In addition, the metabolic profile of PV-, WJ- and CL-MSCs is quiescent as evidenced by undifferentiated MSCs exhibiting low levels of mitochondrial activities and high levels of glycolytic activities [224].

In order to assay the mitochondrial function of PV-, WJ- and CL-MSCs in ischemic conditions, a Cell Mito Stress test was performed to in both normal and after OGD/R (lower part of Figure 17). Seahorse XF Cell Mito Stress test showed that all 3 UC-MSCs cellular populations have a comparable mitochondrial respiration in both normal and after OGD/R conditions demonstrating their ability to survive in ischemic conditions (Figure 19).

In addition, a cell viability test showed that all 3 UC-MSCs cellular populations displayed good survival and also efficient proliferation following OGD/R further demonstrating their property to survive in ischemic conditions (lower part of Figure 17 and Figure 20). These results demonstrate the adaptive capacity of PV-, WJ- and CL-MSCs under OGD conditions. This capacity to survive is probably due to their robust mitochondrial function. The three populations of UC-MSCs could be a potential source of mitochondria-based stem cell therapy for stroke.

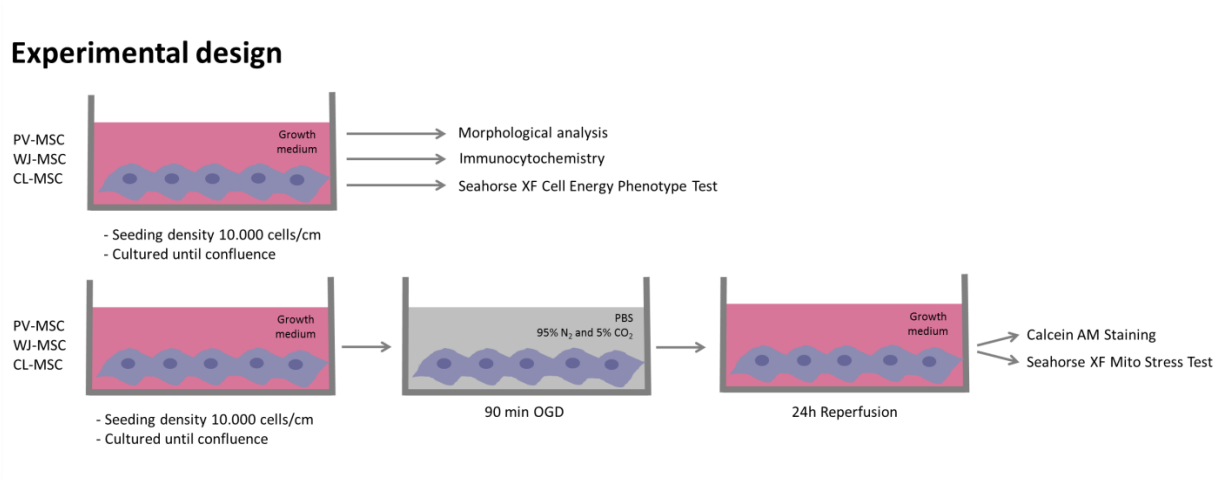

Figure 17. Experimental design

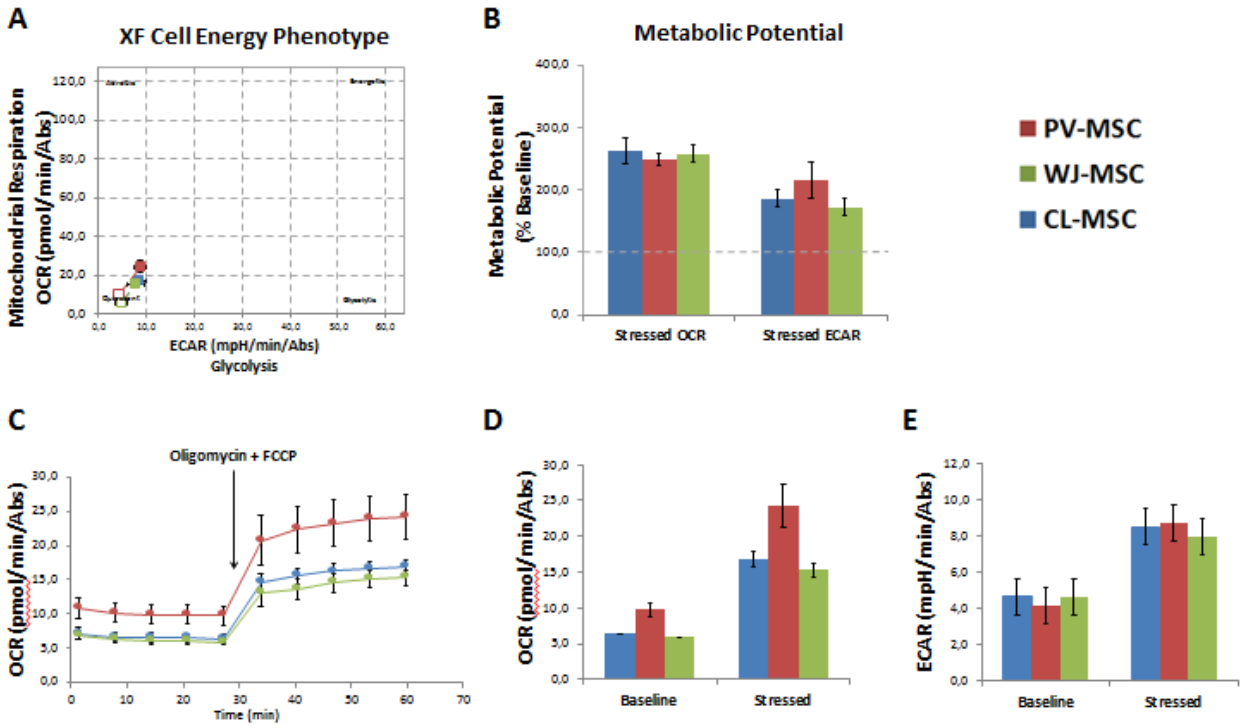

Figure 18. Seahorse XF Cell Energy Phenotype Test performed by using a Seahorse XF96 Analyzer. Oligomycin 1µM, FCCP 1µM. OCR: oxygen consumption rate. ECAR: extracellular acidification rate.

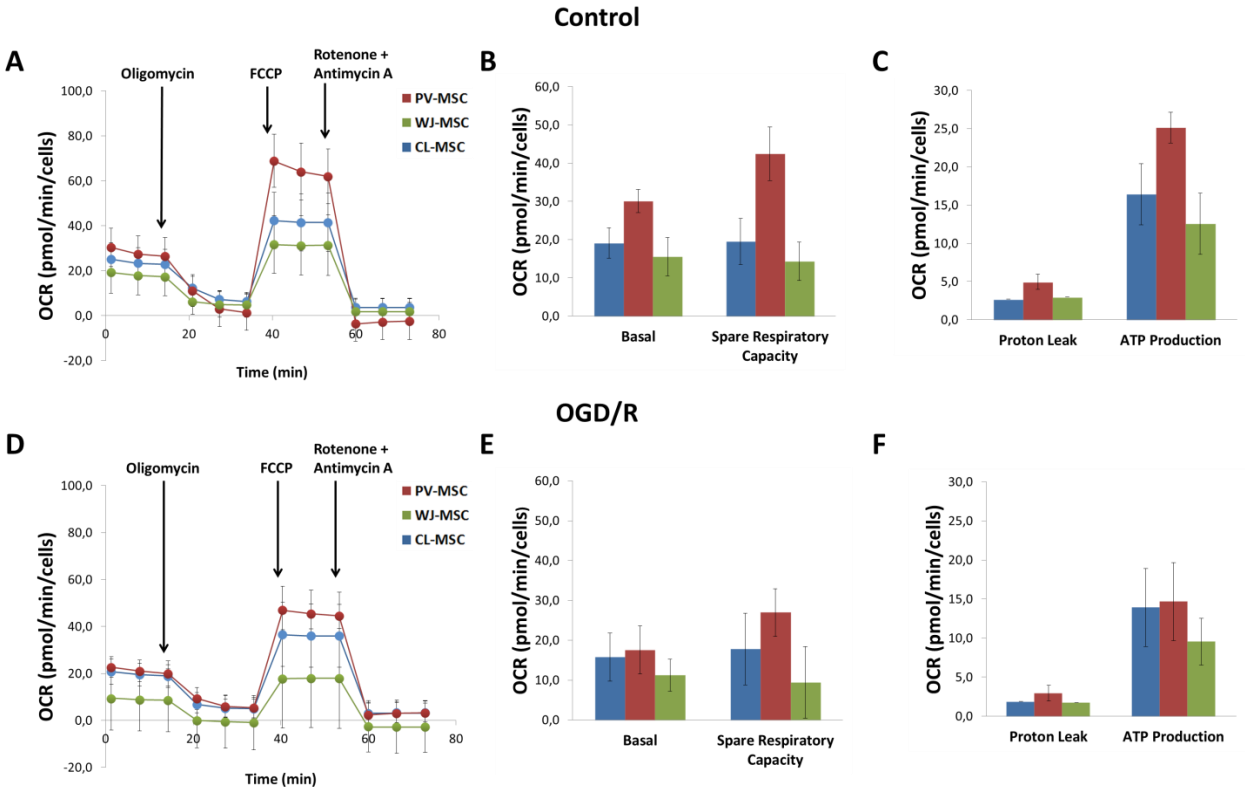

Figure 19. Seahorse XF Mito Stress test shows PV-, WJ- and CL-MSCs in both normal and after OGD/R conditions. OCR: oxygen consumption rate. 1µM Oligomycin, 1µM FCCP, 0.5µM Rotenone + Antimycin A.

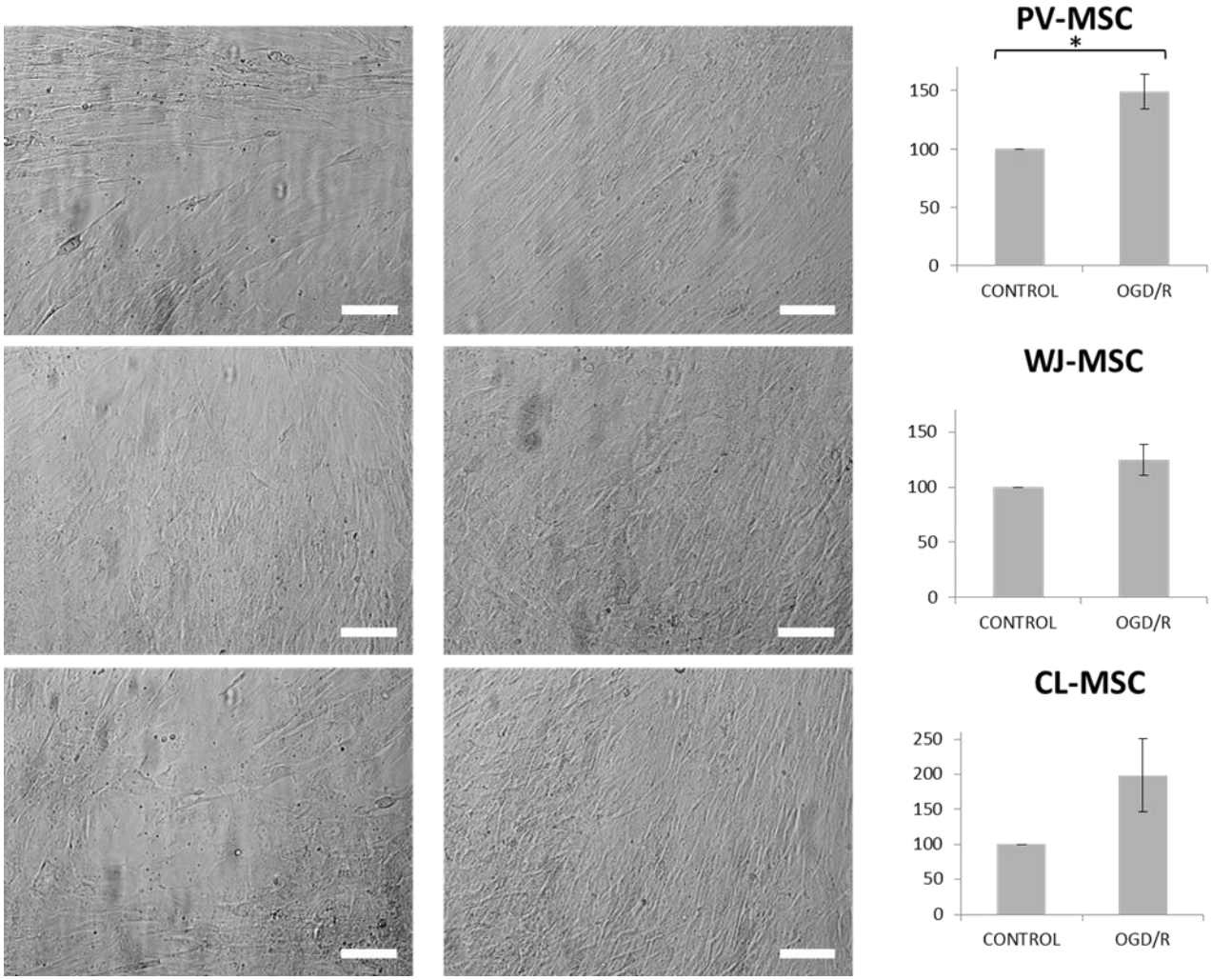

Figure 20. Cell viability tested by using Calcein AM stain in both control and after OGD/R conditions. Magnification 10x, bar 100µm. *P value = 0.0354.

DISCUSSION

Cerebrovascular diseases, such as stroke, result from blood vessel occlusion leading to focal tissue loss and death of endothelial cells and multiple neural populations, referred to as neurovascular unit. Recent evidence suggests the central role of mitochondria dysfunction in the progression of ischemic damage [7]. Following oxygen and glucose deprivation, the mitochondrial function is impaired resulting in exacerbation of excitotoxicity, failure of energetic metabolism, oxidative stress, inflammation and neural death. Ischemia, edema and other factors, can cause damage to the surrounding intact tissue [6].

Recently, stem cell-based therapies have been identified as promising strategies for the treatment of stroke [225]. Stem cell repair mechanisms include (1) cell replacement, (2) bystander effect via secretion products and (3) stimulation of endogenous stem cells proliferation and migration from the neurogenic niche to the injured site [6] [226]. (4) New evidence indicates the transfer of healthy mitochondria from stem cells to ischemic cells as a novel encouraging strategy for the stem cell-based therapy of stroke [7] [6].

UC-MSCs are a promising cellular source for the treatment of stroke due to their self-renewal and multipotent differentiation potential, immunomodulatory and anti-inflammatory properties, as well as ease of collection procedures without ethical concerns [14] [227]. Since UC-MSCs receive blood supply only from three vessels, these cells are normally adapted to survive in a relatively hypoxic and glucose poor environment leading to the hypothesis that these cells may have a beneficial potential for the treatment of ischemic pathologies, such as stroke [15]. Laboratory studies showed that UC-MSCs isolated by distinct regions of the UC seem to have different characteristics [155]. However, it is not still clear whether a MSC population of the UC may have a better therapeutic potential than other stem cells.

The goal of this project is to characterize the MSCs of human UC with a focus on each stem cell repair mechanism mentioned above. In particular, this study revealed that UC-MSCs have anti-inflammatory, neurogenic and angiogenic properties, as well as potential abilities to promote proliferation and migration of NSCs from the neurogenic niches to the ischemic region and protection against ischemic damage via mitochondrial function.

The evolution of ischemic brain damage is strongly affected by an inflammatory reaction that involves soluble mediators, such as cytokines and chemokines, and specialized cells activated locally or recruited from the periphery [228]. Inflammation contributes to the progression of tissue damage. UC-MSCs present low immunogenicity and anti-inflammatory proprieties and they can modulate the immune system response by cytokines, growth factors, as well as the lack of co-stimulatory molecules. This study demonstrated that UC-MSCs expressed Gal-1 and B7-H3 as revealed by 2D-western blot and mass spectrometry-based proteomic analyses of UC-MSCs lysates. Gal-1 has recently been identified as a key molecule that plays important roles in the regulation of neural progenitor cell proliferation in two neurogenic regions: the SVZ of the lateral ventricle and the SGZ of the hippocampal DG [229]. Gal-1 has been shown to promote neurite outgrowth in peripheral and central nerves [229]. In the normal adult mouse brain, endogenous Gal-1 is expressed in these SVZ GFAP-expressing astrocytes and regulates the proliferation of endogenous neural stem/progenitor cells (NSPCs) in the SVZ through its carbohydrate binding ability [229]. However, the effect of Gal-1 on the proliferation of NSPCs after brain injury has not been studied yet. This endogenous protein is potentially involved in ischemia-driven neurogenesis and thus is potentially applicable as a new drug in regenerative therapy of stroke [230]. B7-H3 belongs to the B7 superfamily, a group of molecules that costimulate or down-modulate T cell responses. In the presence of strong activation signals, B7-H3 potently and consistently down-modulated human T cell responses by decreasing the expression of IL-2 [217]. For the first time, La Rocca et al. demonstrated in both undifferentiated and chondrogenic-like cells the presence of B7-H3 (CD276) in UC-MSCs [13].

In this study, Gal3BP was identified in UC-MSCs lysate. Gal3BP is a lectin galactoside-binding binding soluble protein that modulates Gal-1 and Gal-3. It has been shown to drive the of different immune cells [231]. In addition, Gal3BP induces VEGF secretion and promotes angiogenesis [232]. Serum level of Gal-1, and Gal-3 were upregulated in large artery atherosclerotic stroke patients, while no difference between patients and controls was reported serum level of Gal3BP [233]. Gal-3, a key player in inflammation in stroke and other neurological diseases, has been identified in UC-MSCs lysates (

Table 8) [234]. Galectin-12 has been also identified in UC-MSCs lysates (

Table 8). Gal-12 has been shown to be involved in regulating growth, differentiation, lipolysis, and inflammation. In addition, Gal-12 has been reported as a key player in regulation of

glucose homeostasis and energetic metabolism [235]. Indeed, galectin-12-deficient mice showed a high metabolic rate, as indicated by higher oxygen consumption in galectin-12-deficient adipocytes compared to controls [235]. Despite the controversial role of galectins in inflammation and cancer progression, further investigation about galectins in the context of brain repair is needed.

Several proteins involved in immunomodulation during pregnancy have been identified in UC-UC-MSCs such as PZP, pregnancy-specific beta-1-glycoprotein 1 (PSG1), PSG4, IDO1 and IDO2 in cell lysates (

Table 8).

PZP is a glycoprotein which is functionally and structurally related to A2M, also identified in UC-UC-MSCs lysates (

Table 8). PZP has been suggested as a key protein in protecting the fetus from attack of maternal immune system by inhibition of T cell proliferation and IL-2 production [236].

Moreover, pregnancy-specific glycoproteins PSG1 and PSG4 have been found in UC-MSCs lysate lysate (

Table 8). PSGs have immunoregulatory, pro-angiogenic, and anti-platelet functions. In particular, PSG1 may promote immune tolerance, affect trophoblast function, and angiogenesis in the pregnant uterus through induction of TGFB1 and VEGFA [237].

Furthermore, IDO1 and IDO2 are implicated in maternal-fetus tolerance through the tryptophan catabolism, an essential amino acid obtained through the diet [238]. The action of IDO1 leads to tryptophan depletion, but also to the production of tryptophan degradation products that have been shown to irreversibly suppress T-cells, B-cells and NK cells proliferation in vitro while DCs remained unaffected contributing to DC tolerogenesis through increased recruitment of regulatory T-cells (Treg) [239]. In CNS, IDO1 has been associated with suppression of neural inflammation. In particular, the expression of IDO1 can be induced in microglial cells by T helper cells that release IFNγ, triggering a negative feedback loop to decrease neural inflammation in autoimmune encephalomyelitis (EAE), an animal model of multiple sclerosis [240]. IDO2 has been suggested essential for IDO1-dependent induction of Treg, which was defective in mice genetically deficient in IDO2 [241].

In summary, these anti-inflammatory and immunomodulatory proprieties make UC-MSCs a good candidate to the cellular therapy of CNS diseases, such as stroke for at least two reasons. First, UC-MSCs' secreted factors could reduce progression of the damage by reducing the anti-inflammatory response. Second, the tolerogenic propriety of the UC-MSCs could reduce the risks of immune-rejection in transplantation.

MMPs and TIMPs have been implicated in neuroinflammation and BBB disruption, but also in the remodeling of ECM that allows the migration of NSCs from neurogenic niches to the injure site promoting endogenous repair mechanisms [220]. In this study, immunohistochemistry and mass spectrometry analyses showed expression of MMPs (MT-MMP1, MMP-2, MMP-3 and MMP-9) and TIMPs (TIMP-1, TIMP-2 and TIMP-3) in UC-MSCs.

By regulating the integrity and composition of the ECM structure, these enzyme systems play a pivotal role in the control of signals elicited by matrix molecules, which regulate cell proliferation, differentiation and cell death [222]. Regulation of MMP expression and activation is very complex and tightly controlled. MMPs are synthesized as zymogens and are secreted into the extracellular space as inactive zymogens [220]. ProMMPs are activated by disruption of the zinc-thiol interaction between the catalytic site and the pro-domain [220]. The pro-peptide of the zymogen has to be proteolytically cleaved by other MMPs or proteases for an MMP to be active. For instance, pro-MMP-9 is activated in MMP-9 by MMP-2 and MMP-3 [220]. Pro-MMP-2 is activated in MMP-2 by MT1-MMP in a complex with TIMP-2 [220]. The activities of MMPs are regulated by tissue inhibitors of MMPs (TIMPs) [220]. Four members of this family have been characterized [220]. In particular, TIMP-2 inhibits MMP-2, whereas TIMP-1 is a MMP inhibitor with specificity for several MMPs [220].

During neuroinflammation and ischemia, molecular cascades are initiated with the purpose of removing damaged cells and preparing the brain for repair [222]. Early after the injury, constitutive proteases are activated and begin the process of disassembling the extracellular matrix, opening the BBB, and initiating cell death by apoptosis [222]. The second stage of injury involves MMPs in processes of angiogenesis and neurogenesis [222]. In this second phase, treatment with MMP inhibitors may interfere with repair [222]. Remodeling of the ECM characterizes the third phase when gliosis forms impenetrable scar tissues that block the regrowth and re-projection of axons [222]. The action of the MMPs on the basal lamina and tight junction proteins (TJPs) in endothelial cells is the final common pathway for opening of the BBB, which

allows cells to enter the CNS and attack invading organisms [222]. This is probably a protective mechanism during CNS infection, but when no infection exists, this inflammatory response contributes to tissue damage [222].

The two major inducible MMPs that have been identified in the neuroinflammatory response are MMP-3 and MMP-9, which are associated with a significant opening of the BBB [222] [242]. Endothelial cells are positive mainly for MMP-9, pericytes express MMP-3 and -9, while astrocytes express MMP-2 and MT1-MMP in the endfeet that surround the endothelial cells [222] [242]. This pattern of MMPs facilitates the opening of the BBB in inflammation, but also allows for the gradual changes in the extracellular matrix that are most likely on going and may involve the action of the MMP-2/MT1-MMP complex remodeling the matrix to prevent excessive build-up [222] [242]. In the reperfusion model, there is an early increase in MMP-2, which is transient, but results in the early reversible opening of the BBB [222] [242]. MMP inhibitors have been used in a number of animal studies to block BBB injury, reduce infarct size and cell death [222] [242]. However, the same inhibitors blocked neurogenesis and neurovascular remodeling during delayed phases after stroke [222] [242]. These results underscore the complexity of the effects of MMPs during ischemic brain injury, ranging from detrimental effects during the early phases after stroke to beneficial roles at later stages [222] [242].

Improvements in drug design and increased understanding of the timing of MMP expression should improve our therapeutic options with MMPs and MMPs inhibitors. A key feature supporting the efficacy of exogenous stem cell transplantation may be the ability of exogenous cells to alter the expression of MMPs and extracellular matrix metalloproteinases (ECMs), facilitating the creation of a biobridge between the neurogenic and ischemic sites [243]. Recent work in the setting of traumatic brain injury (TBI) has shown that transplanted exogenous MSCs are able to guide the migration of endogenous cells from the neurogenic site to the area of injury in the cortex via a biobridge paved with MMPs and ECMs [243]. This migration observed in the transplanted rats corresponded to a nine-fold increase in MMP-9 expression and activity [5].

In this study, not only MMPs and TIMPs, but also several other proteases and proteases inhibitors were identified by mass spectrometry analysis of UC-MSCs. MMPs are members of an extended family of metazicins which also includes “a disintegrin and metalloproteases” (ADAMs) and “ADAMs with ThromboSpondin motifs” (ADAMTS) [244]. Here, MT1-MMP, ADAMTS-like protein (ADAMTSL)-1 and ADAMTSL-4 have been identified in proteomic analysis of UC-MSCs

lysates. Although their functions are still little-known, ADAMTSL-1 and ADAMTSL-4 have an important role in ECM. ADAMTSL-4 is a biomarker that allows distinguishing cardioembolic stroke from large vessel stroke [245].

In summary, the preliminary results of this study, in regards to the expression of MMPs and TIMPs as well as ADAMs, ADAMTSs and Serpins, showed that the UC-MSCs could promote the endogenous repair mechanisms. Future studies should be done to better understand the useful proprieties of UC-MSCs. Future objectives will include zymography assay to evaluate if the MMPs, expressed by UC-MSCs, are in inactive or active zymogen form. Moreover, in vivo study should be done to evaluate the effects of the UC-MSCs and their secretion products on stroke.

Alongside the bystander effect, literature data support the neural and angiogenic differentiation differentiation potential of UC-MSCs [186] [195]. Here in this study, several proteins involved in neurogenesis, gliogenesis, axonogenesis, neuron and glia differentiation, synaptic signaling, myelination, learning, memory and adult behavior as well as blood vessel development and morphogenesis, angiogenesis and endothelial cell migration were detected in UC-MSCs cell lysates. Different CNS receptors have been identified in UC-MSCs cell lysates such as 5-hydroxytryptamine (serotonin) receptor 2C (HTR2C), acid sensing ion channel subunit 1 (ASIC1), cholinergic receptor nicotinic alpha 3 subunit (CHRNA3), dopamine receptor (DR) D1, DRD4, gamma-aminobutyric acid receptor subunit pi (GABRP), glutamate ionotropic receptor kainate type subunit 3 (GRIK3), glutamate metabotropic receptor (GRM) 8, glycine receptor alpha 3 (GLRA3), unc-5 netrin receptor (UNC5) A and UNC5C (

Table 8). These phenotypic evaluations of UC-MSCs reveals that expression markers.

In addition, UC-MSCs produced different neurotrophic factors and factors associated with neurogenesis and differentiation such as fibroblast growth factor (FGF) 12, GDNF, mesencephalic astrocyte derived neurotrophic factor (MANF), microcephalin (MCPH1), NMDA receptor synaptonuclear signaling and neuronal migration factor (NSMF) and neuroblast differentiation-associated protein AHNAK (AHNAK).

GDNF is a member of the TGF-β family that promotes survival and recovery of mature neurons under pathological conditions such as ischemia, hypoxia, and oxidative stress [246] [247]. Several studies have shown that infusion of GDNF enhances neurogenesis after stroke by activation of several survival signals and inhibition of death signals such as caspase-9 and -3 [248]

[249]. In addition, ischemia increases NOS activity, which can be attenuated by GDNF suggesting also an import role of GDNF against oxidative stress [250]. Administration of GDNF protein, or GDNF overexpression, has been reported to reduce brain infarction and restored locomotor activity in stroke rats [251] [252]. Similar neuroprotective effects have been found after transplantation of GDNF containing cells to the stroke brain [253]. Recently, WJ-MSCs grafts were observed to significantly increase GDNF expression in the host brain in an animal model of stroke [254].

In a similar fashion, MANF has been shown to be upregulated in the glial cells under focal cerebral ischemia, and increased by several endoplasmic reticulum stress inducers and nutrient deprivation in cultured primary glial cells suggesting a neuroprotective role after stroke [255]. In addition, post stroke MANF administration promoted functional recovery in stroke animals [256].

Protein kinase C gamma (PRKCG) is expressed exclusively in neurons of the brain and spinal cord cord [285]. Here, PRKCG was detected in UC-MSCs cell lysates supporting their neurogenic potential (

Table 8). Several studies have reported increasing levels of PRKCG after stroke associated with detrimental effects after ischemia, but mediated beneficial signaling processes during reperfusion injury [257].

Furthermore, in UC-MSCs cell lysates expressed cell-surface and soluble proteins semaphorins (SEMA-3A, 3G, 4C and 5C) and their receptors plexins (PLXN-A4, B2 and B3) involved in regulation of axon guidance and development of neuronal connectivity as well as cell–cell interactions, differentiation, morphology and function. However, SEMA-3A increases vascular permeability and inhibits angiogenesis leading to deleterious effects after ischemia, SEMA-3G promotes angiogenesis [258] [259].

Angiogenesis, neurogenesis and synaptic plasticity are the main processes implicated in neurorepair [260]. Besides neural markers mentioned above, UC-MSCs express proteins are involved in angiogenesis and BBB protection including angiopoietin (ANGPT) 4, ANGPT-like 3 (ANGPTL3) angiomotin (AMOT), angio associated migratory cell protein (AAMP), myeloid growth factor (MYDGF), PSG1 and vascular endothelial growth factor receptor 3 (VEGFR3) (

Table 8).

ANGPT4 promotes endothelial cell survival, migration and angiogenesis [261]. ANGPTL3 is primarily known for its key role in lipid metabolism, and drugs targeting ANGPTL3 are currently tested in phase 1 and 2 studies on metabolic disorders [262]. Of note, ANGPTL3 has been shown to induce endothelial cell adhesion and in vivo angiogenesis [262].

AMOT is an angiostatin-binding protein that promotes endothelial cell migration and angiogenesis and participates in the assembly of endothelial cell-cell junctions [263]. In addition, AMOT has been shown as a component of the Hippo pathway with tumor-suppressing function through the inhibition of YAP and TAZ oncoproteins, suggesting its essential role in tight junction integrity and stabilization of endothelial cell-cell contacts [264] [265]. Interestingly, two AMOT isoforms have been identified, AMOT-80 and AMOT-130, and both are expressed in CNS in which drive spine maturation [266].

Moreover, AAMP promotes angiogenesis and can be regulated by astrocytes, leading to the hypothesis that the regulation of extracellular AAMP in endothelial cells by astrocytes may support the angiogenesis of the nervous system [267].

Another identified protein in UC-MSCs is MYDGF which has been reported to promote cardiac myocytes survival and angiogenesis following myocardial infarction by inhibition of cardiac myocytes apoptosis and reducing infarct size [268]. MYDGF may be another active growth factor involved in tissue repair after ischemic injury.

Furthermore, VEGFR3 promotes proliferation, survival and migration of endothelial cells, and regulates angiogenic sprouting [269] [270]. The activation of VEGFR-3 signaling in response to oxidative stress promotes endothelial cell survival protecting against ROS-induced cell damage [271]. In addition, VEGF-C/VEGFR-3 signaling has been reported to act directly on NSCs by regulating adult neurogenesis in SVZ of the brain [272]. The upregulation of VEGFR3 has been shown in SVZ astrocytes and immature neurons after focal ischemia, suggesting that VEGFR-3 may be involved in promoting neurogenesis after ischemic stroke [273].

As noted above, UC is supported from three blood vessels only and, therefore, the UC-MSCs are adapted to survive in a low oxygen and glucose environment leading to the hypothesis that can be one of the best sources for the treatment of ischemic diseases [15]. Mitochondria dysfunction is a direct consequence of oxygen and glucose deprivation during stroke and impaired mitochondria contributes to oxidative stress, neuronal death and inflammation [3]. Emerging

evidence of mitochondria transfer from stem cells to ischemic cells paved the way for mitochondrial-based stem cell therapy of stroke [10] [7] [6]. Although several studies have shown that the regulation of energetic metabolism is critical for the MSCs functions and proliferation/differentiation dynamics, few studies have been focused on the energetic metabolism and mitochondrial function of the UC-MSCs [146] [224] [274]. In addition, growing evidence suggests the existence of three different populations of UC-MSCs (PV-, WJ- and CL-MSCs) [15]. However, whether a population is superior to another is not still clear [155]. Likewise, whether the different anatomical distance from the vessels of the three MSCs population in the UC might result in a different energetic metabolism and in a growing resistance and survival capacity in a poor oxygen and glucose environment has not been investigated. With this gap in knowledge, PV-, WJ- and CL-MSCs were isolated from human UCs in order to understand (1) the energetic metabolism profile, (2) the mitochondrial function and (3) their survival capacity in both normal and after ischemic/reperfusion conditions.

The energy metabolism profiling of the three UC-MSC populations was performed by using a Seahorse XF96 Analyzer (Figure 18 and Figure 19). Studies in BM-MSCs showed that these cells displayed a glycolytic metabolism in undifferentiated state, while a switch to OXPHOS metabolism occurred during the differentiation [224]. These studies were performed with different methods including the measure of mitochondrial mass, determination of mtDNA copy number, western blot analysis of glycolytic and mitochondrial enzymes, assay of the expression of mitochondrial biogenesis-associated genes, measurement of intracellular ATP content, OCR measurement by using the 782 OxygenMeter and quantization of radioactive labeled glucose [224] [275] [276]. Past studies have used the Seahorse analyzer for OCR measurement in differentiated AD-MSCs and iPSC-derived mesenchymal progenitor cells [277] [278] [279]. A study analyzed the UC-MSCs metabolism by measuring the dissolved O_2 and pH values in the culture medium using the SFR-Shake Flask Reader [146].

Here, for the first time, the energetic metabolism of the three populations of MSCs of human UC was analyzed by using the Seahorse Analyzer. The Seahorse Analyzer allows a real time measure of OCR and ECAR in baseline condition and after the injection of drugs. The results of the XF Cell Energy Phenotype Test showed that PV-, WJ- and CL-MSCs are characterized by a similar energetic metabolism (Figure 18). In particular, the three MSC types exhibited a quiescent phenotype. Thus, PV-, WJ- and CL-MSCs maintained both mitochondrial and glycolytic activities at

low levels. Under stress conditions (Oligomycin + FCCP injection) the three types of MSCs displayed an increase in the glycolytic pathway likely to balance the reduction of mitochondrial respiration. Moreover, a Seahorse XF Cell Mito Stress test was performed in both normal and after OGD/R to analyze the mitochondrial activity of PV-, WJ- and CL-MSCs in ischemic conditions (Figure 19). Although the OCR undergoes a slight decrease in OGD/R groups, all the three UC-MSC populations showed a comparable robust resistance and adaption to ischemic conditions as also demonstrated by the cell viability test. Indeed, the survival of cells was not affected by OGD/R treatment but surprisingly the number of the cells increased suggesting a powerful ability of all the UC-MSCs to survive in ischemic conditions (Figure 20). Taken together, these results demonstrate the adaptive capacity of PV-, WJ- and CL-MSCs to ischemic environments due to their maintained mitochondrial function. Thus, the three populations of UC-MSCs might be a promising source of mitochondria for mitochondrial stem cells-based therapy of stroke. All three types of UC-MSCs displayed a similar energetic metabolism and mitochondrial function. Both Seahorse tests showed that PV-MSCs showed the highest OCR values suggesting a superior mitochondrial activity in these cells. A further support of this result is the more consistent reduction of OCR of PV-MSCs after OGD/R compared to WJ- and CL-MSCs (Figure 19). CL-MSCs were the cells least affected by OGD/R condition (Figure 19), suggesting their robust survival in ischemic environment. Further investigations are needed to better understand whether these slight but significant differences among the three UC-MSCs are due to a different number of healthy mitochondria in the cells and/or to better adaptation of mitochondria to ischemic conditions. Despite these limitations, UC-MSCs appear to afford more effective protection against ischemic reperfusion injury.

Arguably, UC-MSCs expressed several proteins involved in protection against ischemia and oxidative stress as demonstrated by the proteomic analysis showed in

Table 8. These protective systems include different HSPs (heat shock proteins, HSPA12A, HSPA1L, HSPA4, HSPA8, HSPB1, HSPB6, HSP90AA1, HSP90AB1 and HSPA9), antioxidant enzymes (glutathione S-transferase pi 1, Prxs (PRDX1, PRDX2, PRDX4, PRDX5, PRDX6, probable glutathione peroxidase 8, SOD1, SOD2, Trx domain-containing protein 12, Trx, Trx-dependent peroxide reductase mitochondrial), hypoxia inducible factor (HIF) 3A and hypoxia up-regulated 1 (HYOU1).

HSPs and antioxidant enzymes can reduce the oxidative stress and the ROS-associated damage in ischemic pathologies including stroke [280]. HIF induces genes involved in cell survival

and protection in response to hypoxia, indicating its neuroprotective effects on stroke in pre-clinical studies [280].

In summary, these build of evidence shows several benefits of UC-MSCs including differentiation potential, anti-inflammatory properties, neuro- and angioprotective abilities, anti-oxidative and hypoxia, making them a promising cellular source for stem cell-based treatment of CNS diseases including stroke. In addition, UC-MSCs have an elevated capacity of survival and adaption to OGD/R conditions due to their energetic metabolism and mitochondrial function suggesting that all three types of UC-MSCs could be an effective source of healthy mitochondria for stem cell-based therapy in ischemic pathologies.

CONCLUSIONS AND FUTURE DIRECTIONS

In conclusion, this study characterized the UC-MSCs at proteomic, histologic and metabolic level, providing compelling evidence of a promising potential for the use of UC-MSCs in the treatment of CNS diseases, specifically stroke. In particular, UC-MSCs express several neural markers, immunomodulatory molecules, neuro- and angioprotective factors including proteins that promote neurogenesis, angiogenesis, as well as molecules involved in ECM remodeling and BBB protection. In addition, some of these factors are secreted suggesting a strong by-stander effect of UC-MSCs. Moreover, the Seahorse analysis performed for the first time in PV-, WJ- and CL-MSCs of the human UC showed that the three MSC populations have a peculiar energetic metabolism profile. The great capacity of survival under ischemic conditions of the three UC-MSCs due to their mitochondrial function suggests that these UC-MSCs may represent an effective donor cells for mitochondrial-based stem cells therapy of stroke.

Three objectives were pursued. First, a proteomic analysis of the single UC-MSC populations was performed to analyze the potential biological differences among specific MSC sources, allowing us to better assess the optimal cell source. The preliminary results of this study showed UC-MSC expression of MMPs and TIMPs, suggesting that the UC-MSCs could promote endogenous repair mechanisms possibly through enhancing extracellular matrices. Finally, the results of the energetic metabolism of PV-, WJ- and CL-MSCs built the foundation for a mitochondrial-based stem cell therapy for stroke. Future studies geared towards translating these laboratory findings to clinical application will focus on mitochondrial transfer from PV-, WJ- and CL-MSCs into ischemic cells, which may prove therapeutic for stroke.

ACKNOWLEDGMENTS

- To Dr. Giampiero La Rocca, PhD, and Dr. Cesar V. Borlongan, MA, PhD, the best mentors of the world who always believed in my potentials and imparted me passion and indispensable teachings for the wonderful scientific research job.
- To Dr. Rita Anzalone, PhD, a teacher of science and life who gave me precious advices to improve me like scientist and woman.
- To Dr. Salvatore Saieva, PhD, with whom I started my internship and my PhD at Department of Experimental Biomedicine and Clinical Neurosciences (BIONEC), Section of Histology and Human Anatomy, School of Medicine and Surgery University of Palermo, Palermo, Italy, and I built up a nice friendship.
- To La Rocca's laboratory group of BIONEC, with whom I worked during my PhD and who made me a better researcher and person: Dr. Salvatore Saieva, PhD; Dr. Melania Lo Iacono, PhD; Dr. Simona Corrao, PhD; Dr. Tiziana Corsello, PhD, Maria Elena Trapani and Giusi Alberti.
- To Borlongan's laboratory group of the Center of Excellence for Aging and Brain Repair (CEABR), Department of Neurosurgery and Brain Repair, Morsani College of Medicine, University of South Florida, Tampa, Florida, USA, with whom I pursued my PhD international program and to whom I will always be grateful to have enriched my personal store of knowledge and experiences: Dr. Yuji Kaneko, PhD; Dr. Jea Young Lee, PhD; Dr. Kaya Xu, MD; Dr. Sandra Acosta, PhD; Hung Nguyen (soon to be Dr.); Trenton Lippert; Julian Tuazon; Roger Lin; Michael Grant Liska.

- To Dr. Jea Young Lee, PhD (CEABR); Hung Nguyen (CEABR) and Dr. Eleonora Napoli, PhD (Department of Molecular Biosciences, School of Veterinary Medicine, University of California, Davis, California, USA) for their precious teachings and contribute to my PhD project.
- To my Italian and International friends in Palermo and Tampa that made my PhD life fun.
- To my family, whose love does not know distances and boundaries and who always believed in my potential supporting and encouraging me to achieve my accomplishments and to make my dreams come true.

REFERENCES

[1] Benjamin, E. J., Virani, S. S., Callaway, C. W., Chamberlain, A., Chang , A. R., Cheng, S., et al. (2018). Heart Disease and Stroke Statistics-2018 Update: A Report From the American Heart Association. *Circulation, 137* (12), e67-e492.

[2] Gravanis, I., & Tsirka, S. E. (2008). Tissue-type plasminogen activator as a therapeutic target in stroke. *Expert Opin Ther Targets, 12* (2), 159-70.

[3] Yang, J. L., Mukdaab, S., & Chen, S. D. (2018). Diverse roles of mitochondria in ischemic stroke. *Redox Biol., 16* (2018), 263-275.

[4] Watts, L. T., Lloyd, R., Garling, R. J., & Duong, T. T. (2013). Stroke Neuroprotection: Targeting Mitochondria. *Brain Sci., 3* (2), 540-60.

[5] Tajiri, N., Duncan, K., Antoine, A., Pabon, M., Acosta, S. A., de la Peña, I., et al. (2014). Stem cell-paved biobridge facilitates neural repair in traumatic brain injury. *Front Syst Neurosci., 8* (116), 1-6.

[6] Russo, E., Napoli, E., & Borlongan, C. V. (2018). Healthy mitochondria for stroke cells. *Brain Circulation, 4* (3), 95-98.

[7] Russo, E., Nguyen, H., Lippert, T., Tuazon, J., Borlongan, C. V., & Napoli, E. (2018). Mitochondrial targeting as a novel therapy for stroke. *Brain Circulation, 4* (3), 84-94.

[8] Hsu, Y. C., Wu, Y. T., Yu, T. H., & Wei, Y. H. (2016). Mitochondria in mesenchymal stem cell biology and cell therapy: From cellular differentiation to mitochondrial transfer. *Semin Cell Dev Biol., 52*, 119-31.

[9] Paliwal, S., Chaudhuri, R., Agrawal, A., & Mohanty, S. (2018). Regenerative abilities of mesenchymal stem cells through mitochondrial transfer. *J Biomed Sci., 25* (1), 31.

[10] Borlongan, C. V., Nguyen, H., Lippert, T., Russo, E., Tuazon, J., Xu, K., et al. (2018). May the force be with you: transfer of healthy mitochondria from stem cells to stroke cells. *Journal of Cerebral Blood Flow and Metabolism, [ahead of print]*.

[11] Ilic, D., & Polak, J. M. (2011). Stem cells in regenerative medicine: introduction. *Br Med Bull., 98*, 117-26.

[12] Ullah, I., Subbarao, R. B., & Rho, G. J. (2015). Human mesenchymal stem cells - current trends and future prospective. *Biosci Rep., 35* (2), pii: e00191.

[13] La Rocca, G., Lo Iacono, M., Corsello, T., Corrao, S., Farina, F., & Anzalone, R. (2013). Human Wharton's jelly mesenchymal stem cells maintain the expression of key immunomodulatory molecules when subjected to osteogenic, adipogenic and chondrogenic differentiation in vitro: new perspectives for cellular therapy. *Curr Stem Cell Res Ther., 8* (1), 100-13.

[14] Magatti, M., Abumaree, M. H., Silini, A. R., Anzalone, R., Saieva, S., Russo, E., et al. (2016). Chapter 6. The Immunomodulatory Features of Mesenchymal Stromal Cells Derived from Wharton's Jelly, Amniotic Membrane, and Chorionic Villi: In Vitro and In Vivo Data. In O. Parolini (Ed.), *Placenta: The Tree of Life* (pp. 91-128). CRC Press.

[15] Davies, J. E., Walker, J. T., & Keating, A. (2017). Concise Review: Wharton's Jelly: The Rich, but Enigmatic, Source of Mesenchymal Stromal Cells. *Stem Cells Transl Med., 6* (7), 1620-1630.

[16] Deb, P., Sharma, S., & Hassan, K. M. (2010). Pathophysiologic mechanisms of acute ischemic stroke: An overview with emphasis on therapeutic significance beyond thrombolysis. *Pathophysiology, 17* (3), 197-218.

[17] Brott, T., Adams , H. P., Olinger, C. P., Marler, J. R., Barsan, W. G., & al. (1989). Measurements of acute cerebral infarction: a clinical examination scale. *Stroke, 20*, 864-870.

[18] Meyer, B. C., Hemmen, T. M., Jackson, C. M., & Lyden, P. D. (2002). Modified National Institutes of Health Stroke Scale for use in stroke clinical trials: prospective reliability and validity. *Stroke, 33* (5), 1261-6.

[19] Meyer, B. C., & Lyden, P. D. (2009). The modified National Institutes of Health Stroke Scale: its time has come. *Int J Stroke, 4*, 267-273.

[20] Knecht , S., Hesse, S., & Oster, P. (2011). Rehabilitation after stroke. *Dtsch Arztebl Int., 108* (36), 600-6.

[21] Aqueveque, P., Ortega P, P., Pino, E., Saavedra, F., Germany, E., & Gomez, B. (2017). After Stroke Movement Impairments: A Review of Current Technologies for Rehabilitation. In U. Tan (Ed.), *Physical Disabilities - Therapeutic Implications* (pp. 95-116). InTech.

[22] Leśniak, M., Bak, T., Czepiel, W., Seniów, J., & Członkowska, A. (2008). Frequency and prognostic value of cognitive disorders in stroke patients. *Dement Geriatr Cogn Disord., 26* (4), 356-63.

[23] Hommel, M., Trabucco-Miguel, S., Joray , S., Naegele, B., Gonnet, N., & al. (2009). Social dysfunctioning after mild to moderate first-ever stroke at vocational age. *J Neurol Neurosurg Psychiatry, 80* (4), 371-375.

[24] Stonesifer, C., Corey, S., Ghanekar, S., Diamandis, Z., Acosta, S. A., & Borlongan, C. V. (2017). Stem cell therapy for abrogating stroke-induced neuroinflammation and relevant secondary cell death mechanisms. *Prog Neurobiol., 158*, 94-131.

[25] Dobkin, B. H., & Carmichael, S. T. (2016). The Specific Requirements of Neural Repair Trials for Stroke. *Neurorehabil Neural Repair, 30* (5), 470-8.

[26] Bernhardt, J., Hayward, K. S., Kwakkel, G., Ward, N. S., Wolf, S. L., Borschmann, K., et al. (2017). Agreed definitions and a shared vision for new standards in stroke recovery research: The Stroke Recovery and Rehabilitation Roundtable taskforce. *Int J Stroke, 12* (5), 444-450.

[27] Bansal , S., Sangha, K. S., & Khatri, P. (2013). Drug treatment of acute ischemic stroke. *AmJ Cardiovasc Drugs., 13* (1), 57-69.

[28] Dailey, T., Metcalf, C., Mosley YI, Y. I., Sullivan, R., Shinozuka, K., Tajiri, N., et al. (2013). An Update on Translating Stem Cell Therapy for Stroke from Bench to Bedside. *J Clin Med., 2* (4), 220-241.

[29] Bélanger, M., Allaman, I., & Magistretti, P. J. (2011). Brain Energy Metabolism: Focus on Astrocyte-Neuron Metabolic Cooperation. *Cell Metab., 14* (6), 724-38.

[30] Sims, N. R., & Muyderman, H. (2010). Mitochondria, oxidative metabolism and cell death in stroke. *Biochim Biophys Acta, 1802* (1), 80-91.

[31] Lipton, P. (1999). Ischemic Cell Death in Brain Neurons. *Physiol Rev., 79* (4), 1431-568.

[32] Falkowska, A., Gutowska, I., Goschorska, M., Nowacki, P., Chlubek, D., & Baranowska-Bosiacka, I. (2015). Energy Metabolism of the Brain, Including the Cooperation between Astrocytes and Neurons, Especially in the Context of Glycogen Metabolism. *Int J Mol Sci., 16* (11), 25959–25981.

[33] (2003). Hemodynamic Events Associated with Acute Focal Brain Ischemia and Reperfusion. Ischemic Penumbra. In E. Gusev, & V. I. Skvortsova, *Brain Ischemia* (p. 9-19). Boston, MA: Springer.

[34] Rossi, D. J., Brady, J. D., & Mohr, C. (2007). Astrocyte metabolism and signaling during brain ischemia. *Nat Neurosci., 10* (11), 1377-86.

[35] (2003). Metabolic Acidosis and Ischemic Damage. In E. Gusev, & V. I. Skvortsova , *Brain Ischemia* (p. 96-100). Boston, MA: Springer.

[36] Robbins, N. M., & Swanson, R. A. (2014). Opposing effects of glucose on stroke and reperfusion injury:acidosis, oxidative stress, and energy metabolism. *Stroke, 45* (6), 1881-6.

[37] Nadler, J. V. (2012). Plasticity of Glutamate Synaptic Mechanisms. In J. L. Noebels, M. Avoli, M. A. Rogawski, R. W. Olsen, & A. V. Delgado-Escueta (Eds.), *Jasper's Basic Mechanisms of the Epilepsies, Fourth Edition (Contemporary Neurology Series 80).* USA: Oxford University Press.

[38] Rama Bretón, R., & García Rodriguez, J. C. (2012). Excitotoxicity and Oxidative Stress in Acute Ischemic Stroke. In J. C. García Rodríguez (Ed.), *Acute Ischemic Stroke.* IntechOpen.

[39] Dirnagl, U., Iadecola, C., & Moskowitz, M. A. (1999). Pathobiology of ischaemic stroke: an integrated view. *Trends Neurosci., 22* (9), 391-7.

[40] Lee, J. M., Zipfel, G. J., & Choi, D. W. (1999). The changing landscape of ischaemic brain injury mechanisms. *Nature, 399* (6738 Suppl), A7-14.

[41] Schousboe, A., Scafidi, S., Bak, L. K., Waagepetersen, H. S., & McKenna, M. C. (2014). Glutamate metabolism in the brain focusing on astrocytes. *Adv Neurobiol., 11*, 13-30.

[42] Schinder, A. F., Olson, E. C., Spitzer, N. C., & Montal, M. (1996). Mitochondrial Dysfunction Is a Primary Event in Glutamate Neurotoxicity. *Journal of Neuroscience, 16* (19), 6125-6133.

[43] Shenoda, B. (2015). The role of Na+/Ca2+ exchanger subtypes in neuronal ischemic injury. *Transl Stroke Res., 6* (3), 181-90.

[44] Chen, Z., Mou, R., Feng, D., Wang, Z., & Chen, G. (2017). The role of nitric oxide in stroke. *Med Gas Res., 7* (3), 194–203.

[45] Fischer, F., Hamann, A., & Osiewacz, H. D. (2012). Mitochondrial quality control: an integrated network of pathways. *Trends Biochem Sci., 37* (7), 284-92.

[46] Quijano, C., Trujillo, M., Castro, L., & Trostchansky, A. (2016). Interplay between oxidant species and energy metabolism. *Redox Biol., 8*, 28-42.

[47] Rodrigo, R., Fernández-Gajardo, R., Gutiérrez, R., Matamala, J. M., Carrasco, R., Miranda-Merchak, A., et al. (2013). Oxidative Stress and Pathophysiology of Ischemic Stroke: Novel therapeutic opportunities. *CNS Neurol Disord Drug Targets, 12* (5), 698-714.

[48] Abramov, A. Y., Scorziello, A., & Duchen, M. R. (2007). Three distinct mechanisms generate oxygen free radicals in neurons and contribute to cell death during anoxia and reoxygenation. *J Neurosci., 27* (5), 1129-38.

[49] Bedard, K., & Krause, K. H. (2007). The NOX family of ROS-generating NADPH oxidases: physiology and pathophysiology. *Physiol Rev., 87* (1), 245-313.

[50] Daiber, A., Di Lisa, F., Oelze, M., Kröller-Schön, S., Steven, S., Schulz, E., et al. (2017). Crosstalk of mitochondria with NADPH oxidase via reactive oxygen and nitrogen species signalling and its role for vascular function. *Br J Pharmacol., 174* (12), 1670-1689.

[51] Kim, S. H., Kim, K. Y., Yu, S. N., Seo, Y. K., Chun , S. S., Yu, H. S., et al. (2016). Silibinin induces mitochondrial NOX4-mediated endoplasmic reticulum stress response and its subsequent apoptosis. *BMC Cancer., 16*, 452.

[52] Shanmugasundaram, K., Nayak, B. K., Friedrichs, W. E., Kaushik, D., Rodriguez, R., & Block, K. (2017). NOX4 functions as a mitochondrial energetic sensor coupling cancer metabolic reprogramming to drug resistance. *Nat Commun., 8* (1), 997.

[53] Ježek, J., Jabůrek, M., Zelenka, J., & Ježek, P. (2010). Mitochondrial phospholipase A2 activated by reactive oxygen species in heart mitochondria induces mild uncoupling. *Physiol Res., 59* (5), 737-47.

[54] Niizuma, K., Yoshioka, H., Chen, H., Kim, G. S., Jung, J. E., Katsu, M., et al. (2010). Mitochondrial and apoptotic neuronal death signaling pathways in cerebral ischemia. *Biochim Biophys Acta, 1802* (1), 92-9.

[55] Liu, F., Lu, J., Manaenko, A., Tang, J., & Hu, Q. (2018). Mitochondria in Ischemic Stroke: New Insight and Implications. *Aging and Disease, 9* (5), 1-14.

[56] Kumar, R., Bukowski, M. J., Wider, J. M., Reynolds, C. A., Calo, L., Lepore, B., et al. (2016). Mitochondrial dynamics following global cerebral ischemia. *Mol Cell Neurosci., 76*, 68-75.

[57] Saxton, W. M., & Hollenbeck, P. J. (2012). The axonal transport of mitochondria. *J Cell Sci., 125* (9), 2095–2104.

[58] Rugarli, E. I., & Langer, T. (2012). Mitochondrial quality control: a matter of life and death for neurons. *The EMBO Journal, 31*, 1336–1349.

[59] Rami, A., & Kögel, D. (2008). Apoptosis meets autophagy-like cell death in the ischemic penumbra: Two sides of the same coin? *Autophagy, 4* (4), 422-426.

[60] Mills, E. L., Kelly, B., & O'Neill, L. A. (2017). Mitochondria are the powerhouses of immunity. *Nat Immunol., 18* (5), 488-498.

[61] *NIH Fact Sheets: Regenerative medicine*. (2010). Retrieved from NIH: https://report.nih.gov/nihfactsheets/ViewFactSheet.aspx?csid=62

[62] Horch, R. E., Popescu, L. M., & Polykandriotis, E. (2016). History of Regenerative Medicine. In S. G. (Ed.), *Regenerative Medicine - from Protocol to Patient.* (3 ed., pp. 1-19). Springer, Cham.

[63] Barnes, J. (Ed.). (1984). *The complete works of Aristotle: the revised Oxford edition.* (Bollingen series LXXI ed., Vol. 2). Princeton, New Jersey , 08540 USA: Princeton University Press.

[64] Lenhoff, H. M., & Lenhoff, S. G. (1991). Abraham Trembley and the origins of research on regeneration in animals. In. In C. E. Dinsmore (Ed.), *A History of Regeneration Research. Milestones in the Evolution of a Science.* (pp. 47–66.). Cambridge: Cambridge University Press.

[65] Harrison, R. G. (1907). Observations on the living developing nerve fiber. *Anat. Rec., 1* (5), 116–118.

[66] Harrison, R. G. (1910). The outgrowth of the nerve fiber as a mode of protoplasmic movement. *J. Exp. Zool, 9* (4), 787–846.

[67] Maienschein, J. (2011). Regenerative medicine's historical roots in regeneration, transplantation, and translation. *Dev Biol., 358* (2), 278-84.

[68] Dameshek, W. (1957). Bone marrow transplantation; a present-day challenge. *Blood, 12* (4), 321-3.

[69] De la Morena, M. T., & Gatti, R. A. (2011). A history of bone marrow transplantation. *Hematol Oncol Clin North Am., 25* (1), 1-15.

[70] Kolios, G., & Moodley, Y. (2013). Introduction to stem cells and regenerative medicine. *Respiration, 85* (1), 3-10.

[71] Weissman, I. L. (2000). Stem cells: units of development, units of regeneration, and units in evolution. *Cell, 100* (1), 157-68.

[72] Becker, A. J., McCulloch, E. A., & Till, J. E. (1963). Cytological demonstration of the clonal nature of spleen colonies derived from transplanted mouse marrow cells. *Nature, 197*, 452-4.

[73] Till, J. E., & McCulloch, E. A. (1961). A direct measurement of the radiation sensitivity of normal mouse bone marrow cells. *Radiat Res., 14*, 213-22.

[74] Wu, A. M., Till, J. E., Siminovitch , L., & McCulloch, E. A. (1968). Cytological evidence for a relationship between normal hematopoietic colony-forming cells and cells of the lymphoid system. *J Exp Med., 127* (3), 455-64.

[75] Smith, A. (2006). A glossary for stem-cell biology. *Nature, 441*, 1060 .

[76] Thomson, J. A., Itskovitz-Eldor, J., Shapiro, S. S., Waknitz, M. A., Swiergiel, J. J., Marshall, V. S., et al. (1998). Embryonic stem cell lines derived from human blastocysts. *Science, 282* (5391), 1145-7.

[77] Reubinoff, B. E., Pera, M. F., Fong, C. Y., Trounson, A., & Bongso, A. (2000). Embryonic stem cell lines from human blastocysts: somatic differentiation in vitro. *Nat Biotechnol., 18* (4), 399-404.

[78] De Wert, G., & Mummery, C. (2003). Human embryonic stem cells: research, ethics and policy. *Hum Reprod., 18* (4), 672-82.

[79] The Hinxton Group. An International consortium on stem cells, e. a. (2006). *http://www.hinxtongroup.org/wp_eu_map.html*. Tratto da www.hinxtongroup.org.

[80] Lovell-Badge, R. (2008). The regulation of human embryo and stem-cell research in the United Kingdom. *Nature Reviews Molecular Cell Biology, 9* (12), 998–1003 .

[81] Beltrame, L. (2017). The Italian Way to Stem Cell Research: Rethinking the Role of Catholic Religion in Shaping Italian Stem Cell Research Regulations. *Dev World Bioeth., 17* (3), 157-166.

[82] Human embryonic stem cell research in the US: time for change? (2010). *Nat Cell Biol., 12* (7), 627.

[83] Volarevic, V., Simovic Markovic, B., Gazdic, M., Volarevic, A., Jovicic, N., Arsenijevic, N., et al. (2018). Ethical and Safety Issues of Stem Cell-Based Therapy. *Int J Med Sci., 15* (1), 36–45.

[84] Kroon, E., Martinson, L. A., Kadoya, K., Bang, A. G., Kelly, O. G., Eliazer, S., et al. (2008). Pancreatic endoderm derived from human embryonic stem cells generates glucose-responsive insulin-secreting cells in vivo. *Nat Biotechnol., 26* (4), 443-52.

[85] Prokhorova, T. A., Harkness, L. M., Frandsen, U., Ditzel, N., Schrøder, H. D., Burns, J. S., et al. (2009). Teratoma formation by human embryonic stem cells is site dependent and enhanced by the presence of Matrigel. *Stem Cells Dev., 18* (1), 47-54.

[86] Shi, Y., Inoue, H., Wu, J. C., & Yamanaka, S. (2017). Induced pluripotent stem cell technology: a decade of progress. *Nat Rev Drug Discov., 16* (2), 115-130.

[87] Takahashi, K., & Yamanaka, S. (2006). Induction of pluripotent stem cells from mouse embryonic and adult fibroblast cultures by defined factors. *Cell, 126* (4), 663-76.

[88] Takahashi, K., Tanabe, K., Ohnuki, M., Narita, M., Ichisaka, T., Tomoda, K., et al. (2007). Induction of pluripotent stem cells from adult human fibroblasts by defined factors. *Cell, 131* (5), 861-72.

[89] Yu, J., Vodyanik, M. A., Smuga-Otto, K., Antosiewicz-Bourget, J., Frane, J. L., Tian, S., et al. (2007). Induced pluripotent stem cell lines derived from human somatic cells. *Science, 318* (5858), 1917-20.

[90] O'Donoghue, K., & Fisk, N. M. (2004). Fetal stem cells. *Best Pract Res Clin Obstet Gynaecol., 18* (6), 853-75.

[91] Lindvall, O. (2003). Stem cells for cell therapy in Parkinson's disease. *Pharmacol Res., 47* (4), 279-87.

[92] Lo, B., & Parham, L. (2009). Ethical Issues in Stem Cell Research. *Endocr Rev., 30* (3), 204–213.

[93] Wadman, M. (2015). The truth about fetal tissue research. *Nature, 528* (7581), 178-181.

[94] Gage, F. H. (2000). Mammalian neural stem cells. *Science, 287* (5457), 1433-8.

[95] Gage, F. H., & Temple, S. (2013). Neural Stem Cells: Generating and Regenerating the Brain. *Neuron., 80* (3), 588-601.

[96] Ernst, A., Alkass, K., Bernard, S., Salehpour, M., Perl, S., Tisdale, J., et al. (2014). Neurogenesis in the striatum of the adult human brain. *Cell, 156* (5), 1072-83.

[97] Nunes, M. C., Roy, N. S., Keyoung, H. M., Goodman, R. R., McKhann, G. 2., Jiang, L., et al. (2003). Identification and isolation of multipotential neural progenitor cells from the subcortical white matter of the adult human brain. *Nat Med., 9* (4), 439-47.

[98] Feldmann, R. E., & Mattern, R. (2006). The human brain and its neural stem cells postmortem: from dead brains to live therapy. *Int J Legal Med., 120* (4), 201-11.

[99] Eriksson, P. S., Perfilieva, E., Björk-Eriksson, T., Alborn, A. M., Nordborg , C., Peterson, D. A., et al. (1998). Neurogenesis in the adult human hippocampus. *Nat Med., 4* (11), 1313-7.

[100] van den Berge, S. S., Middeldorp, J., Zhang, C. E., Curtis, M. A., Leonard, B. W., Mastroeni, D., et al. (2010). Longterm quiescent cells in the aged human subventricular neurogenic system specifically express GFAP-delta. *Aging Cell, 9* (3), 313-26.

[101] van Strien, M. E., Sluijs, J. A., Reynolds, B. A., Steindler, D. A., Aronica, E., & Hol , E. M. (2014). Isolation of neural progenitor cells from the human adult subventricular zone based on expression of the cell surface marker CD271. *Stem Cells Transl Med., 3* (4), 470-80.

[102] Pagano, S. F., Impagnatiello, F., Girelli, M., Cova, L., Grioni, E., Onofri, M., et al. (2000). Isolation and characterization of neural stem cells from the adult human olfactory bulb. *Stem Cells, 18* (4), 295-300.

[103] Kuwabara, T., & Asashima, M. (2012). Regenerative medicine using adult neural stem cells: the potential for diabetes therapy and other pharmaceutical applications. *J Mol Cell Biol., 4* (3), 133-9.

[104] Behnan, J., Stangeland, B., Langella, T., Finocchiaro, G., Tringali, G., Meling, T. R., et al. (2017). Identification and characterization of a new source of adult human neural progenitors. *Cell Death Dis., 8* (8), e2991.

[105] Plock, J. A., Schnider, J. T., Solari, M. G., Zheng, X. X., & Gorantla, V. S. (2013). Perspectives on the use of mesenchymal stem cells in vascularized composite allotransplantation. *Front Immunol., 4* (175), 1-7.

[106] Zomer, H. D., Vidane, A. S., Gonçalves, N. N., & Ambrósio, C. E. (2015). Mesenchymal and induced pluripotent stem cells: general insights and clinical perspectives. *Stem Cells Cloning, 8*, 125-34.

[107] in 't Anker, P. S., Noort, W. A., Scherjon, S. A., Kleijburg-van der Keur, C., Kruisselbrink, A. B., van Bezooijen, R. L., et al. (2003). Mesenchymal stem cells in human second-trimester bone marrow, liver, lung,

and spleen exhibit a similar immunophenotype but a heterogeneous multilineage differentiation potential. *Haematologica, 88* (8), 845-52.

[108] Le Blanc, K., Götherström, C., Ringdén, O., Hassan, M., McMahon, R., Horwitz, E., et al. (2005). Fetal mesenchymal stem-cell engraftment in bone after in utero transplantation in a patient with severe osteogenesis imperfecta. *Transplantation, 79* (11), 1607-14.

[109] Jiao, F., Wang, J., Dong, Z. L., Wu, M. J., Zhao, T. B., Li, D. D., et al. (2012). Human mesenchymal stem cells derived from limb bud can differentiate into all three embryonic germ layers lineages. *Cell Reprogram., 14* (4), 324-33.

[110] Pittenger, M. F., Mackay, A. M., Beck, S. C., Jaiswal, R. K., Douglas, R., Mosca, J. D., et al. (1999). Multilineage potential of adult human mesenchymal stem cells. *Science, 284* (5411), 143-7.

[111] Bunnell, B. A., Flaat, M., Gagliardi, C., Patel, B., & Ripoll, C. (2008). Adipose-derived Stem Cells: Isolation, Expansion and Differentiation. *Methods, 45* (2), 115-20.

[112] Huang, G. T., Gronthos, S., & Shi, S. (2009). Mesenchymal stem cells derived from dental tissues vs. those from other sources: their biology and role in regenerative medicine. *J Dent Res., 88* (9), 792-806.

[113] Schüring, A. N., Schulte, N., Kelsch, R., Röpke, A., Kiesel, L., & Götte, M. (2011). Characterization of endometrial mesenchymal stem-like cells obtained by endometrial biopsy during routine diagnostics. *Fertil Steril., 95* (1), 423-6.

[114] Allickson, J. K., Sanchez, A., Yefimenko, N., Borlongan, C. V., & Sanberg, P. R. (2011). Recent studies assessing the proliferative capability of a novel adult stem cell identified in menstrual blood. *Open Stem Cell J., 3* (2011), 4-10.

[115] Ab Kadir, R., Zainal Ariffin, S. H., Megat Abdul Wahab, R., Kermani, S., & Senafi, S. (2012). Characterization of mononucleated human peripheral blood cells. *ScientificWorldJournal, 2012* (843843).

[116] Rotter, N., Oder, J., Schlenke, P., Lindner, U., Böhrnsen, F., Kramer, J., et al. (2008). Isolation and characterization of adult stem cells from human salivary glands. *Stem Cells Dev., 17* (3), 509-18.

[117] Bartsch, G., Yoo, J. J., De Coppi, P., Siddiqui, M. M., Schuch, G., Pohl, H. G., et al. (2005). Propagation, expansion, and multilineage differentiation of human somatic stem cells from dermal progenitors. *Stem Cells Dev., 14* (3), 337-48.

[118] Riekstina, U., Muceniece, R., Cakstina, I., Muiznieks, I., & Ancans, J. (2008). Characterization of human skin-derived mesenchymal stem cell proliferation rate in different growth condition. *Cytotechnology, 58* (3), 153-62.

[119] Morito, T., Muneta, T., Hara, K., Ju, Y. J., Mochizuki, T., Makino, H., et al. (2008). Synovial fluid-derived mesenchymal stem cells increase after intra-articular ligament injury in humans. *Rheumatology (Oxford), 47* (8), 1137-43.

[120] Williams, J. T., Southerland, S. S., Souza, J., Calcutt, A. F., & Cartledge, R. G. (1999). Cells isolated from adult human skeletal muscle capable of differentiating into multiple mesodermal phenotypes. *Am Surg., 65* (1), 22-6.

[121] Branch, M. J., Hashmani, K., Dhillon, P., Jones, D. R., Dua, H. S., & Hopkinson, A. (2012). Mesenchymal stem cells in the human corneal limbal stroma. *Invest Ophthalmol Vis Sci., 53* (9), 5109-16.

[122] Chong, J. J., Chandrakanthan, V., Xaymardan, M., Asli, N. S., Li, J., Ahmed, I., et al. (2011). Adult cardiac-resident MSC-like stem cells with a proepicardial origin. *Cell Stem Cell, 9* (6), 527–540.

[123] Hennrick, K. T., Keeton, A. G., Nanua, S., Kijek, T. G., Goldsmith, A. M., Sajjan, U. S., et al. (2007). Lung cells from neonates show a mesenchymal stem cell phenotype. *Am J Respir Crit Care Med., 175* (11), 1158-64.

[124] Raynaud, C. M., Maleki, M., Lis, R., Ahmed, B., Al-Azwani, I., Malek, J., et al. (2012). Comprehensive characterization of mesenchymal stem cells from human placenta and fetal membrane and their response to osteoactivin stimulation. *Stem Cells Int., 2012* (658356).

[125] In 't Anker, P. S., Scherjon, S. A., Kleijburg-van der Keur, C., Noort, W. A., Claas, F. H., Willemze, R., et al. (2003). Amniotic fluid as a novel source of mesenchymal stem cells for therapeutic transplantation. *Blood, 102*, 1548-1549.

[126] Romanov, Y. A., Svintsitskaya, V. A., & Smirnov, V. N. (2003). Searching for alternative sources of postnatal human mesenchymal stem cells: candidate MSC-like cells from umbilical cord. *Stem Cells, 21*, 105-110.

[127] Lee, O. K., Kuo, T. K., Chen, W. M., Lee, K. D., Hsieh, S. L., & Chen, T. H. (2004). Isolation of multipotent mesenchymal stem cells from umbilical cord blood. *Blood, 103* (5), 1669-75.

[128] Friedenstein, A. J., Chailakhyan, R. K., Latsinik, N. V., Panasyuk, A. F., & Keiliss-Borok, I. V. (1974). Stromal cells responsible for transferring the microenvironment of the hemopoietic tissues. Cloning in vitro and retransplantation in vivo. *Transplantation, 17* (4), 331-40.

[129] Horwitz, E. M., Le Blanc, K., Dominici, M., Mueller, I., Slaper-Cortenbach, I., Marini, F. C., et al. (2005). Clarification of the nomenclature for MSC: The International Society for Cellular Therapy position statement. *Cytotherapy, 7* (5), 393-5.

[130] Caplan, A. I. (1991). Mesenchymal stem cells. *J Orthop Res., 9* (5), 641-50.

[131] Dominici, M., Le Blanc, K., Mueller, I., Slaper-Cortenbach, I., Marini, F., Krause, D., et al. (2006). Minimal criteria for defining multipotent mesenchymal stromal cells. The International Society for Cellular Therapy position statement. *Cytotherapy, 8* (4), 315-7.

[132] Caplan, A. I. (2007). Adult Mesenchymal Stem Cells for Tissue Engineering versus Regenerative medicine. *J. Cell. Physiology, 213*, 341-347.

[133] Ryan, J. M., Barry, F. P., Murphy, J. M., & Mahon, B. P. (2005). Mesenchymal stem cells avoid allogeneic rejection. *J Inflamm (Lond)., 2* (8).

[134] Ankrum, J. A., Ong, J. F., & Karp, J. M. (2014). Mesenchymal stem cells: immune evasive, not immune privileged. *Nat Biotechnol., 32* (3), 252-60.

[135] Rao, M. S., & Mattson, M. P. (2001). Stem cells and aging: expanding the possibilities. *Mech Ageing Dev., 122* (7), 713-34.

[136] Stolzing, A., Jones, E., McGonagle, D., & Scutt, A. (2008). Age-related changes in human bone marrow-derived mesenchymal stem cells: consequences for cell therapies. *Mech Ageing Dev., 129* (3), 163-73.

[137] Marcus, A. J., & Woodbury, D. (2008). Fetal stem cells from extra-embryonic tissues: do not discard. *J. Cell. Mol. Med., 12* (3), 730-742.

[138] Vu, Q., Xie, K., Eckert, M., Zhao, W., & Cramer, S. C. (2014). Meta-analysis of preclinical studies of mesenchymal stromal cells for ischemic stroke. *Neurology, 82* (14), 1277–1286.

[139] Squillaro, T., Peluso, G., & Galderisi, U. (2016). Clinical Trials With Mesenchymal Stem Cells: An Update. *Cell Transplant., 25* (5), 829-48.

[140] Wang, L., Ting, C., Yen, M., Liu, K., Sytwu, H., Wu, K. K., et al. (2016). Human mesenchymal stem cells (MSCs) for treatment towards immune- and inflammation-mediated diseases: review of current clinical trials. *J Biomed Sci., 23*, 76.

[141] Dalous, J., Larghero, J., & Baud, O. (2012). Transplantation of umbilical cord–derived mesenchymal stem cells as a novel strategy to protect the central nervous system: technical aspects, preclinical studies, and clinical perspectives. *Pediatr Res., 71* (4 Pt 2), 482-90.

[142] Wharton, T. W. (1996). *Adenographia. Translated by S. Freer.* (Vol. 1656:243). Oxford, UK: Oxford University Press.

[143] Sobolewski, K., Bańkowski, E., Chyczewski, L., & Jaworski, S. (1997). Collagen and glycosaminoglycans of Wharton's jelly. *Biol Neonate., 71* (1), 11-21.

[144] Nanaev, A. K., Kohnen, G., Milovanov, A. P., Domogatsky, S. P., & Kaufmann, P. (1997). Stromal differentiation and architecture of the human umbilical cord. *Placenta, 18* (1), 53-64.

[145] Karahuseyinoglu, S., Cinar O, O., Kilic , E., Kara, F., Akay, G. G., Demiralp, D. O., et al. (2007). Biology of Stem Cells in Human Umbilical Cord Stroma: In Situ. *Stem Cells, 25* (2), 319-31.

[146] Lavrentieva, A., Majore, I., Kasper, C., & Hass, R. (2010). Effects of hypoxic culture conditions on umbilical cord-derived human mesenchymal stem cells. *Cell Commun Signal., 8* (18).

[147] McElreavey, K. D., Irvine, A. I., Ennis, K. T., & McLean, W. H. (1991). Isolation, culture and characterisation of fibroblast-like cells derived from the Wharton's jelly portion of human umbilical cord. *Biochem Soc Trans., 19* (1), 29S.

[148] Takechi, K., Kuwabara, Y., & Mizuno, M. (1993). Ultrastructural and immunohistochemical studies of Wharton's jelly umbilical cord cells. *Placenta, 14* (2), 235-45.

[149] Xiao, B., Rao, F., Guo, Z. Y., Sun, X., Wang, Y. G., Liu, S. Y., et al. (2016). Extracellular matrix from human umbilical cord-derived mesenchymal stem cells as a scaffold for peripheral nerve regeneration. *Neural Regen Res., 11* (7), 1172-9.

[150] Lo Iacono, M., Russo, E., Anzalone, R., Baiamonte, E., Alberti, G., Gerbino, A., et al. (2018). Wharton's Jelly Mesenchymal Stromal Cells Support the Expansion of Cord Blood–derived CD34+ Cells Mimicking a Hematopoietic Niche in a Direct Cell–cell Contact Culture System. *Cell Transplantation, 27* (1), 117-129.

[151] Farias, V. A., Linares-Fernández, J. L., Peñalver, J. L., Payá Colmenero, J. A., Ferrón, G. O., Duran, E. L., et al. (2011). Human umbilical cord stromal stem cell express CD10 and exert contractile properties. *Placenta, 32* (1), 86-95.

[152] Hutchison, N., Fligny, C., & Duffiel, J. S. (2013). Resident mesenchymal cells and fibrosis. *Biochimica et Biophysica Acta (BBA) - Molecular Basis of Disease, 1832* (7), 962-971.

[153] Subramanian, A., Fong, C. Y., Biswas, A., & Bongso, A. (2015). Comparative Characterization of Cells from the Various Compartments of the Human Umbilical Cord Shows that the Wharton's Jelly Compartment Provides the Best Source of Clinically Utilizable Mesenchymal Stem Cells. *PLoS One, 10* (6), e0127992.

[154] Spurway, J., Logan, P., & Pak, S. (2012). The development, structure and blood flow within the umbilical cord with particular reference to the venous system. *Australas J Ultrasound Med., 15* (3), 97–102.

[155] Conconi, M. T., Di Liddo, R., Tommasini, M., Calore, C., & Parnigotto, P. P. (2011). Phenotype and Differentiation Potential of Stromal Populations Obtained from Various Zones of Human Umbilical Cord: An Overview. *The Open Tissue Engineering and Regenerative Medicine Journal, 4*, 6-20.

[156] Wang, H. S., Hung, S. C., Peng, S. T., Huang, C. C., Wei, H. M., Guo, Y. J., et al. (2004). Mesenchymal stem cells in the Wharton's jelly of the human umbilical cord. *Stem Cells, 22* (7), 1330-7.

[157] Jeschke, M. G., Gauglitz, G. G., Phan, T. T., Herndon, D. N., & Kita, K. (2011). Umbilical Cord Lining Membrane and Wharton's Jelly-Derived Mesenchymal Stem Cells: the Similarities and Differences. *The Open Tissue Engineering and Regenerative Medicine Journal, 4* (special issue 1), 21-27.

[158] Fong, C. Y., Richards, M., Manasi, N., Biswas, A., & Bongso, A. (2007). Comparative growth behaviour and characterization of stem cells from human Wharton's jelly. *Reproductive BioMedicine Online, 15* (6), 708-718 .

[159] Seshareddy, K., Troyer, D., & Weiss, M. L. (2008). Method to isolate mesenchymal-like cells from Wharton's Jelly of umbilical cord. *Methods Cell Biol., 86*, 101-19.

[160] Sarugaser, R., Lickorish, D., Baksh, D., Hosseini, M. M., & Davies, J. E. (2005). Human umbilical cord perivascular (HUCPV) cells: a source of mesenchymal progenitors. *Stem Cells, 23* (2), 220-9.

[161] Mennan, C., Wright, K., Bhattacharjee, A., Balain, B., Richardson, J., & Roberts, S. (2013). Isolation and characterisation of mesenchymal stem cells from different regions of the human umbilical cord. *Biomed Res Int., 2013*, 916136.

[162] Huang, L., Wong, Y. P., Gu, H., Cai, Y. J., Ho, Y., Wang, C. C., et al. (2011). Stem cell-like properties of human umbilical cord lining epithelial cells and the potential for epidermal reconstitution. *Cytotherapy , 13* (2), 145-55.

[163] Sivalingam, J., Krishnan, S., Ng, W. H., Lee, S. S., Phan, T. T., & Kon, O. L. (2010). Biosafety Assessment of Site-directed Transgene Integration in Human Umbilical Cord–lining Cells. *Mol Ther., 18* (7), 1346–1356.

[164] Sarugaser, R., Ennis, J., Stanford, W. L., & Davies, J. E. (2009). Isolation, propagation, and characterization of human umbilical cord perivascular cells (HUCPVCs). *Methods Mol Biol., 482*, 269-79.

[165] Salehinejad, P., Alitheen, N. B., Ali, A. M., Omar, A. R., Mohit, M., Janzamin, E., et al. (2012). Comparison of different methods for the isolation of mesenchymal stem cells from human umbilical cord Wharton's jelly. *In Vitro Cell Dev Biol Anim., 48* (2), 75-83.

[166] Yannarelli, G., Dayan, V., Pacienza , N., Lee, C. J., Medin, J., & Keating, A. (2013). Human umbilical cord perivascular cells exhibit enhanced cardiomyocyte reprogramming and cardiac function after experimental acute myocardial infarction. *Cell Transplant., 22* (9), 1651-66.

[167] Tsang, W. P., Shu, Y., Kwok, P. L., Zhang, F., Lee, K. K., Tang, M. K., et al. (2013). CD146+ human umbilical cord perivascular cells maintain stemness under hypoxia and as a cell source for skeletal regeneration. *PLoS One, 8* (10), e76153.

[168] Saltik, B. C., & Gökçınar Yağcı, B. (2017). Expansion of human umbilical cord blood hematopoietic progenitors with cord vein pericytes. *Turkish Journal of Biology, 41*, 49-57.

[169] Martin-Rendon, E., Sweeney D, D., Lu, F., Girdlestone, J., & Watt, S. M. (2008). 5-Azacytidine-treated human mesenchymal stem/progenitor cells derived from umbilical cord, cord blood and bone marrow do not generate cardiomyocytes in vitro at high frequencies. *Vox Sang, 95* (2), 137-48.

[170] Sarugaser, R., Hanoun, L., Keating, A., Stanford, W. L., & Davies, J. E. (2009). Human mesenchymal stem cells self-renew and differentiate according to a deterministic hierarchy. *PLoS One, 4* (8), e6498.

[171] Schugar, R. C., Chirieleison, S. M., Wescoe, K. E., Schmidt, B. T., Askew, Y., Nance, J. J., et al. (2009). High harvest yield, high expansion, and phenotype stability of CD146 mesenchymal stromal cells from whole primitive human umbilical cord tissue. *J Biomed Biotechnol., 2009* (789526).

[172] Xu, L., Zhou, J., Liu, J., Liu, Y., Wang, L., & Jiang, R. (2017). Different Angiogenic Potentials of Mesenchymal Stem Cells Derived from Umbilical Artery, Umbilical Vein, and Wharton's Jelly. *Stem Cells Int.*, *2017* (3175748).

[173] Pires, A. O., Mendes-Pinheiro B, B., Teixeira FG, F. G., Anjo, S. I., Ribeiro-Samy, S., Gomes, E. D., et al. (2016). Unveiling the Differences of Secretome of Human Bone Marrow Mesenchymal Stem Cells, Adipose Tissue-Derived Stem Cells, and Human Umbilical Cord Perivascular Cells: A Proteomic Analysis. *Stem Cells Dev., 25* (14), 1073-83.

[174] Szaraz, P., Librach, M., Maghen, L., Iqbal, F., Barretto, T. A., Kenigsberg, S., et al. (2016). In Vitro Differentiation of First Trimester Human Umbilical Cord Perivascular Cells into Contracting Cardiomyocyte-Like Cells. *Stem Cells Int., 2016*, 7513252.

[175] Dayan, V., Yannarelli, G., Billia, F., Filomeno, P., Wang, X. H., Davies, J. E., et al. (2011). Mesenchymal stromal cells mediate a switch to alternatively activated monocytes/macrophages after acute myocardial infarction. *Basic Res Cardiol., 106* (6), 1299-310.

[176] Kadam, S. S., Tiwari, S., & Bhonde, R. R. (2009). Simultaneous isolation of vascular endothelial cells and mesenchymal stem cells from the human umbilical cord. *In Vitro Cell Dev Biol Anim., 45* (1-2), 23-7.

[177] Prasanna, S. J., Gopalakrishnan, D., Shankar, S. R., & Vasandan, A. B. (2010). Pro-inflammatory cytokines, IFNgamma and TNFalpha, influence immune properties of human bone marrow and Wharton jelly mesenchymal stem cells differentially. *PLoS One, 5* (2), e9016.

[178] Tong, C. K., Vellasamy, S., Tan, B. C., Abdullah, M., Vidyadaran, S., Seow, H. F., et al. (2011). Generation of mesenchymal stem cell from human umbilical cord tissue using a combination enzymatic and mechanical disassociation method. *Cell Biol Int., 35* (3), 221-6.

[179] Oktar, P. A., Yildirim, S., Balci, D., & Can, A. (2011). Continual expression throughout the cell cycle and downregulation upon adipogenic differentiation makes nucleostemin a vital human MSC proliferation marker. *Stem Cell Rev., 7* (2), 413-24.

[180] La Rocca, G., Anzalone, R., Corrao, S., Magno, F., Loria , T., Lo Iacono, M., et al. (2009). Isolation and characterization of Oct-4+/HLA-G+ mesenchymal stem cells from human umbilical cord matrix: differentiation potential and detection of new markers. *Histochem Cell Biol., 131* (2), 267-82.

[181] Fong, C. Y., Chak, L. L., Biswas, A., Tan, J. H., Gauthaman, K., Chan, W. K., et al. (2011). Human Wharton's jelly stem cells have unique transcriptome profiles compared to human embryonic stem cells and other mesenchymal stem cells. *Stem Cell Rev., 7* (1), 1-16.

[182] Weiss, M. L., Anderson, C., Medicetty, S., Seshareddy, K. B., Weiss, R. J., VanderWerff, I., et al. (2008). Immune properties of human umbilical cord Wharton's jelly-derived cells. *Stem Cells, 26* (11), 2865-74.

[183] Prasanna, S. J., & Jahnavi, V. S. (2011). Wharton's jelly mesenchymal stem cells as off-the -shelf cellular therapeutics: A closer look into their regenerative and immunomodulatory properties. *Open Tissue Eng. Regen. Med. J., 4*, 28–38.

[184] Kyurkchiev, D., Bochev, I., Ivanova-Todorova, E., Mourdjeva, M., Oreshkova, T., Belemezova, K., et al. (2014). Secretion of immunoregulatory cytokines by mesenchymal stem cells. *World J Stem Cells., 6* (5), 552-70.

[185] Mitchell, K. E., Weiss, M. L., Mitchell, B. M., Martin, P., Davis, D., Morales, L., et al. (2003). Matrix cells from Wharton's jelly form neurons and glia. *Stem Cells, 21* (1), 50-60.

[186] Leite, C., Silva, N. T., Mendes, S., Ribeiro, A., de Faria, J. P., Lourenço, T., et al. (2014). Differentiation of human umbilical cord matrix mesenchymal stem cells into neural-like progenitor cells and maturation into an oligodendroglial-like lineage. *PLoS One, 9* (10), e111059.

[187] Messerli, M., Wagner, A., Sager, R., Mueller, M., Baumann, M., Surbek, D. V., et al. (2013). Stem cells from umbilical cord Wharton's jelly from preterm birth have neuroglial differentiation potential. *Reprod Sci., 20* (12), 1455-64.

[188] Peng, J., Wang, Y., Zhang, L., Zhao, B., Zhao, Z., Chen, J., et al. (2011). Human umbilical cord Wharton's jelly-derived mesenchymal stem cells differentiate into a Schwann-cell phenotype and promote neurite outgrowth in vitro. *Brain Res Bull., 84* (3), 235-43.

[189] Ding, D. C., Shyu, W. C., Chiang, M. F., Lin, S. Z., Chang, Y. C., Wang, H. J., et al. (2007). Enhancement of neuroplasticity through upregulation of beta1-integrin in human umbilical cord-derived stromal cell implanted stroke model. *Neurobiol Dis., 27* (3), 339-53.

[190] Wang, S. H., Lin, S. J., Chen, Y. H., Lin, F. Y., Shih, J. C., Wu, C. C., et al. (2009). Late outgrowth endothelial cells derived from Wharton jelly in human umbilical cord reduce neointimal formation after vascular injury: involvement of pigment epithelium-derived factor. *Arterioscler Thromb Vasc Biol., 29* (6), 816-22.

[191] Anzalone, R., Lo Iacono, M., Corrao, S., Magno, F., Loria, T., Cappello, F., et al. (2010). New emerging potentials for human Wharton's jelly mesenchymal stem cells: immunological features and hepatocyte-like differentiative capacity. *Stem Cells Dev., 19* (4), 423-38.

[192] Anzalone, R., Lo Iacono, M., Loria, T., Di Stefano, A., Giannuzzi, P., Farina, F., et al. (2011). Wharton's jelly mesenchymal stem cells as candidates for beta cells regeneration: extending the differentiative and immunomodulatory benefits of adult mesenchymal stem cells for the treatment of type 1 diabetes. *Stem Cell Rev., 7* (2), 342-63.

[193] Kadam, S. S., & Bhonde, R. R. (2010). Islet neogenesis from the constitutively nestin expressing human umbilical cord matrix derived mesenchymal stem cells. *Islets, 2* (2), 112-20.

[194] Campard, D., Lysy, P. A., Najimi, M., & Sokal, E. M. (2008). Native umbilical cord matrix stem cells express hepatic markers and differentiate into hepatocyte-like cells. *Gastroenterology, 134* (3), 833-48.

[195] Hsieh, J. Y., Wang, H. W., Chang, S. J., Liao, K. H., Lee, I. H., Lin, W. S., et al. (2013). Mesenchymal stem cells from human umbilical cord express preferentially secreted factors related to neuroprotection, neurogenesis, and angiogenesis. *PLoS One, 8* (8), e72604.

[196] Kita, K., Gauglitz, G. G., Phan, T. T., Herndon, D. N., & Jeschke, M. G. (2010). Isolation and characterization of mesenchymal stem cells from the sub-amniotic human umbilical cord lining membrane. *Stem Cells Dev., 19* (4), 491-502.

[197] Deuse, T., Stubbendorff, M., Tang-Quan, K., Phillips, N., Kay, M. A., Eiermann, T., et al. (2011). Immunogenicity and immunomodulatory properties of umbilical cord lining mesenchymal stem cells. *Cell Transplant., 20* (5), 655-67.

[198] Reza, H. M., Ng, B. Y., Phan, T. T., Tan, D. T., Beuerman, R. W., & Ang, L. P. (2011). Characterization of a novel umbilical cord lining cell with CD227 positivity and unique pattern of P63 expression and function. *Stem Cell Rev., 7* (3), 624-38.

[199] Gonzalez, R., Griparic, L., Umana, M., Burgee, K., Vargas, V., Nasrallah, R., et al. (2010). An efficient approach to isolation and characterization of pre- and postnatal umbilical cord lining stem cells for clinical applications. *Cell Transplant., 19* (11), 1439-49.

[200] Tajiri, N., Kaneko, Y., Shinozuka, K., Ishikawa, H., Yankee, E., McGrogan, M., et al. (2013). Stem Cell Recruitment of Newly Formed Host Cells via a Successful Seduction? Filling the Gap between Neurogenic Niche and Injured Brain Site. *PLoS One, 8* (9), e74857.

[201] Spees, J. L., Olson, S. D., Whitney, M. J., & Prockop, D. J. (2006). Mitochondrial transfer between cells can rescue aerobic respiration. *Proc Natl Acad Sci U S A, 103* (5), 1283-8.

[202] Hayakawa, K., Esposito, E., Wang, X., Terasaki, Y., Liu, Y., Xing, C., et al. (2016). Transfer of mitochondria from astrocytes to neurons. *Nature, 535* (7613), 551-5.

[203] Plotnikov, E. Y., Babenko, V. A., Silachev, D. N., Zorova, L. D., Khryapenkova, T. G., Savchenko, E. S., et al. (2015). Intercellular Transfer of Mitochondria. *Biochemistry (Mosc), 80* (5), 542-8.

[204] Nguyen, H., Zarriello, S., Rajani, M., Tuazon, J., Napoli, E., & Borlongan, C. V. (2018). Understanding the Role of Dysfunctional and Healthy Mitochondria in Stroke Pathology and Its Treatment. *Int J Mol Sci., 19* (7), pii: E2127.

[205] Hayakawa, K., Chan, S. J., Mandeville, E. T., Park, J. H., Bruzzese, M., Montaner, J., et al. (2018). Brief Reports: Protective Effects of Endothelial Progenitor Cell-Derived Extracellular Mitochondria in Brain Endothelium. *Stem Cells, 36* (9), 1404-1410.

[206] Huang, P. J., Kuo, C. C., Lee, H. C., Shen, C. I., Cheng, F. C., Wu, S., et al. (2016). Transferring Xenogenic Mitochondria Provides Neural Protection Against Ischemic Stress in Ischemic Rat Brains. *Cell Transplant., 25* (5), 913-27.

[207] Chen, J., Wang, Q., Feng, X., Zhang, Z., Geng, L., Xu, T., et al. (2016). Umbilical Cord-Derived Mesenchymal Stem Cells Suppress Autophagy of T Cells in Patients with Systemic Lupus Erythematosus via Transfer of Mitochondria. *Stem Cells Int., 2016*, 4062789.

[208] Lin, H. Y., Liou, C. W., Chen, S. D., Hsu, T. Y., Chuang, J. H., Wang, P. W., et al. (2015). Mitochondrial transfer fromWharton's jelly-derived mesenchymal stem cells to mitochondria-defective cells recaptures impaired mitochondrial function. *Mitochondrion, 22*, 31-44.

[209] Chuang, Y. C., Liou, C. W., Chen, S. D., Wang, P. W., Chuang, J. H., Tiao, M. M., et al. (2017). Mitochondrial Transfer from Wharton's Jelly Mesenchymal Stem Cell to MERRF Cybrid Reduces Oxidative Stress and Improves Mitochondrial Bioenergetics. *Oxid Med Cell Longev., 2017*, 5691215.

[210] Jin, L. T., Hwang, S. Y., Yoo, G. S., & Choi, J. K. (2006). A mass spectrometry compatible silver staining method for protein incorporating a new silver sensitizer in sodium dodecyl sulfate-polyacrylamide electrophoresis gels. *Proteomics, 6* (8), 2334-7.

[211] Shevchenko A, T. H. (2006). In-gel digestion for mass spectrometric characterization of proteins and proteomes. *Nat Protoc., 1(6)*, 2856-60.

[212] Gasteiger, E., Gattiker, A., Hoogland, C., Ivanyi, I., Appel, R. D., & Bairoch, A. (2003). ExPASy: the proteomics server for in-depth protein knowledge and analysis. *Nucleic Acids Res., 31*, 3784-3788.

[213] The UniProt Consortium. (2017). UniProt: the universal protein knowledgebase. *Nucleic Acids Res., 45*, D158-D169.

[214] Huang, D. W., Sherman, B. T., & Lempicki, R. A. (2009). Systematic and integrative analysis of large gene lists using DAVID Bioinformatics Resources. *Nature Protoc., 4* (1), 44-57.

[215] Kaneko, Y., Tajiri, N., Shojo, H., & Borlongan, C. V. (2014). Oxygen–Glucose-Deprived Rat Primary Neural Cells Exhibit DJ-1 Translocation into Healthy Mitochondria: A Potent Stroke Therapeutic Target. *CNS Neurosci Ther., 20* (3), 275–281.

[216] Camby, I., Le Mercier, M., Lefranc, F., & Kiss, R. (2006). Galectin-1: a small protein with major functions. *Glycobiology, 16* (11), 137R–157R.

[217] Leitner, J., Klauser, C., Pickl, W. F., Stöckl, J., Majdic, O., Bardet, A. F., et al. (2009). B7-H3 is a potent inhibitor of human T-cell activation: No evidence for B7-H3 and TREML2 interaction. *Eur J Immunol., 39* (7), 1754-64.

[218] Chapoval, A. I., Ni, J., Lau, J. S., Wilcox, R. A., Flies, D. B., Liu, D., et al. (2001). B7-H3: a costimulatory molecule for T cell activation and IFN-gamma production. *Nat Immunol., 2* (3), 269-74.

[219] Ling, V., Wu, P. W., Spaulding, V., Kieleczawa, J., Luxenberg, D., Carreno, B. M., et al. (2003). Duplication of primate and rodent B7-H3 immunoglobulin V- and C-like domains: divergent history of functional redundancy and exon loss. *Genomics, 82* (3), 365-77.

[220] Page-McCaw, A., Ewald, A. J., & Werb, Z. (2007). Matrix metalloproteinases and the regulation of tissue remodelling. *Nat Rev Mol Cell Biol., 8* (3), 221-33.

[221] Almalki SG, A. D. (2016). Effects of matrix metalloproteinases on the fate of mesenchymal stem cells. *Stem Cell Res Ther., 7(1):129.*

[222] Candelario-Jalil E, Y. Y. (2009). Diverse roles of matrix metalloproteinases and tissue inhibitors of metalloproteinases in neuroinflammation and cerebral ischemia. *Neuroscience., 158(3)*, 983-94.

[223] Shaikh, A., & Bhartiya, D. (2012). Pluripotent Stem Cells in Bone Marrow and Cord Blood. In T. E. Moschandreou (Ed.), *Blood Cell - An Overview of Studies in Hematology* (pp. 69-88). IntechOpen.

[224] Hu, C., Fan, L., Cen, P., Chen, E., Jiang, Z., & Li, L. (2016). Energy Metabolism Plays a Critical Role in Stem Cell Maintenance and Differentiation. *Int J Mol Sci., 17* (2), 253.

[225] Neal, E. G., Liska, M. G., Lippert, T., Lin, R., Gonzalez, M., Russo, E., et al. (2018). An update on intracerebral stem cell grafts. *Expert Review of Neurotherapeutics, 18* (7), 557-572.

[226] Russo, E., Lippert, T., Tuazon, J. P., & Borlongan, C. V. (2018). Advancing stem cells: New therapeutic strategies for treating central nervous system disorders. *Brain Circulation, 4* (3), 81-83.

[227] Li, Y., Hu , G., & Cheng, Q. (2015). Implantation of human umbilical cord mesenchymal stem cells for ischemic stroke: perspectives and challenges. *Front. Med., 9* (1), 20–29.

[228] Amantea, D., Tassorelli, C., Petrelli, F., Certo, M., Bezzi, P., Micieli, G., et al. (2014). Understanding the multifaceted role of inflammatory mediators in ischemic stroke. Amantea D, Tassorelli C, Petrelli F, Certo M, Bezzi P, Micieli G, Corasaniti MT, Bagetta G. *Curr Med Chem., 21* (18), 2098-117.

[229] Sakaguchi, M. O. H. (2012). Neural stem cells, adult neurogenesis, and galectin-1: from bench to bedside. *Dev Neurobiol., 72(7)*, 1059-67.

[230] Ishibashi, S. K. T. (2007). Galectin-1 regulates neurogenesis in the subventricular zone and promotes functional recovery after stroke. *Exp Neurol., 207(2)*, 302-13.

[231] Läubli, H., Alisson-Silva, F., Stanczak, M. A., Siddiqui, S., Deng, L., Verhagen, A., et al. (2014). Lectin Galactoside-binding Soluble 3 Binding Protein (LGALS3BP) Is a Tumor-associated Immunomodulatory Ligand for CD33-related Siglecs. *J Biol Chem., 289* (48), 33481–33491.

[232] Piccolo, E., Tinari, N., Semeraro, D., Traini, S., Fichera, I., Cumashi, A., et al. (2013). LGALS3BP, lectin galactoside-binding soluble 3 binding protein, induces vascular endothelial growth factor in human breast cancer cells and promotes angiogenesis. *J Mol Med, 91*, 83–94.

[233] He, X. W., Li, W. L., Li, C., Liu, P., Shen, Y. G., Zhu, M., et al. (2017). Serum levels of galectin-1, galectin-3, and galectin-9 are associated with large artery atherosclerotic stroke. *Scientific Reports, 7*, 40994.

[234] Venkatraman, A., Hardas, S., Patel, N., Singh Bajaj, N., Arora, G., & Arora, P. (2018). Galectin-3: an emerging biomarker in stroke and cerebrovascular diseases. *Eur J Neurol., 25* (2), 238-246.

[235] Wan, L., Yang, R. Y., & Liu, F. T. (2018). Galectin-12 in Cellular Differentiation, Apoptosis and Polarization. *Int J Mol Sci., 19* (1), 176.

[236] Skornicka, E. L., Kiyatkina, N., Weber, M. C., Tykocinski, M., & Koo, P. H. (2004). Pregnancy zone protein is a carrier and modulator of placental protein-14 in T-cell growth and cytokine production. *Cell Immunol., 232* (1-2), 144-56.

[237] Ha, C. T., Wu, J. A., Irmak, S., Lisboa, F. A., Dizon, A. M., Warren, J. W., et al. (2010). Human pregnancy specific beta-1-glycoprotein 1 (PSG1) has a potential role in placental vascular morphogenesis. *Biol Reprod., 83* (1), 27-35.

[238] Sedlmay, P., Blaschitz, A., & Stocker, R. (2014). The Role of Placental Tryptophan Catabolism. *Front Immunol., 5*, 230.

[239] Mbongue, J. C., Nicholas, D. A., Torrez, T. W., Kim, N. S., Firek, A. F., & Langridge, W. H. (2015). The Role of Indoleamine 2, 3-Dioxygenase in Immune Suppression and Autoimmunity. *Vaccines (Basel), 3* (3), 703–729.

[240] Kwidzinski, E., & Bechmann, I. (2007). IDO expression in the brain: a double-edged sword. *J Mol Med (Berl), 85* (12), 1351-9.

[241] Metz, R., Smith, C., DuHadaway, J. B., Chandler, P., Baban, B., Merlo, L. M., et al. (2014). IDO2 is critical for IDO1-mediated T-cell regulation and exerts a non-redundant function in inflammation. *Int Immunol., 26* (7), 357–367.

[242] Morancho, A., Rosell, A., García-Bonilla, L. & Montaner, J. (2010). Metalloproteinase and stroke infarct size: role for anti-inflammatory treatment? *Ann N Y Acad Sci., 1207*, 123-33.

[243] Sullivan R, D. K. (2015). A possible new focus for stroke treatment - migrating stem cells. *Expert Opin Biol Ther., 15(7)*, 949-58.

[244] Yang, P., Baker, K. A., & Hagg, T. (2006). The ADAMs family: Coordinators of nervous system development, plasticity and repair. *Progress in Neurobiology, 79* (2), 73-94.

[245] Jickling, G. C., & Sharp, F. R. (2015). Biomarker panels in ischemic stroke. *Stroke, 46* (3), 915–920.

[246] Abe, K., Hayash, T., & Itoyama, Y. (1997). Amelioration of brain edema by topical application of glial cell line-derived neurotrophic factor in reperfused rat brain. *Neurosci. Lett., 231*, 37-40.

[247] Kitagawa, H., Hayashi, T., Mitsumoto, Y., Koga, N., Itoyama, Y., & Abe, K. (1998). Reduction of ischemic brain injury by topical application of glial cell line-derived neurotrophic factor after permanent middle cerebral artery occlusion in rats. *Stroke, 29*, 1417-1422.

[248] Kobayashi, T., Ahlenius, H., Thored, P., Kobayashi, R., Kokaia, Z., & Lindvall, O. (2006). Intracerebral infusion of glial cell line-derived neurotrophic factor promotes striatal neurogenesis after stroke in adult rats. *Stroke, 37* (9), 2361-7.

[249] Jin, G., Omori, N., Li, F., Nagano, I., Manabe, Y., Shoji, M., et al. (2003). Protection against ischemic brain damage by GDNF affecting cell survival and death signals. *Neurol Res., 25* (3), 249-53.

[250] Wang, Y., Chang, C. F., Morales, M., Chiang, Y. H., & Hoffer, J. (2002). Protective effects of glial cell line-derived neurotrophic factor in ischemic brain injury. *Ann N Y Acad Sci., 962*, 423-37.

[251] Wang, Y., Lin, S. Z., Chiou, A. L., Williams, L. R., & Hoffer, B. J. (1997). Glial cell line-derived neurotrophic factor protects against ischemia-induced injury in the cerebral cortex. *J Neurosci., 17* (11), 4341-8.

[252] Harvey, B. K., Chang, C. F., Chiang, Y. H., Bowers, W. J., Morales, M., Hoffer, B. J., et al. (2003). HSV amplicon delivery of glial cell line-derived neurotrophic factor is neuroprotective against ischemic injury. *Exp Neurol., 183* (1), 47-55.

[253] Chiang, Y. H., Lin, S. Z., Borlongan, C. V., Hoffer, B. J., Morales, M. F., & Wang, Y. (1999). Transplantation of fetal kidney tissue reduces cerebral infarction induced by middle cerebral artery ligation. *J Cerebral Blood Flow Metab., 19* (12), 1329-35.

[254] Wu, K. J., Yu, S. J., Chiang, C. W., Lee, Y. W., Yen, L., Tseng, P. C., et al. (2018). Neuroprotective action of human Wharton's Jelly derived-mesenchymal stromal cell transplants in a rodent model of stroke. *Cell Transplantation, [ahead of print]*.

[255] Shen, Y., Sun, A., Wang, Y., Cha, D., Wang, H., Wang, F., et al. (2012). Upregulation of mesencephalic astrocyte-derived neurotrophic factor in glial cells is associated with ischemia-induced glial activation. *J Neuroinflammation, 9*, 254.

[256] Mätlik, K., Anttila, J. E., Kuan-Yin, T., Smolander, O. P., Pakarinen, E., Lehtonen, L., et al. (2018). Poststroke delivery of MANF promotes functional recovery in rats. *Sci Adv., 4* (5), eaap8957.

[257] Bright, R., & Mochly-Rosen, D. (2005). The Role of Protein Kinase C in Cerebral Ischemic and Reperfusion Injury. *Stroke, 36* (12), 2781-90.

[258] Mecollari, V., Nieuwenhuis, B., & Verhaagen, J. (2014). A perspective on the role of class III semaphorin signaling in central nervous system trauma. *Front Cell Neurosci., 8*, 328.

[259] Worzfeld, T., & Offermanns, S. (2014). Semaphorins and plexins as therapeutic targets. *Nat Rev Drug Discov., 13* (8), 603-21.

[260] Font, M. A., Arboix, A., & Krupinski, J. (2010). Angiogenesis, Neurogenesis and Neuroplasticity in Ischemic Stroke. *Curr Cardiol Rev., 6* (3), 238-44.

[261] Lee, H. J., Cho, C. H., Hwang, S. J., Choi, H. H., Kim, K. T., Ahn, S. Y., et al. (2004). Biological characterization of angiopoietin-3 and angiopoietin-4. *FASEB J., 18* (11), 1200-8.

[262] Carbone, C., Piro, G., Merz, V., Simionato, F., Santoro, R., Zecchetto, C., et al. (2018). Angiopoietin-Like Proteins in Angiogenesis, Inflammation and Cancer. *Int J Mol Sci., 19* (2), pii: E431.

[263] Troyanovsky, B., Levchenko, T., Månsson, G., Matvijenko, O., & Holmgren, L. (2001). Angiomotin: an angiostatin binding protein that regulates endothelial cell migration and tube formation. *J Cell Biol., 152* (6), 1247-54.

[264] Zhao, B., Li, L., Lu , Q., Wang, L. H., Liu, C. Y., Lei, Q., et al. (2011). Angiomotin is a novel Hippo pathway component that inhibits YAP oncoprotein. *Genes Dev., 25* (1), 51-63.

[265] Ernkvist, M., Birot, O., Sinha, I., Veitonmaki, N., Nyström, S., Aase, K., et al. (2008). Differential roles of p80- and p130-angiomotin in the switch between migration and stabilization of endothelial cells. *Biochim. Biophys. Acta., 1783*, 429–437.

[266] Wigerius, M., Quinn, D., Diab, A., Clattenburg, L., Kolar, A., Qi, J., et al. (2018). The polarity protein Angiomotin p130 controls dendritic spine maturation. *J Cell Biol., 217* (2), 715-730.

[267] Beckner, M. E., Jagannathan, S., & Peterson, V. A. (2002). Extracellular angio-associated migratory cell protein plays a positive role in angiogenesis and is regulated by astrocytes in coculture. *Microvasc Res., 63* (3), 259-69.

[268] Korf-Klingebiel, M., Reboll, M. R., Klede, S., Brod, T., Pich, A., Polten, F., et al. (2015). Myeloid-derived growth factor (C19orf10) mediates cardiac repair following myocardial infarction. *Nat Med., 21* (2), 140-9.

[269] Makinen, T., Veikkola, T., Mustjoki, S., Karpanen, T., Catimel, B., Nice, E. C., et al. (2001). Isolated lymphatic endothelial cells transduce growth, survival and migratory signals via the VEGF-C/D receptor VEGFR-3. *EMBO J., 20*, 4762-4773.

[270] Nilsson, I., Bahram, F., Li, X., Gualandi, L., Koch, S., Jarvius, M., et al. (2010). VEGF receptor 2/-3 heterodimers detected in situ by proximity ligation on angiogenic sprouts. *EMBO J., 29*, 1377-1388.

[271] Wang, J. F., Zhang, X., & Groopman, J. E. (2004). Activation of vascular endothelial growth factor receptor-3 and its downstream signaling promote cell survival under oxidative stress. *J. Biol. Chem., 279*, 27088-27097.

[272] Calvo, C. F., Fontaine, R. H., Soueid, J., Tammela, T., Makinen, T., Alfaro-Cervello, C., et al. (2011). Vascular endothelial growth factor receptor 3 directly regulates murine neurogenesis. *Genes Dev., 25* (8), 831-44.

[273] Shin, Y. J., Choi, J. S., Choi, J. Y., Cha, J. H., Chun, M. H., & Lee, M. (2010). Enhanced expression of vascular endothelial growth factor receptor-3 in the subventricular zone of stroke-lesioned rats. *Neurosci Lett., 469* (2), 194-8.

[274] Skiles, M. L., Brown, K. S., Tatz, W., Swingle, K., & Brown, H. L. (2018). Quantitative analysis of composite umbilical cord tissue health using a standardized explant approach and an assay of metabolic activity. *Cytotherapy, 20* (4), 564-575.

[275] Chen, C. T., Shih, Y. R., Kuo, T. K., Lee, O. K., & Wei, Y. H. (2008). Coordinated Changes of Mitochondrial Biogenesis and Antioxidant Enzymes During Osteogenic Differentiation of Human Mesenchymal Stem Cells. *Stem Cells, 26* (4), 960-8.

[276] Fillmore, N., Huqi, A., Jaswal, J. S., Mori, J., Paulin, R., Haromy, A., et al. (2015). Effect of Fatty Acids on Human Bone Marrow Mesenchymal Stem Cell Energy Metabolism and Survival. *PLoS One, 10* (3), e0120257.

[277] Balhara, B., Burkart, A., Topcu, V., Lee, Y. K., & Cowan, C. K. (2015). Severe insulin resistance alters metabolism in mesenchymal progenitor cells. *Endocrinology, 156* (6), 2039-48.

[278] Moisan, A., Lee, Y. K., Zhang, J. D., Hudak, C. S., Meyer, C. A., Prummer, M., et al. (2015). White-to-brown metabolic conversion of human adipocytes by JAK inhibition. *Nat Cell Biol., 17* (1), 57-67.

[279] van den Beukel, J. C., Grefhorst, A., Hoogduijn, M. J., Steenbergen, J., Mastroberardino, P. G., Dor, F. J., et al. (2015). Women have more potential to induce browning of perirenal adipose tissue than men. *Obesity (Silver Spring), 23* (8), 1671-9.

[280] Shirley, R., Ord, E. N., & Work, L. M. (2014). Oxidative Stress and the Use of Antioxidants in Stroke. *Antioxidants (Basel), 3* (3), 472–501.